Title
Behavioral genetic analysis of the spatial and temporal resolution of vision in the zebrafish, Danio rerio

Author
Smear, Matt

Publication Date
2005

Peer reviewed|Thesis/dissertation

Behavioral genetic analysis of the spatial and temporal resolution of vision in the zebrafish, *Danio rerio*

by

Matt Smear

DISSERTATION

Submitted in partial satisfaction of the requirements for the degree of

DOCTOR OF PHILOSOPHY

in

Neuroscience

in the

GRADUATE DIVISION

of the

UNIVERSITY OF CALIFORNIA, SAN FRANCISCO

Acknowledgements

I would like to thank our collaborators Mu-Ming Poo and Whit Tao for their contributions to my work. Without their electrophysiological expertise my work would be incomplete. I'd also like to thank the Baier Lab for providing a collegial and nourishing environment for my maturation as a scientist. Wendy Staub kept our lab running and our fish living, and she covered for me too many times to count. Koji Takahashi's technical assistance in molecular biology was instrumental to my success. Patrick Page-McGaw and Ann Wehman gave me a crash course in molecular biology and genomics, and without their help we'd have taken much longer to clone the *blu* gene. Michael Orger was an inspiring collaborator and a great friend. We developed the OMR system together, and Mike is such a great and smart person that I benefited immeasurably from our association. Most of all, I'd like to thank Herwig, my thesis advisor, for allowing me to pursue such a wide-ranging project. Herwig's mentoring strikes the perfect balance between hand's on micromanagement and hand's off detachment. I always felt that I had his full support, and yet I never felt him breathing down my neck.

I'd like to thank my girlfriend Andrea for bringing so much joy and moral support to my life. My parent's unstintingly self-sacrificing support got me to where I am today. Finally, I'd like to thank my brother Chris, who inspired me to go into Neuroscience.

Behavioral genetic analysis of the spatial and temporal resolution of vision in the zebrafish, *Danio rerio*

Matthew Charles Smear

Abstract

It is unclear whether the properties of neuronal circuits beyond the retina limit the spatial and temporal resolution of vision. The kinetics of neurotransmission at central synapses should limit an animal's ability to see rapid movements. Accurate retinotopy should be essential for the perception of fine spatial detail. We have tested these predictions using the zebrafish *blumenkohl (blu)* mutant. Positional cloning revealed that the *blu* gene encodes *vglut2a*, a vesicular glutamate transporter expressed by retinal ganglion cells. *blu* mutants' retinotectal synapses show diminished responses to high frequency electrical stimulation, which should reduce the visibility of fast-moving visual stimuli. Single retinal axons in *blu* mutants arborize over a larger area in the tectum, blurring the fine detail of the retinotopic map, which should compromise spatial acuity. We tested these hypotheses using assays for optomotor responses and prey capture. Our study provides experimental support for previously untested principles of sensory coding.

Table of Contents

Introduction 1

Chapter 1: The *blumenkohl* gene encodes a vesicular glutamate transporter expressed by retinal ganglion cells 8

Chapter 2: *blumenkohl* mutants show impairments in presynaptic release of glutamate 21

Chapter 3: Retinotectal axon arbors are enlarged in the *blu* mutant, suggesting homeostatic compensation 38

Chapter 4: *blu* mutants have reduced acuity in two visual behaviors 63

Conclusion 86

References 99

List of Figures

Figure 1. The *blu* gene encodes Vglut2a. 19

Figure 2. Properties of retinotectal synaptic transmission in blu mutants. 34

Figure 3. *blu* mutant synapses transmit deficiently at high stimulation rates. 36

Figure 4. *blu* mutants have enlarged RGC axon arbors. 56

Figure 5. Chimera analysis of RGC arbor morphology. 58

Figure 6. The OMR of *blu* mutants has reduced spatial and temporal resolution. 82

Figure 7. Prey capture by *blu* mutants has reduced spatial resolution. 84

Introduction

The vertebrate visual system encodes with high precision the spatiotemporal distribution of photons entering the retina. The spatial and temporal resolution of the visual system can be predicted by the Nyquist theorem. In the retina, the spacing of photoreceptors (Geisler, 1984) and retinal ganglion cells (Wassle and Boycott, 1991) set how densely images are sampled and thus determine the spatial resolution of vision. In the temporal domain, phototransduction kinetics set an upper bound to the ability to discriminate events in time (Baylor, 1996). The representation of the visual scene at the photoreceptors then passes through two to four layers of neural processing before being transmitted into the brain via the axons of retinal ganglion cells (RGCs). Since all visual information passes through RGCs, the properties of its output must constrain the spatial and temporal resolution of vision.

The axons of RGCs project to their targets in an ordered fashion. A ubiquitous design feature of connectivity and function in the visual as well as other sensory systems is topographic mapping, that is, preservation of the spatial order of the sensory surface being represented (Kaas, 1997). Why is topographic mapping so prevalent? Biologically useful information is often obtainable by performing local comparisons, for example comparing the input from one part of the sensory surface with the input from another nearby part of the sensory surface. The cardinal example of this type of computation would be center-surround receptive fields of the retina (Hartline, 1940; Kuffler, 1953), in which the brightness of a given region is compared with the region surrounding it. In order to perform these kinds of local computations, the neurons that represent nearby

parts of the sensory surface must be connected to each other. In general, it is good design to minimize wire length by positioning connected neurons close together, since long projections are disadvantageous in several ways (Cajal, 1995; Chklovskii et al., 2002). They take up a lot of space, they lengthen the time it takes to propagate the signal, and they are metabolically costly. Wire-length minimization can thus explain the organization of retinotopic, somatotopic, and cochleotopic (tonotopic) maps. The principle of wire-length minimization is also satisfied by maps which represent a computationally derived variable, for example mappings of auditory space obtained from interaural comparisons (Knudsen et al., 1987). It may even explain mapping in the olfactory bulb, a brain area which represents a much higher-dimensional signal (odor identity) than other sensory systems. Glomeruli that represent related chemical groups are mapped close together (Rubin and Katz, 1999), perhaps thus facilitating lateral-inhibition-like computations.

In order for brain areas to possess topographically mapped functional organization, their afferent input must preserve the spatial order of the receptor surface (Kaas, 1997). Thus as information transfers from receptors to the neurons to which they connect, and then through successive layers of neurons, the spatial organization at the receptor layer is preserved anatomically. Thus, two receptors at opposite ends of the receptor surface connect to neurons at opposite ends of the brain area. Neighboring receptors are represented by neighboring neurons in the downstream brain area. This is achieved by having neurons project their axons to the next stage in an order which reflects the organization of their cell bodies.

The fidelity of topographic mapping is determined by two factors. First, the size of individual axon arbors determines how many postsynaptic neurons a given presynaptic neuron connects to. Second, the extent to which the targeting of axon arbors preserves the order of their cell bodies determines how well that order is transmitted to the next stage. Taken together, these two factors determine how wide a region of the afferent area a given postsynaptic neuron connects to and consequently should play a causal role in receptive field size. In the visual system, the receptive field size of a retinorecipient neuron should be set by the distribution within the ganglion cell layer of the RGCs from which it receives synaptic input, as has been demonstrated in the cat retinogeniculate connection (Usrey et al., 1999). Thus, a neuron with a large receptive field is connected to a broadly-distributed population of RGCs. A neuron with a small receptive field receives input from a population of RGCs circumscribed to a small portion of the ganglion cell layer. Since the size and structure of visual neurons' receptive fields are set by the arrangement of their synaptic inputs (Barlow, 1975; Reid and Alonso, 1995), the spatial resolution of vision should depend on the accuracy of retinotopic mapping (Barlow, 1975; Kaas, 1997; Marshall, 1942).

Temporal resolution depends on the time it takes to activate and quench the phototransduction cascade (Baylor, 1996). Photoreceptors are tonically depolarized and release large amounts of neurotransmitter in the dark. The output of the phototransduction cascade is the closing of ion channels, thus hyperpolarizing the photoreceptor terminal and reducing the amount of transmitter released. At the next stage of processing, the dynamic range of the photoreceptor signal is divided, with ON-bipolar cells responding to the reductions in photoreceptor release consequent from light

increment, and OFF-bipolar cells responding to increases of neurotransmitter release due to light decrement (Sterling, 2003). Because photoreceptors represent a broad bandwidth of temporal signals, the photoreceptor signal is also subdivided into narrower temporal bands. For example, different morphological classes of OFF-bipolar cell are sensitive to different ranges of temporal modulations. Their differential sensitivity is conferred by the different time courses of deactivation of the glutamate receptors they express (DeVries, 2000). The temporal resolution of vision is thus set by the class of bipolar cell sensitive to the fastest modulation rates.

Subsequently, the temporal resolution of vision is set by the kinetics of neurotransmission at downstream synapses. In order for fast changes in the visual image to be represented in the activity of neurons downstream of the photoreceptors, synapses must transmit effectively when presynaptic neurons fire at high rates. One well-known effect of repetitive firing on synaptic transmission is short-term synaptic plasticity (Zucker and Regehr, 2002). Some synapses increase the amount of neurotransmitter they release when stimulated repetitively, an effect known as short-term facilitation. Other synapses decrease transmitter release to repetitive stimulation, an effect called short-term depression. Based on the evidence of classic studies of neuromuscular transmission, these short-term changes are traditionally thought to be dependent on a synapse's initial probability of release. Synapses which release at low probability tend to show facilitation, which is attributed to the accumulation of residual calcium over successive spikes (Katz and Miledi, 1968). Synapses with a high probability of release deplete their supply of filled vesicles, and thus release less neurotransmitter over the course of a stimulus train (Del Castillo, 1954). Short-term plasticity then can work as a filter on synaptic

transmission, boosting transmission when a presynaptic cell fires at frequencies which evoke net facilitation, and attenuating transmission when a presynaptic cell fires at frequencies which produce net depression (Fortune and Rose, 2001; Tsodyks and Markram, 1997).

Short-term plasticity thus has an important potential influence on the temporal resolution of vision. It may modulate transmission by RGC synapses. RGCs with linear receptive fields modulate their spike rate to match the modulation rate of a sinusoidal grating stimulus (Bilotta and Abramov, 1989; Hochstein and Shapley, 1976). Thus if a visual stimulus is modulated rapidly enough to evoke RGC firing at a rate which causes synaptic release to depress, then this stimulus will not be transmitted effectively to postsynaptic neurons, thus making the stimulus less visible to the animal. Thus, the kinetics of transmission at central synapses should determine whether fast changes in the visual image can be seen (Fortune and Rose, 2001; Tsodyks and Markram, 1997).

Whether visual circuits beyond the retina constrain visual resolution has not been rigorously tested, due in large part to the difficulty of combining psychophysical measurements with experimental perturbations in one model system. We have taken a combined genetic and psychophysical approach in zebrafish to this problem. Zebrafish depend on vision for numerous behaviors, including prey capture, predator avoidance, schooling, and the execution of innate reflexes to steady light and motion (Neuhauss, 2003). Zebrafish retinal ganglion cells (RGCs) extend long axons primarily to the optic tectum, where they elaborate single terminal arbors. Each axonal arbor covers only about 3-6% of the tectal surface in the zebrafish larva and may overlap substantially with

neighboring arbors (Gnuegge et al., 2001; Schmidt et al., 2000; Stuermer, 1988); our own unpublished observations). The retinotectal projection is highly ordered; neighboring RGCs project to neighboring positions in the tectum, forming a precise retinotopic map (Stuermer, 1988). The *blumenkohl* (*blu*) mutation was originally isolated in a screen for retinotectal axon guidance phenotypes (Baier et al., 1996; Trowe et al., 1996).

By positional cloning, we show that the *blu* mutation disrupts *vglut2a*, a vesicular glutamate transporter closely related to mammalian VGLUT2. This family of proteins mediates glutamate uptake by presynaptic vesicles and is necessary and sufficient for glutamatergic transmission (Bellocchio et al., 2000; Fremeau et al., 2004; Fremeau et al., 2001; Takamori et al., 2001; Wojcik et al., 2004). Zebrafish *vglut2a* is expressed in RGCs and is largely, but not exclusively, responsible for glutamatergic transmission at the retinotectal synapse. We show that retinal input to the tectum is only modestly impaired in *blu* mutants, due partly to co-expression of another Vglut isoform in RGCs and partly to specific compensatory mechanisms.

Despite their grossly normal retinotectal transmission, RGCs in *blu* mutants have phenotypes which should compromise the spatial and temporal acuity of their vision. Retinotectal synapses in mutants exhibit larger depression during high-frequency stimulation compared to wildtype. Short-term depression of this kind is thought to function as a low-pass filter on the transfer of information across synapses (Fortune and Rose, 2001; Tsodyks and Markram, 1997). Because rapidly modulated visual stimuli evoke high firing rates in RGCs (Bilotta and Abramov, 1989; Hochstein and Shapley, 1976), we asked if this physiological change leads to a deficit in the detection of fast

changing visual scenes. In a behavioral test employing the optomotor response (OMR; the reflexive swimming to follow visual motion) (Orger et al., 2000), we confirmed that *blu* mutants responded normally to slow-drifting gratings, but much less so to rapidly modulated stimuli. We go on to show that individual axon arbors cover a nearly twofold larger tectal area, thus degrading the retinotopic map. In agreement with prediction that the precision of retinotopic mapping should be important for spatial acuity (Barlow, 1975; Kaas, 1997; Marshall, 1942), *blu* mutants display spatial deficits in two visual behaviors. When the animals were presented with the movement of fine gratings, their OMR was diminished relative to wildtype. Moreover, *blu* mutants have a selective deficit in capturing small prey items. Thus, this mutant's perceptual deficits match the perturbations of CNS circuitry, providing genetic evidence for two important neurological constraints on visual acuity.

Chapter 1: The *blumenkohl* gene encodes a vesicular glutamate transporter expressed by retinal ganglion cells

The *blumenkohl* (blu^{tz257}) mutant was originally isolated in a screen for phenotypes affecting the projection of retinal ganglion cell (RGC) axons to the tectum (Baier et al., 1996) (Trowe et al., 1996). In blu^{tz257} mutants, small groups of RGC axons were shown to cover a larger-than-normal area of the tectal neuropil. We hypothesized that this anatomical phenotype would impair vision in a manner analagous to the way in which poor optics blurs images. To test this hypothesis, we compared the acuity of *blu* mutants' optomotor response (OMR) to that of their siblings. Our initial results showed that *blu* mutants' OMR had impaired visual acuity, so we decided to clone the *blu* gene. For forward genetics, zebrafish have proven to be the most tractable vertebrate species utilized (Talbot and Hopkins, 2000). While not yet as awesomely powerful as fly or worm genetics, with a bit of luck, one can clone zebrafish genes in a reasonable amount of time. To clone the *blu* gene, we took advantage of the genetic and physical maps that were available for the zebrafish genome at the time we began this project.

In order to genetically map a mutant gene, whatever the species, one must be able to rapidly and reliably distinguish mutants from wildtype siblings. The physiological, anatomical, and behavioral phenotypes I focus on in this thesis are quite interesting, but they are too subtle and difficult to demonstrate to allow the rapid and reliable sorting

which is necessary for genetic mapping. Fortunately, *blu* mutants have another behavioral phenotype, in a behavior called visual background adaptation (VBA). VBA allows zebrafish to adjust the distribution of melanin pigmentation in their skin to match ambient light levels, and is thought to serve as a camouflage mechanism. When placed on a dark background, melanin granules (also called melanosomes) become widely distributed within the processes of the pigment cells, the melanophores, making the fish appear dark. When placed on a light background, melanosomes become aggregated, and the fish look pale. A direct projection from the retina to the hypothalamus is thought to provide the sensory input to this adaptation response (for review, see Balm and Groeneveld, 1998). The melanophores of *blu* mutants have dispersed melanin even at very high light levels, a phenotype frequently observed in blind or visually impaired fish (Neuhauss et al., 1999); Muto et al., in press). The VBA phenotype in *blu* is not due to a defect in melanophore-autonomous function, because bath application of norepinephrine, which causes wild-type fish to aggregate their melanin granules in the dark, can completely aggregate the melanin granules of *blu* mutants. Since melanophores in *blu* mutants can be aggregated in response to external signals, the defect must either be in the part of the visual system that measures ambient light levels and/or the system that signals from there to the melanophores.

The dark appearance of fish with VBA phenotypes makes them very easy to sort – "even a monkey could do it" (H. Baier, direct quotation). The VBA phenotype in *blu* allows them to be distinguished from wild-type siblings with perfect reliability, which is crucial not only for genetic mapping (in 1200 mutant embryos collected for mapping, we never had a mis-score) but also for the behavioral analyses discussed later in this thesis.

The behavioral assays we used to test *blu* mutants test multiple fish simultaneously. The behavior is scored by measuring some index of performance of all the fish in a given tank. Only by separating mutants and wildtype fish into different tanks can their behavior be compared. The ability to sort *blu* mutants on the basis of their VBA phenotype is thus crucial to the work we describe here. Later in this chapter I will discuss why we think *blu* mutants have this phenotype.

We genetically mapped the *blu* mutation using microsatellite markers (Shimoda et al., 1999). Microsatellites (also called simple sequence length polymorphisms (SSLPs)) are tracts of sequence which consist of highly repetitive di-, tri-, or tetranucleotide repeats. These tracts of repetitive sequence are highly polymorphic in length and thus easy to score after PCR-amplification and gel electrophoresis. By performing a "genome scan", in which a battery of markers distributed throughout the genome are checked for linkage, we localized the *blu* gene to chromosome 7. We performed fine mapping on 200 embryos with 3 markers we found to be closely linked to the gene. One of these markers, z28221, showed no recombinants after genotyping these 200 embryos, and still showed none after 1000 additional embryos were tested. Such a low recombination frequency indicates a very short physical distance between the marker and the gene. Because our other closest markers were so much farther away, we sought to generate additional markers, in order to better circumscribe the genetic region in which the *blu* gene resides. Looking for additional polymorphisms to use as markers, we generated primers oriented outward from z28221 and used them to sequence genomic DNA. To our pleasant surprise, we found that the sequence obtained from these reactions included sequence belonging to a novel zebrafish gene, indicating that z28221 resided in the intron of a

gene. Moreover, BLAST analysis of this gene revealed that it was highly homologous to two genes, originally named BNPI (brain-specific Na^{2+}-dependent inorganic phosphate transporter) and DNPI (differentiation-associated Na^{2+}-dependent inorganic phosphate transporter) which had recently been shown to mediate vesicular glutamate uptake (Bellocchio et al., 2000; Fremeau et al., 2001; Takamori et al., 2000).

BNPI was identified in a screen for transcripts which are upregulated in cerebellar granule cells exposed to subtoxic levels of NMDA (Ni et al., 1994). DNPI was first characterized as a transcript expressed during the differentiation of exocrine pancreas AR42J cells into neuroendocrine cells (Aihara et al., 2000). Both genes were found by homology searching to belong to a family of proteins defined as Na^{2+}-dependent inorganic phosphate transporters. Consistent with this function, both proteins were shown to increase Na^{2+}-dependent inorganic phosphate transport in *Xenopus* oocytes (Aihara et al., 2000; Ni et al., 1994). The first evidence that this gene family might be important for glutamatergic neurotransmission came from the *C. elegans* mutant EAT-4, which has defects in feeding behavior (Avery, 1993). The EAT-4 gene was later cloned and found to be highly homologous to BNPI (Lee et al., 1999). Feeding, and several other behaviors in which EAT-4 is deficient, including pharyngeal muscle contraction and the tap-withdrawal response, require glutamatergic transmission (Lee et al., 1999), while behaviors mediated by other neurotransmitter pathways are spared. Glutamatergic transmission is greatly reduced at the pharyngeal muscle in EAT-4 mutants (Lee et al., 1999), yet the pharyngeal muscle in EAT-4 mutants responds normally to iontophoretically-applied glutamate (Dent et al., 1997), implying that EAT-4 protein functions presynaptically.

Following these studies in worms, Rob Edwards' group began to investigate the role of BNPI in mammals. By light microscopy, they showed that BNPI was expressed by glutamatergic neurons. Further, they showed by electron microscopy and biochemical fractionation that BNPI localized to synaptic vesicles (Bellocchio et al., 1998). It was originally suggested that the role of BNPI in glutamate signaling was to increase cytoplasmic phosphate concentrations, since the glutamate-synthesizing enzyme is activated by phosphate (Lee et al., 1999). The real role of BNPI in glutamatergic neurotransmission, however, was shown to be much more direct. Membranes purified from cells transfected with BNPI possess glutamate uptake activity (Bellocchio et al., 2000; Takamori et al., 2000), which mimics the substrate selectivity and energy dependence of glutamate uptake characterized in synaptic vesicles purified from brain (Maycox et al., 1990). BNPI expression is thus sufficient for vesicular glutamate uptake. Furthermore, transfection of GABAergic neurons with BNPI enables them to release glutamate synaptically, thus demonstrating that BNPI expression is sufficient for glutamatergic neurotransmission (Takamori et al., 2000). BNPI was thus shown to be a vesicular glutamate transporter, and was renamed VGLUT1. Soon after, additional members of the VGLUT gene family were identified. DNPI was shown to transport glutamate in vitro, and was renamed VGLUT2 (Fremeau et al., 2001). Interestingly, VGLUT2 and VGLUT1 are expressed in essentially non-overlapping subsets of glutamtergic neurons mature mammals (Fremeau et al., 2001). Finally, a previously undescribed gene was shown to be the third member of this gene family, and was named VGLUT3 (Fremeau et al., 2002). Interestingly, this gene is expressed in neurons not thought to use glutamate as a neurotransmitter. All three transporters have very similar affinities and transport kinetics for glutamate, so the reason for their strikingly different expression patterns remains mysterious.

Glutamatergic signaling plays an important role in the development of neural circuits (Goodman and Shatz, 1993; Katz and Shatz, 1996), including RGC axon arbor morphogenesis (Hua and Smith, 2004; Ruthazer and Cline, 2004). We felt that given the RGC axon phenotype in *blu* mutants and the proximity of our closest marker, this putative VGLUT homolog was a strong candidate gene, so we decided to clone it. We generated cDNA from *blu* mutants and wildtype larvae from the same strain, and amplified an internal fragment of the cDNA using primers complementary to sequence we had obtained from genomic DNA. Since this part of the genome had not yet been sequenced by the Zebrafish Genome Project, we could not amplify the gene using gene-specific primers, since we had no way of knowing the sequence of the rest of the gene. Instead, we used 5' and 3' rapid amplification of cDNA ends (RACE) to amplify sequence out to the ends of the cDNA. Using RACE, we were able to amplify all of the coding sequence and much of the 5' and 3' untranslated regions of the gene from mutant and wildtype.

On the basis of very strong sequence conservation, we can confidently say that this gene is a vesicular glutamate transporter. The amino acid sequences of the VGLUT genes are incredibly well-conserved throughout phylogeny, an indication of their essential function in glutamatergic neurotransmission and thus behavior. The gene we have cloned is 76% identical to mouse VGLUT1, and 89% identical to mouse VGLUT2. Almost all of the divergent sequence in different VGLUT proteins resides either at the N- and C- terminals, especially in an approximately 60-aa stretch of the protein at the C-terminal end. Within this region our gene is 55% identical to VGLUT2 and 41% identical to VGLUT1. In addition, the region on Chromosome 7 in which our gene is located is syntenic to the regions of the human and mouse genomes where VGLUT2 is located. This gene is thus orthologous to mammalian VGLUT2. We later learned that another group had cloned parts of this and several other VGLUT genes (Higashijima et

al., 2004). One of the genes was an additional VGLUT2 isoform. We henceforth refer to the VGLUT gene we have cloned as *vglut2a*.

While cloning the *vglut2a* gene from mutant and wildtype cDNA, we found that for some reactions, we obtained shorter bands in wildtype than in mutants. Sequencing confirmed this observation. The sequence obtained from *blu* mutant cDNA was missing a 114 nt stretch of sequence present in wildtype cDNA. As a result of this absence, the coding frame of the mutant transcript is shifted, and the next upstream codon becomes a stop. This mutation thus results in a much shorter encoded protein – 154 aa instead of the wildtype 584 aa. The protein will thus lack several transmembrane domains (Fremeau et al., 2001), thereby nullifying the vesicular glutamate transport activity of the protein.

The absence of such a large chunk of sequence from the *blu* mutant transcript could result from two possible genetic lesions. Either a mutation causes the gene to be spliced improperly, omitting an exon, or, the chunk of sequence had been deleted from genomic DNA. Because this mutation was obtained from an ethylnitrosurea (ENU) mutagenesis screen, which mostly causes point mutations, a splicing error seemed to be the most likely explanation. To determine the genetic lesion responsible for this change in the *blu* mutant transcript, we sequenced genomic DNA from mutant and wildtype using primers from sequence within the missing chunk and immediately outside it. The missing sequence was present and normal in *blu* mutants. It corresponds to exon 4 of the gene. The 5' splice site of this gene (which is intronic), has a T → A substitution in the conserved consensus sequence GT at the 5' end of the adjacent intron (Fig. 1B). This GT is required for splicing (Gesteland et al., 1999). In its absence, the 5' splice site of the next upstream intron joins with the 3' splice site of the next downstream intron, thereby editing exon 4 out of the mutant transcript (Fig. 1C). This genetic lesion thus explains the missing sequence from the *blu* allele of *vglut2a*.

Given this strong evidence that *vglut2a* function is nullified in *blu* mutants, we attempted to rescue the mutation. We screened a library of phage artificial chromosomes (PACs) containing zebrafish genomic contigs for the presence of z28221 by PCR. We obtained 3 PAC clones from which z28221 could be amplified. Using a picospritzer, we pressure injected a solution containing a high concentration (150-400 ng/μl) of these solutions into one-cell stage embryos obtained from a cross of *blu* heterozygotes. The injected embryos, and an equal number of uninjected embryos were scored for their VBA by an investigator blind to which fish had been injected. The fish scored as wildtype were genotyped for z28221. Of the injected fish, 13 of 200 scored as mutant, compared to none of the 200 uninjected fish. Thus, a genomic clone containing a normal copy of the *vglut2a* gene can rescue *blu* mutants' VBA phenotype. Taken together, linkage analysis, sequencing, and rescue data show that the blu^{tz257} allele encodes a likely null of *vglut2a*.

We next wanted to determine where the *blu* gene is expressed. We obtained oligonucleotide probes for *vglut2a*, as well as probes for two other *vglut* isoforms, named *vglut2b* and *vglut1a* on the basis of sequence homology (generous gift of Joe Fetcho's lab)(Higashijima et al., 2004). The sequence to which these probes hybridize is almost completely in UTR, and quite divergent from other VGLUT family members, thus ensuring specificity despite the high degree of sequence conservation across the gene family. Using these probes, we performed *in situ* hybridization on 7dpf larvae. Whole-mount staining of the eye revealed that *vglut2a* is expressed in RGCs. Cells in the inner nuclear layer express *vglut1a*, while *vglut2b* is not expressed in the retina.

In the brain, *vglut2a* and *vglut2b* are expressed in a largely overlapping set of areas, including the olfactory epithelia, the brain stem, and the ventral diencephalons, including the hypothalamus. The normal expression of *vglut2a* in the hypothalamus may explain the severity of the VBA phenotype, since the hypothalamus is thought to mediate VBA. Despite this overlap, there are notable differences in the expression pattern of these two genes. In addition to the absence of *vglut2b* in RGCs, *vglut2b* is absent from a patch of cells in the posterior forebrain which expresses *vglut2a* strongly. In the tectum, many cells express *vglut2b,* while *vglut2a* is largely absent in this area. Staining for *vglut1a* is very strong in the cerebellum, and also present in the olfactory bulb and hindbrain.

We also wanted to determine the expression pattern of *vglut2a* protein, which would have allowed us to determine the protein's subcellular localization. We obtained the anti-mouse VGLUT2 antibody, but it gave non-specific staining patterns in cryo-sections and Western blots. We attempted to raise an antibody to the *vglut2a* protein, which would have allowed us to visualize the protein's subcellular localization as well as determine whether the mutation is indeed a protein null. We generated a GST-fusion protein using the sequence coding for the 60-aa C-terminal region of the *vglut2a* protein which has the most divergent sequence. Unfortunately, antisera obtained from rabbits injected with the fusion protein also gave non-specific staining in sections and Western blots. Nevertheless, given the *vglut2a* gene's high degree of sequence conservation, it is exceedingly likely that it performs the same function as its homologs in other species. In light of its expression in RGCs and our interest in its role in visual function, we next investigated the effects of the *blu* mutation on synaptic transmission by RGCs, by recording from optic tectal neurons.

METHODS

Mapping, cloning, rescue, and expression analysis

Heterozygous *blu*^{tz257} carriers in a mixed TL and Tübingen strain background were crossed to the polymorphic WIK strain. We deduced the map position of *blu* first by bulk-segregant analysis with simple-sequence length polymorphism markers (Shimoda et al., 1999) and then by single-embryo linkage analysis using 1,205 F2 embryos, which yielded a marker, *z28221*, which failed to recombine with the *blu* phenotype. The genomic sequence adjoining on both sides was PCR-amplified, cloned and sequenced, revealing *z28221*'s location to be in an intron of a gene. BLAST analysis identified the sequence as a *vglut2* homolog. Starting from primers generated within this sequence, we used 5'- and 3'- RACE to clone full length cDNA for the wildtype (TL) and mutant alleles of *vglut2a*, revealing a 114-bp stretch missing from the *blu* mRNA. Because the missing sequence in the *blu* mRNA suggested an exon skip, we PCR-amplified, cloned, and sequenced genomic DNA containing the splice sites surrounding the putative missing exon. To test for rescue, a phage artificial chromosome (PAC) genomic clone library (obtained from D. Stainier's lab, UCSF) was screened for *z28221*. From positive clones, purified PAC DNA was diluted in Danieau buffer [58 mM NaCl, 0.7 mM KCl, 0.4 mM MgSO4, 0.6 mM Ca (NO3)2, 5 mM HEPES (pH 7.6)] and injected into one-cell-stage embryos at 100 ng/ml or 200 ng/ml using a picospritzer (World Precision Instruments). Injected and uninjected larvae were scored by VBA phenotype, blind to whether they had been injected, and genotyped with *z28221*. Whole-mount RNA *in situ* hybridization was performed as previously described (Keegan et al., 2002). Hybridized probe was detected

Figure 1, Smear et al.

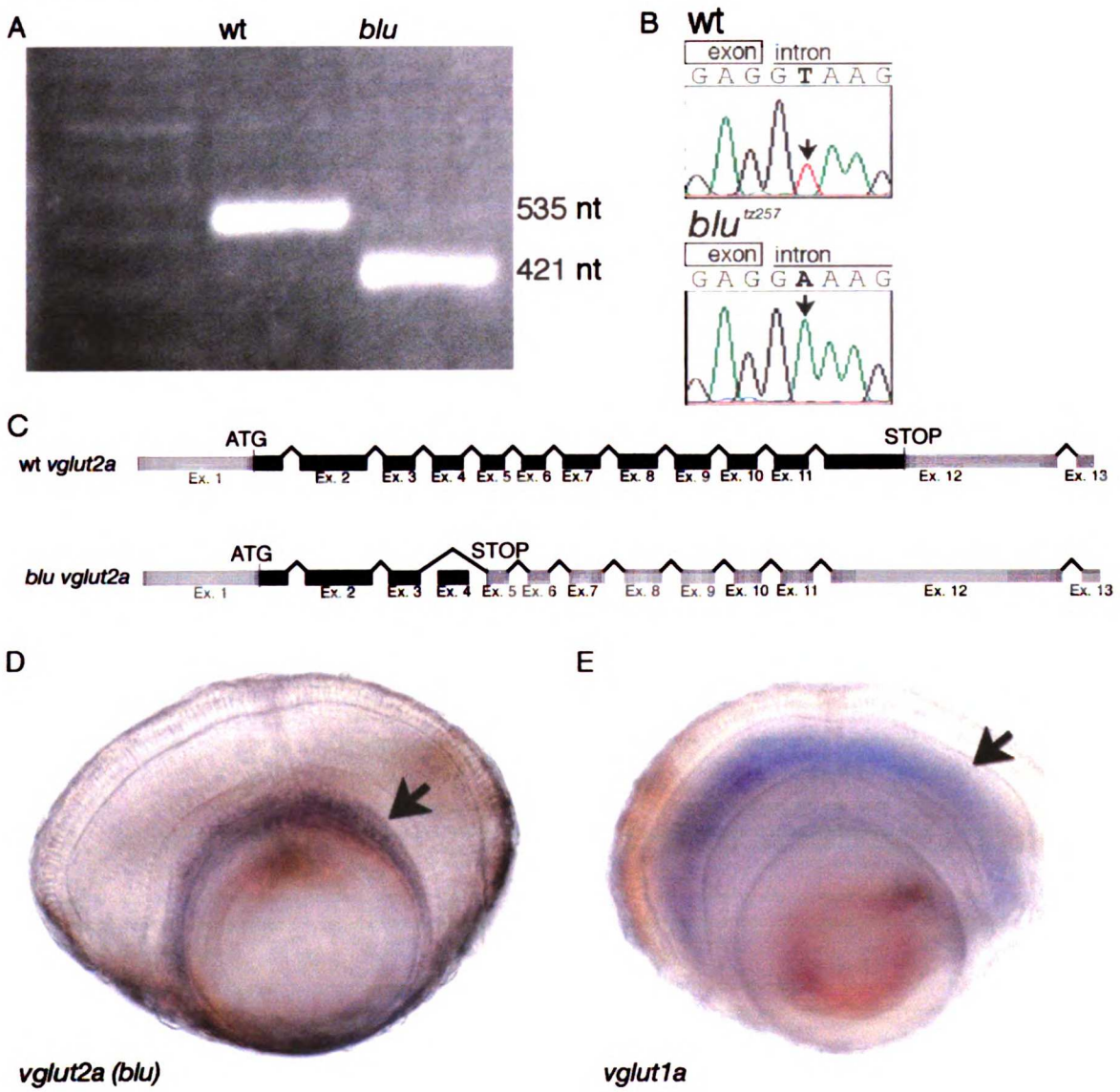

Figure 1. The *blu* gene encodes Vglut2a. **A,** RT-PCR amplification of a fragment of *vglut2a* containing exon 4. Subsequent sequencing showed that the wt fragment is 535 nt, and the *blu* fragment is 421 nt. **B,** Genomic DNA sequence from the 5' splice site affected in blu^{tz257}. **C,** Schematic representation of the *vglut2a* gene and the blu^{tz257} allele. Translated regions are colored black and untranslated regions are grey. In blu^{tz257}, exon 4 is skipped, producing a premature stop codon. **D,** Expression of *vglut2a* in zebrafish eye (7 dpf), removed from larva after fixation. Arrowhead points to the RGC layer, in which *vglut2a* is expressed. **e,** Expression of *vglut1a* in isolated zebrafish eye (7 dpf). Arrowhead points to the bipolar cells in the inner nuclear layer, in which *vglut1a* is expressed.

Chapter 2: *blumenkohl* mutants show impairments in presynaptic release of glutamate

Chemical synaptic transmission transpires when an action potential depolarizes a pre-synaptic terminal, opening voltage-gated Ca^{2+} channels. The ensuing calcium influx causes neurotransmitter-filled vesicles to fuse with the terminal's membrane at release sites and exocytose their contents into the synaptic cleft. Synaptic signaling thus requires that vesicles contain high concentrations of neurotransmitters. Active transport activities mediated by specific transporter proteins generate the steep concentration gradients across vesicular membranes necessary for effective synaptic communication (Liu and Edwards, 1997). The vesicular glutamate transporter proteins have been shown to mediate transmembrane glutamate transport with properties identical to that of synaptic vesicle membranes purified from the brain (Bellocchio et al., 2000; Maycox et al., 1990; Takamori et al., 2000). Consistent with the crucial function of vesicular glutamate transporters in synaptic transmission, mice in which the VGLUT1 gene is deleted have profound defects in glutamatergic transmission (Fremeau et al., 2004; Wojcik et al., 2004). Additionally, transfection of inhibitory neurons with the VGLUT1 gene is sufficient to endow them with exocytotic glutamate release (Takamori et al., 2000).

We wanted to ascertain whether the *blu* mutation affects glutamatergic transmission in zebrafish. We chose to study transmission at synapses formed between RGC terminals

and neurons in the optic tectum for several reasons. By *in situ* hybridization, we had shown that *vglut2a* is prominently expressed in RGCs. RGCs project to ten arborization fields in the zebrafish brain (Burrill and Easter, 1994), with the optic tectum being by far the largest and most superficial, and thus the most experimentally accessible. Also, the fact that the *blu* mutation affects retinotectal axon arbor morphogenesis, a phenotype which we hypothesized might be due to deficient glutamate release, hinted that this synapse might have a phenotype in synaptic transmission. Finally, our major goal in studying this mutant was to determine whether its neural phenotypes caused phenotypes in visual behaviors. All visual information passes through RGCs on its way from the retina to the brain, a process to which synaptic transmission is essential.

We recorded from optic tectal neurons intracellularly using whole-cell patch recordings *in vivo* (Engert et al., 2002; Zhang et al., 1998). Tectal neurons in mutants are not different from wildtype in their basic eletrophysiological properties (resting membrane potential and input resistance: mutant, 53 ± 6 mV, 1535 ± 128 MΩ, n = 25; wildtype, 54 ± 5 mV, 1498 ± 115 MΩ, n=22). When we started these experiments, we knew that *blu* mutants were not blind, and thus must not completely lack glutamatergic transmission from RGCs. Even so, we were surprised to find that excitatory postsynaptic currents (EPSCs) recorded evoked in optic tectal neurons seemed completely normal. Indeed, crude light stimulation (turning the lights on and off) EPSCs evoked equal-sized EPSCs in *blu* mutants and wildtype (Fig. 2A, bottom). Direct electrical stimulation of the optic nerve head, calibrated to activate most if not all of the RGC inputs to the optic tectum, gave normal responses in *blu* mutants. Finally, action potential-dependent

spontaneous EPSCs had identical amplitude distributions in mutants and wildtype (Fig. 2B, C).

Why is glutamatergic transmission so normal at retinotectal synapses, which should lack *vglut2a* function? One possible explanation is that unlike in other vertebrates, retinotectal synaptic transmission is not glutamatergic in zebrafish. We tested this possibility pharmacologically. Synaptic responses elicited by electrically stimulating the RGC inputs are blocked completely by glutamate receptor antagonists 6-cyano-7-nitroquinoxaline-2,3-dione (CNQX) and 2-amino-5-phosphonovalerate (APV) (Fig. 2A, top), but not by GABAa receptor antagonist bicuculline (data not shown), demonstrating that these synapses are exclusively glutamatergic in zebrafish, as they are in other vertebrates. Another possible explanation is that the *blu* allele of *vglut2a* is not a null, and in fact retains substantial glutamate transport activity. In light of the nature of the genetic lesion in *blu,* this possibility is exceedingly unlikely to be true. In the *blu* allele, the consensus GT of a 5' splice site, conserved widely throughout phylogeny, carries a point mutation which abolishes this sequence's role in splicing. The gene's fourth exon is thus edited out of the transcript. As a result of the omission of the gene's 4^{th} exon, the gene's reading frame is shifted, giving rise to a stop in the next upstream codon. Even in the off chance that this stop codon might somehow be 'leaky', allowing the translation machinery to read through and continue translating, the code of the downstream sequence has become a string of nonsense because of the frame-shift. Another possible explanation for the apparent lack of synaptic phenotype in *blu* mutants is that retinotectal synaptic transmission utilizes nonvesicular release of glutamate. Normally, the plasma membrane neurotransmitter transporters work to pump neurotransmitter into neurons or

glial cells, thus removing transmitter from the synaptic cleft. Under some conditions, the direction of uptake can be reversed, thus extruding transporter out of the cell (Attwell et al., 1993). This mechanism of nonvesicluar release has been postulated to function *in vivo*. For example, horizontal cells can release GABA by reversed uptake (Schwartz, 1987), and nonvesicular glutamate release may regulate glutamate receptor clustering at the *Drosophila* neuromuscular junction (Featherstone et al., 2002). But while pathological conditions such as anoxia can produce rapid reversed uptake of glutamate, under normal physiological conditions reversed uptake is too slow to make much contribution to normal synaptic transmission (Attwell et al., 1993). We can thus be rather confident in disregarding nonvesicular release as a possible explanation for *blu* mutants' apparently normal glutamatergic transmission.

Since all of the possibilities sketched above are exceedingly unlikely, by far the best explanation for why *blu* mutants have such strong retinotectal signaling is that RGCs have additional means to load transmitter into synaptic vesicles, most likely through another *vglut* isoform. The two isoforms for which we were able to obtain oligonucleotide probes, *vglut1a* and *vglut2b,* are not expressed by RGCs in wildtype fish, nor is their transcription upregulated in *blu* mutants. BLAST searching of the zebrafish genome reveals uncharacterized sequences likely to encode additional *vglut* isoforms one or more of which may be co-expressed in wildtype RGCs or upregulated in the mutant.

Even if an additional *vglut* isoform is expressed at zebrafish retinotectal synapses, the absence of *vglut2a* function would be expected to have some effect on glutamate release. Since the techniques we have used to examine evoked release were fairly crude,

we wanted to inspect glutamatergic neurotransmission more closely. One potentially important question to ask is if there are multiple vesicular glutamate transporters in RGC presynaptic terminals, how do they localize relative to each other? There are three possible answers to this question. The first possibility is that there are distinct subclasses of glutamatergic synapse in the retinotectal connection, with some expressing *vglut2a* and others expressing another *vglut*. Glutamatergic synapses are organized in this manner in the mature mouse hippocampus (Fremeau et al., 2004)(discussed further below). Another possible mode of organization is that *vglut2a* and the other putative-expressed *vglut* segregate to different populations of vesicles, but that these vesicle populations co-mingle in the same synapses. Third, the *vgluts* might localize to the same vesicles. Which of these three possibilities is true has important implications for glutamatergic neurotransmission in normal fish, as well as the ways in which transmission might be affected in *blu* mutants.

To distinguish between these possibilities, we performed miniature excitatory postsynaptic current (mEPSC) analysis on retinotectal neurotransmission. mEPSCs arise from the spontaneous release of single synaptic vesicles, and their analysis yields valuable information. The amplitude of these currents reflects the intravesicular glutamate concentration, as well as the postsynaptic sensitivity to glutamate, that is, the number and conductivity of ionotropic glutamate channels in the postsynaptic membrane. The frequency of mEPSCs is a function of the probability of release and the number of release sites. The different possibilities for how *vgluts* localize relative to each other make different predictions for how mEPSC amplitude and frequency will be affected by loss of *vglut2a* function. If *vglut2a* and the other *vglut(s)* normally localize to different

vesicles, then the density of transporter molecules per vesicle that express *vgluts* other than *vglut2a* will be unchanged. Having a normal number of vesicular tranporters, these vesicles would be filled to a normal level, and would evoke mEPSCs of normal amplitude. The vesicles that normally express *vglut2a*, on the other hand, will harbor no vesicular transporter molecules in *blu* mutants, and will thus contain glutamate at the same concentration as the extravesicular cytoplasmic concentration. This means that when one of these vesicles is released during a spontaneous exocytotic event, very little or no glutamate will be released – essentially the synapse is shooting blanks (Schuske and Jorgensen, 2004). Since mEPSCs are detected by recording intracellularly from the postsynaptic cell, the spontaneous fusion of essentially empty vesicles will not evoke a detectable postsynaptic current. The frequency of detected events will thus be reduced. This prediction is the same for both the model in which the different classes of vesicles segregate to different synapses and the model in which the different classes are mingled in the same synapses, so additional experiments would be required to distinguish between these models.

If the different *vglut* isoforms colocalize to the same vesicles, however, the predicted results of mEPSC analysis are different. In this scenario, these vesicles will harbor fewer functional transporters. The number of vesicular transporters per vesicle is predicted to be proportional to the steady-state vesicular concentration of transmitter (Gasnier, 2000), and over-expression studies lend support to this idea (Daniels et al., 2004; Wojcik et al., 2004). If this model applies to the zebrafish retinotectal synapse, the amplitude of mEPSCs should be reduced in *blu* mutants, as vesicles will only contain fewer *vglut* protein molecules. As for mEPSC frequency, this model predicts no change.

Vesicles are predicted to contain less glutamate, but they should contain some glutamate, and thus should evoke detectable mEPSCs postsynaptically. If anything, reduction of mEPSC amplitude might be predicted to decrease the frequency of detected mEPSCs, for the following reason. mEPSCs are by definition quite small in amplitude, due to the fact that they reflect the excitation generated by the glutamate contained within a single vesicle. Any reduction in their amplitude may be expected to increase the number of spontaneous release events that escape detection due to being lost in the noise, thereby reducing the frequency of detected mEPSCs.

To perform mEPSC analysis, we recorded intracellularly from optic tectal neurons in the presence of TTX and bicuculline (BMI; Fig. 2B, bottom). Under these conditions, in which voltage-gated Na^{2+} channels are blocked, all glutamatergic post-synaptic currents reflect the spontaneous exocytosis of a glutamate-filled vesicle. We found a difference in the cumulative amplitude distribution of mEPSCs (Fig. 2C) and a reduction in the mean mEPSC amplitude (Fig. 2D, inset) in *blu* mutants. Reduced mEPSC amplitude is consistent with a partial reduction in vesicular glutamate uptake.

We also measured the mEPSC frequency. Based on the fact that mEPSC amplitude is reduced, it would be predicted that mEPSC frequency should also be reduced, because more of the smallest release events would fall beneath the detection threshold. Strikingly, we found instead that mEPSC frequency is increased, which suggests that more is going on at this synapse than just the loss of some vesicular glutamate uptake activity. An increase in mEPSC frequency might be attributable to an increase in release probability or an increase in the number of release sites. An increase in release

probability might reflect an enlargement of the readily releasable pool of vesicles, or it might be due to an increase in the propensity of vesicles to exocytose. An increase in the number of release sites is due to either an increase in the number of active zones at synapses or an increase in the number of synapses. In any event, all of these changes would work to counter the reduction in vesicular glutamate concentration indicated by the diminution of mEPSC amplitude. Whatever the mechanism underlying the change in mEPSC frequency, it may account for the normal evoked EPSC amplitudes described above.

A caveat to these studies is that we cannot isolate mEPSCs evoked by RGC synapses from the other synaptic inputs to optic tectal neurons. Some of these synaptic inputs may not express *vglut2a* and thus may not have any transmission phenotypes in *blu* mutants. To circumvent this problem, we attempted to record evoked mEPSCs from RGC axons by substitituting Sr^{2+} for Ca^{2+} in the medium, which desynchronizes evoked release, allowing individual vesicle-evoked responses to be resolved. By stimulating the optic nerve head in Sr^{2+} medium, we hoped to isolate mEPSCs from the RGC inputs. This technique was unsuccessful, because Sr^{2+} had adverse effects on the health of optic tectal neurons. Nonetheless, RGCs are the predominant synaptic input to the optic tectum, so the contamination of our sample by spontaneous events from other synaptic sources should be minor.

To determine whether the *blu* mutation has any effect on the kinetics of synaptic transmission, we tested short-term plasticity at retinotectal synapses. Short-term plasticity measurements give valuable information about the kinetics of synaptic

transmission. Further, synaptic kinetics can constrain the transfer of information across synapses (Fortune and Rose, 2001; Tsodyks and Markram, 1997), and thus may constrain the animal's vision. Generally, short-term plasticity reflects the simultaneous operation of several often countervailing phenomena, most notably depression, a decrease in synaptic responses during rapid stimulation and facilitation, an increase. Short-term depression is conventionally thought to reflect the depletion of the readily releasable pool of vesicles, while facilitation is attributed to temporal summation of calcium influx within the presynaptic terminal (Zucker and Regehr, 2002). Put simply, synapses with high probability of release tend to show short-term depression, whereas synapses with low probability of release tend to show net facilitation.

To compare the dynamics of synaptic transmission for wildtype and *blu* mutants, we electrically stimulated at the optic nerve head while recording intracellularly from optic tectal neurons. We applied pairs of stimuli, at a range of inter-stimulus intervals (ISIs) between 50 and 500 ms, and measured the paired-pulse ratios (PPR), defined as the amplitude of the second EPSC divided by that of the first. Wild-type retinotectal synapses depressed only slightly to paired stimuli delivered at short ISIs. In contrast, mutant synapses show significantly increased paired-pulse depression, in a strikingly ISI-dependent manner: While the PPRs are similar for mutant and wildtype at the longer ISIs tested (400 ms and greater), a significantly greater depression is seen for mutant synapses at shorter ISIs. The difference of the PPR is most pronounced at an intermediate ISI of 100 ms, but curiously disappears for the very shortest ISI measured (50 ms) (Fig. 3A).

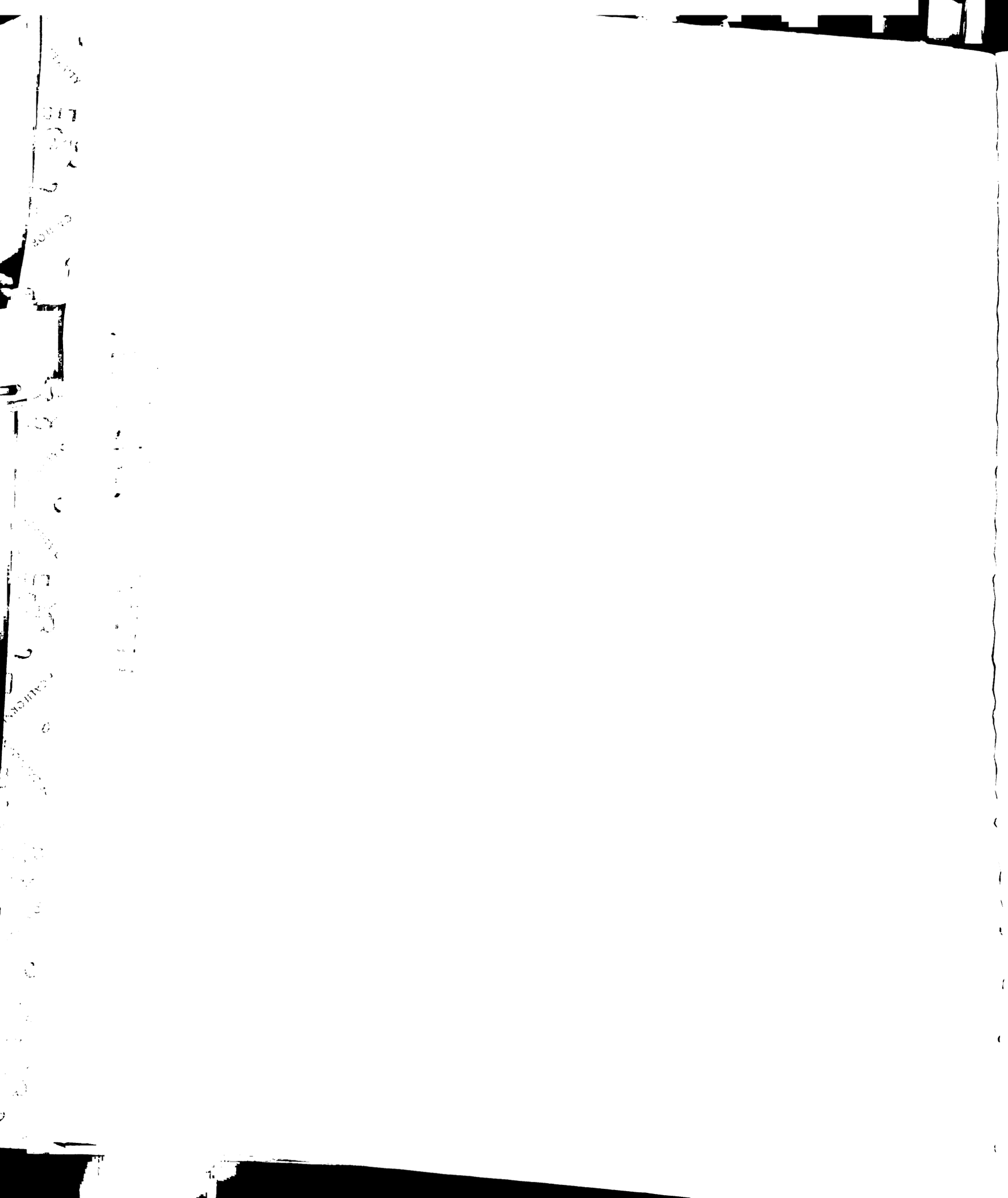

We tested whether this pattern of ISI dependence would also exist for longer trains of stimuli. Additional forms of short-term synaptic plasticity take effect during train stimulation; most notably, accumulation of residual calcium over successive stimuli of a train is thought to recruit vesicles from reserves into the releasable pool (Zucker and Regehr, 2002). For trains at an ISI of 100 ms, mutant cells respond with significantly lower amplitude than wildtype throughout the train. For trains at an ISI of 50 ms, mutant synapses show initially normal responses for the 2nd and sometimes the 3rd pulse, as predicted by the PPR analysis, but are significantly depressed for all subsequent pulses (Fig. 3B). Taken together, our analysis of short-term plasticity demonstrates that *blu* mutant retinotectal synapses are depress at high RGC firing rates (ISI < 400 ms).

What is the mechanism for this reduced ability to transmit at high firing rates? As discussed above, short-term depression is conventionally attributed to the depletion of the readily releasable pool of vesicles. This mechanism alone in insufficient to account for our data, since *blu* mutant synapses give normal responses to the second of a pair of stimuli at the shortest ISIs tested. To explain this result, we propose two kinds of mechanisms, both of which we conceive as compensations for the reduction in vesicular glutamate concentration at these synapses. One class of mechanisms is that *blu* mutant synapses have boosted facilitation which works only for the most rapid of paired stimuli, and which is itself depleted by long trains of rapid action potentials. This might arise for instance by an enlargement of the pool of vesicles recruited for release by the temporal summation of calcium influx during rapid firing. Another possible mechanism to boost facilitation would be if the molecular machinery governing the recruitment of reserve pool vesicles into the releasable pool (thought to be calcium-dependent) (Stevens and

Wesseling, 1998) has increased sensitivity in *blu* mutant synapses. The other kind of mechanism we have considered is that *blu* mutants show short term depression due to retardation of vesicle filling. If, as we argue above, vesicles at RGC synapses contain fewer vesicular glutamate transporters, we would expect not only for the steady state concentration to be reduced, but filling should also be slower (Gasnier, 2000). This retarded filling could cause the observed short term depression phenotype if the responses to repeated stimuli require the exocytosis of recently recycled vesicles which have not yet had time to fill completely. In this scenario, the refilling of vesicles becomes a rate-limiting step for rapid transmission in *blu* mutants. To account for the absence of a phenotype for paired pulses at the shortest ISIs tested, we would postulate a refractory period during which recently recycled vesicles are not competent for release. The deficit for trains of stimuli at short ISI after the 3rd or 4th pulse would reflect the release of vesicles recycled more than one pulse previous. Whatever the mechanism, this phenotype renders these synapses deficient at transmitting information when visual stimuli evoke high firing rates (Fortune and Rose, 2001; Tsodyks and Markram, 1997). In the fourth chapter of this thesis, we describe experiments in which we test visual responses to stimuli predicted to evoke high firing rates from RGCs. In the next chapter, we will present the effects of the *blu* mutation on the arborization of RGC axons.

METHODS

Electrophysiology

For all experiments, mutants were obtained from a cross of two heterozygotes. Wild-type siblings were used as controls. Larval fish at 5-8 dpf were anesthetized with saline containing 0.02% MS222, secured by insect pins to a sylgard-coated dish, and incubated in the recording medium containing (in mM): 134 NaCl, 2.9 KCl, 2.1 CaCl2, 1.2 MgCl2, 10 HEPES, 10 glucose (pH 7.6). The skin over the brain was removed and the brain was split open along the midline to expose the inner surface of the tectum. Experiments were performed at room temperature and the bath was constantly perfused with fresh recording medium, which contains 0.015 mM d-tubocurarine to prevent muscle contraction. Tectal cells were patched under visual control. The micropipettes were made from borosilicate glass capillaries (Kimax), had a resistance in the range of 7-10 MΩ. For perforated patch recording, the recording pipette was tip-filled with internal solution and then back-filled with internal solution containing 200 μg/ml amphotericin B. The internal solution contained (in mM): 110 K-gluconate, 10 KCl, 6 NaCl, 2 MgCl2, 1 CaCl2, 10 HEPES and 10 EGTA (pH 7.4). For whole-cell recording, the internal solution contained: 110 K-gluconate, 10 KCl, 6 NaCl, 1 CaCl2, 10 EGTA, 10 HEPES, 3 ATP.Mg and 0.3 GTP. To record mEPSCs, only whole-cell recording was applied and only 5-6 dpf fish were used for consistency. Recording was made with a patch clamp amplifier (Axopatch 200A; Axon Instruments). The whole-cell capacitance was fully compensated and the series resistance was compensated by 70-75% (lag 60 μs). Signals were filtered at 2 kHz and sampled at 10 kHz using Axoscope software (Axon Instruments). To record

evoked EPSCs, electrical stimulation (0.5 ms, 3-20V voltage step) of RGC fibers was achieved through a glass electrode with 4 μm opening that was placed on the retina close to the optic nerve head, after removal of the lens. To ensure that the evoked EPSCs are monosynaptic, only responses with a delay of onset of less than 5 ms were selected for analysis. All drugs were from Sigma..

Figure 2, Smear et al.

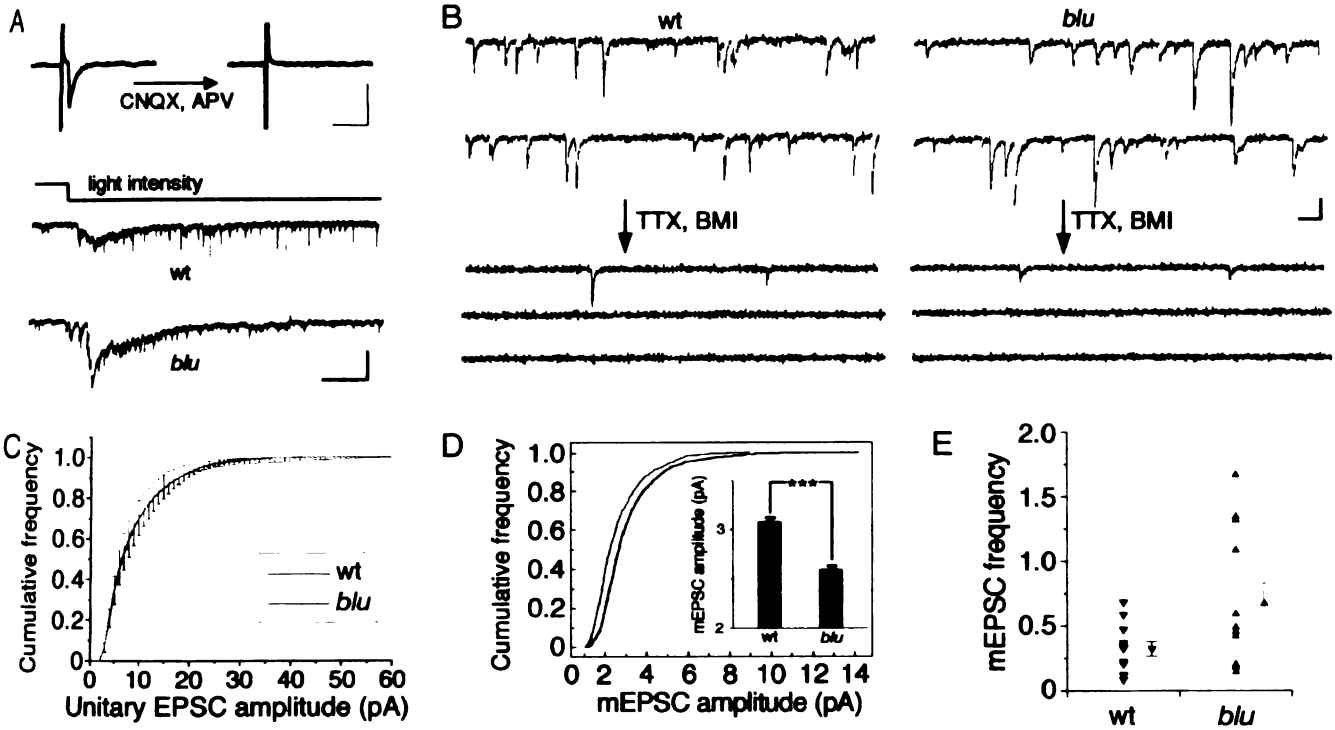

Figure 2. Properties of retinotectal synaptic transmission in blu mutants. **A**, Top, synaptic responses evoked by electrically stimulating optic fibers before and after application of CNQX (10 μM) and D-APV (25 μM) to the tectum. Scale: 10 pA, 20 ms. Bottom, example tectal cell responses elicited by whole field dimming stimulus. The time course of change in the light intensity was represented by the trace on top. Scale: 20 pA, 1 sec. **B**, Example traces of continuous recording of synaptic currents in tectal cells under constant ambient light before and after application of TTX (500 nM) and BMI (10 μM). Most of the recorded spontaneous events are glutamatergic currents according to their kinetics, and reflect action potential-dependent release of retinotectal synapses, since the frequency of miniature EPSCs recorded after TTX and BMI application is much lower. Scale: 5 pA, 50 ms. **C**, Average cumulative frequency of the amplitude of unitary EPSCs, which were identified as single isolated EPSCs during continuous recording of spontaneous currents as shown in B and largely reflect activation of single RGC inputs. Cumulative frequency curve was first made for each cell, and then averaged within the group. Bin size = 1 pA. Wt, n = 16 cells; *blu*, n = 14 cells. **D**, Cumulative distribution of mEPSC amplitudes. 100 mEPSC events were randomly chosen from each cell and then the cumulative frequency curve was plotted for the pooled 1,400 events (n = 14 cells in each group). Two groups are significantly different (P <0.001, Kolmogorov-Smirnov test). Inset, average amplitude of mEPSCs. Bars are s.e.m. ***P <0.001, t-test. Black, wt; red, *blu*. **E**, Frequency of mEPSCs. Triangles on the left in each group represent the average mEPSC frequency measured in individual cells. The average value in the group was shown by the triangle on the right, with bars representing s.e.m. The difference is significant (P < 0.05, Kolmogorov-Smirnov test); n = 14 cells in each group.

Figure 3, Smear et al.

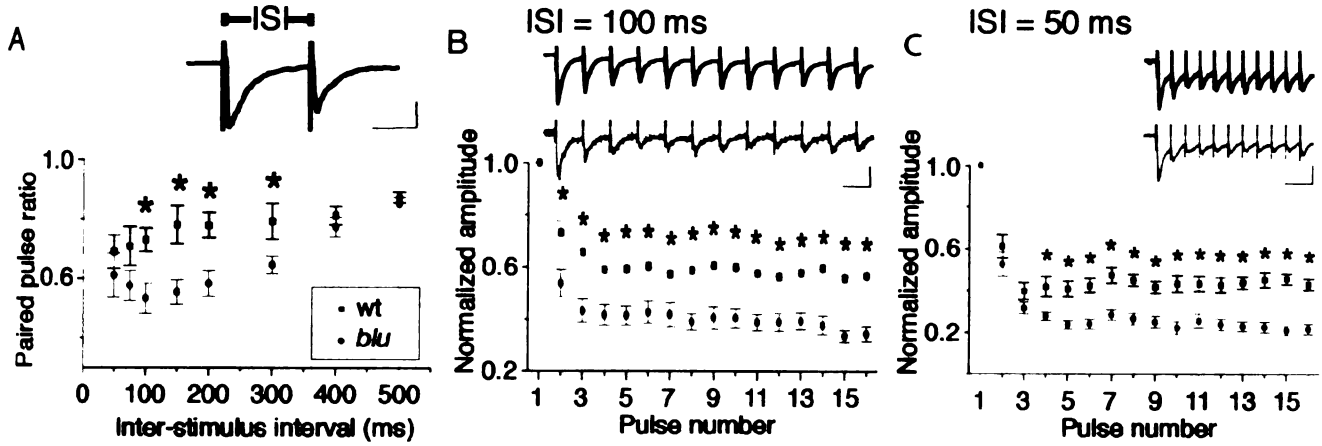

Figure 3. *blu* mutant synapses transmit deficiently at high stimulation rates. **A**, Average paired pulse ratio (amplitude of 2nd response / 1st) at different ISIs. *P < 0.05. n = 10 cells in each group. Inset, example response to paired pulse stimulus. Scale: 20 pA, 50 ms. **B**, Left, dynamics of synaptic strength during train stimulation. The ISI was 100ms. The amplitudes of EPSCs were normalized to that of the first response and averaged according to the number of pulses in the train. Bar: s. e. m. Black, wt (n = 15); red, *blu* (n = 15). *P <0.05, t-test. Inset, example responses recorded from a *blu* mutant (red) and a wild-type (black) sibling fish. Scale: 20 pA, 100 ms. Right, similar presentation except that the ISI was 50 ms. Wt, n = 10; *blu*, n = 12.

Chapter 3: Retinotectal axon arbors are enlarged in the *blu* mutant, suggesting homeostatic compensation

The projection of the retina to its primary midbrain target, called the optic tectum in fish, amphibians, and birds and the superior colliculus in mammals, is arguably the best-studied topographic projection. By virtue of the radial connections leading from the photoreceptors through the inner nuclear layer, retinal ganglion cells (RGCs) form a representation that recapitulates the spatial order of the image formed at the photoreceptor layer (Wassle and Boycott, 1991). RGCs in turn project their axons to various brain areas, including the optic tectum. Once in this area, axons must migrate to and form synapses in topographically appropriate regions of the optic tectal neuropil. In all vertebrate species, RGC axons arrange themselves such that axons from nasal (anterior) retina project to posterior tectum, temporal (posterior) retina to anterior tectum, dorsal retina to lateral (ventral) tectum, and ventral retina to dorsal (medial) tectum (Stuermer, 1988). Interestingly, different species differ markedly in the sequence of events leading to a topographically accurate projection. In mice and chicks, ingrowing RGC axons extend far beyond their topographically appropriate termination zone, and these projections become accurate by an extensive process of interstitial back-branching and refinement (Hindges et al., 2002; Nakamura and O'Leary, 1989). Contrastingly, in frogs and fish, retinal axons grow to their appropriate position much more directly (Kaethner and Stuermer, 1992; O'Rourke and Fraser, 1990). In comparison to frogs, the initial targeting of zebrafish retinal ganglion cell axons is quite accurate, requiring little if

any refinement. It is noteworthy that the rule seems to be that the smaller the tectum, the more accurate the initial projection.

Sperry's pioneering embryological experiments in the regenerating retinotectal projection in newts and frogs remain fundamental to our understanding of topographic mapping. Sperry (1943) showed that regenerating RGC axons grow back to their original positions in the tectum even after eye rotation. Strikingly, this rotated remapping also rotates the animal's visual representation – after eye rotation the frog makes behavioral responses as though the world had rotated. Sperry's work inspired him to propose the chemoaffinity hypothesis, which stated that projecting axons read molecular cues on target neurons, determining the specificity of their connections. Sperry further proposed that these cues might be arranged in complementary gradients, which would identify corresponding positions in the retina and the tectum (Sperry, 1963).

Sperry's ideas have been borne out by later work. Innovative *in vitro* assays developed by Bonhoeffer and colleagues demonstrated that growing RGC axons indeed had differential affinity for tectal membranes harvested from different parts of the tectum (Walter et al., 1987). It was shown that this differential affinity was mediated by graded repulsiveness (Baier and Bonhoeffer, 1992). Later work showed that EphA receptors are expressed in a nasotemporal gradient by RGCs, and their ligands, the Ephrin-As, are expressed in a complementary rostral-caudal gradient in the tectum (Cheng et al., 1995; Drescher et al., 1995), as predicted by Sperry (Sperry, 1963). Heterologous expression of Ephrin-As mimics the repulsive activity of tectal membranes (Drescher et al., 1995; Nakamoto et al., 1996). Loss of function studies showed that these molecular cues were necessary for mapping of the retinotectal projection (Feldheim et al., 2000; Frisen et al.,

1998). It has thus been shown that interactions between different subtypes of Eph receptors and Ephrin ligands are largely responsible for tectal mapping along the anteroposterior and dorsoventral axes of the tectum. The ephrin system has also been shown to play a central role in the mapping of various other projections.

And yet, while the Ephrin system clearly plays a central role in retinotectal mapping, some retinotopy remains in the tecta of the various Ephrin ligand knockout mice, suggesting that retinotectal mapping involves more than just a matter of projecting to the appropriate position on the gradient. The residual retinotectal mapping in the mouse mutants may well be due at least in part to the presence of other graded molecular cues. And yet there is substantial evidence to suggest entirely different mechanisms guiding the formation of the retinotectal map. In the regenerating frog and fish retinotectal projection, ablation of large chunks of the retina prior to reinnervation results in a complete innervation of the tectum by the remaining RGCs' axons (Schmidt and Easter, 1978). Axons thus expand their termination zones despite the fact that according to the absolute levels of a graded guidance cue, axons should only project to positions to which they would project in the presence of a complete cohort of RGC axons. Conversely, partial elimination of the tectum results in a compressed topographic map (Schmidt, 1985; Udin and Gaze, 1983), which again cannot be explained by simple gradient matching of a graded cue. And yet while more sophisticated models of Ephrin signaling may be able to account for these embryological results (Brown et al., 2000a; McLaughlin and O'Leary, 2005), the following embryological experiment most clearly demonstrates the insufficiency of graded cues to explain all aspects of retinotectal map formation.

In frog tadpoles and fish, each tectal lobe receives monocular retinal input, all from the contralateral eye. Constantine-Paton and colleagues demonstrated that when a third eye is grafted onto the frog embryo, this extra eye projects its RGC axons into a tectal lobe together with one of the normal eyes (Constantine-Paton and Law, 1978). The projection of RGCs within a dually-innervated tectal lobe reveals a striking and highly informative pattern. The axons from the two eyes segregate into a pattern of "eye-specific bands": alternating regions receiving input from one eye or the other. The RGC axons from the two eyes should not differ molecularly, but they are differentiated in their activity patterns. This supports the idea that retinotectal mapping is guided by Hebbian mechanism whereby correlated input activity promotes synapse stabilization and uncorrelated activity produces synapse elimination (Hebb, 1949; Stent, 1973). The three-eyed frog experiments argue strongly that Hebbian mechanisms of segregation *can* work in the retinotectal projection, but this does not suffice to demonstrate that Hebbian mechanisms actually *do* play a role in normal development. The activity patterns of the two sets of RGCs dually innervating an experimental tectum will fire in patterns that are essentially completely decorrelated, whether the firing is visually evoked or spontaneous. In a normal eye, spontaneous activity and visually evoked activity will be decreasingly correlated with increasing retinal distance, but it is not clear that these patterns will be sufficiently decorrelated to segregate RGCs at the scales relevant for refinement within the retinotectal map.

Studies of the role of activity in the developing retinotectal projection have utilized pharmacological manipulations, and more recently genetic manipulations. Blocking neural activity with the sodium channel blocker TTX reduces the accuracy of retinotopic

mapping (Gnuegge et al., 2001; Reh and Constantine-Paton, 1985). Similar results are obtained in experiments in which transmission via NMDA channels is blocked by specific blockers APV or MK-801 (Cline and Constantine-Paton, 1989; Schmidt et al., 2000). While these results have been interpreted to support the role of Hebbian mechanisms in topographic refinement, the fact that these manipulations reduce transmission through all the tectum's inputs is also consistent with another interpretation.

Another mechanism which may explain these results is synaptic homeostasis, the strengthening or weakening of a connection in response to a deviation from a set point of activity. Synaptic homeostasis has been described in synapses as diverse as Drosophila neuromuscular synapses (Marek and Davis, 2003), hippocampal neurons *in* vitro (Burrone and Murthy, 2003), and cortical neurons *in vivo* (Turrigiano and Nelson, 2004). While synaptic homeostasis has not yet been prominently studied in the retinotectal system, it seems likely to play an important role in maintaining the appropriate strength of the connection from the eye to the tectum.

So, while it is clear that neural activity plays an important role in the morphological development of axonal arbors (Gnuegge et al., 2001; Hua et al., 2005; Ruthazer et al., 2003; Schmidt et al., 2000), very few studies have tested how partial reduction of synaptic transmission, as opposed to complete blockade, influence the mapping of retinotectal connections. The modest deficit in pre-synaptic release that we have discovered in *blu* mutants allowed us to address this question.

Results

We wanted to examine the fidelity of retinotopy in the retinotectal projection of *blu* mutants. Previous results had shown that small groups (10-100) of RGC axons in *blu* mutants arborized over a larger than normal area. We wanted to test whether this phenotype was attributable to an expansion of individual RGC axon arbors. We first attempted to label single RGCs with the carbocyanine dyes, diI and diO, as had been done in previous studies (e.g., (Kaethner and Stuermer, 1992; Schmidt et al., 2000). While labeling groups of RGCs was not difficult, dye labeling of individual RGC arbors never worked in our hands.

As an alternative, we developed strategies for expressing the green fluorescent protein (GFP) in RGCs. A former student in the lab, Tobias Roeser, had engineered a membrane-targeted GFP, and cloned it into a plasmid downstream of a 6 kb upstream sequence of the *brn3c* gene, which drives expression in RGCs (Xiao et al., 2005). Injection of this plasmid into blastomere-stage zebrafish gives mosaic expression, primarily in RGCs and hair cells (Tokuoka et al., 2002). Lines of fish transfected stably with this construct express the transgene in ~50% of RGCs, which project to a specific subset of the zebrafish retina's 10 arborization fields (Xiao et al., 2005). Interestingly, in the tectal neuropil the transfected cells project to only one of the 4 layers which receive retinal input (Xiao et al., 2005). The transient transgenesis technique gave a small number of individually-resolvable RGC axon arbors. We later adopted another technique, single-cell electroporation of the *Brn3c:mGFP* transgene into the retinal ganglion cell layer (Haas et al., 2002; Hua et al., 2005), with which individually-resolvable RGC arbors can be obtained with much greater efficiency.

We performed all imaging *in vivo,* on unanesthetized 7 dpf fish embedded in agarose. Fish with individually RGC arbors (n = 22 wild-type and n = 11 mutant) were imaged on a laser-scanning confocal microscope (Fig. 4A). Confocal stacks were analyzed morphometrically using Object-Image by an investigator blind to the genotype, similar to previous studies (Tokuoka et al., 2002) (Fig. 4B). Arbors were traced by advancing through the image stack, mouse-clicking along all branches back to the first branch point. We calculated branch number and total branch length by counting the branches in the tracing and totaling up their length. We then obtained the coverage area of the arbor by drawing a convex polygon around the tracing of the arbor after the tracing had been rotated to a plane parallel to the tectal neuropil. Since the arbors are essentially two-dimensional this was defined as the plane in which the arbor had maximal coverage area.

Our morphometric measurements show that *blu* mutant arbors are significantly increased in their total branch length (t-test, $P < 0.05$) and in their coverage area ($P < 0.01$) (Fig. 4C-E). The difference in the number of branches did not reach statistical significance in our sample ($P = 0.25$). Such a change could account to the greater spread of groups of arbors observed previously (Trowe et al., 1996). Furthermore, enlarged arbors may, at least in part, account for the grossly normal evoked EPSCs and for the increase in mEPSC frequency described in the last chapter. The expansion in RGC arbor size in *blu* mutants is likely to be accompanied by an increase in presynaptic active zones. Since synapses in *blu* mutants are weaker than normal, as evidenced by the reduction of mEPSC amplitude, such an increase in the number of synapses would have the effect of compensating for the weakening of individual release sites.

Extensive studies of the role of neural activity in the formation of the retinotectal map suggest several candidate mechanisms for the enlarged RGC axon arbors in *blu* mutants. One possibility is that the mechanism is cell-autonomous. Perhaps RGCs auto-regulate their growth by monitoring their own glutamate release (Kreibich et al., 2004). Since glutamate plays such an important role in intercellular communication, a more interesting mechanism would be non-cell autonomous, of which there are several possibilities. Possibly the most prevalent idea for how activity shapes topographic map development is Hebbian refinement. According to this line of thinking, inputs compete for target space on the basis of their activity patterns (Cline, 2003; Stent, 1973). Another way in which neural activity is thought to influence development can be subsumed under the heading of synaptic homeostasis (Burrone and Murthy, 2003; Marek and Davis, 2003). Evidence from a wide variety of systems demonstrates that synaptic circuits respond to perturbations of their normal activity levels by making changes that counteract the perturbations.

How do we distinguish between these possibilities? Since the *blu* mutant synaptic transmission phenotype acts uniformly across the RGC population, any of the mechanisms listed above could explain *blu* mutants' enlarged arbors. However, the different mechanisms predict different outcomes for a situation in which different arbors differ in their activity level. Fortunately, there exists a technique that can engineer such a situation: chimera analysis. We can thus determine how a single mutant RGC's axon arbor will develop when in the context of an otherwise completely wildtype tectum, and wildtype arbors in the context of an otherwise completely mutant tectum. By transplanting small groups of cells between blastula-stage embryos of different genotypes

(Ho and Kane, 1990), targeting the donor cells to the host blastula in the field fated to become the eye (Woo and Fraser, 1995), we can obtain small donor clones, some of which will give rise to RGCs with individually resolvable axon arbors.

What predictions do the different mechanistic models make for arbor size in the different chimera combinations? The cell-autonomous model predicts that the context is unimportant to the arbor's size. Thus wildtype arbors will be normal sized and *blu* mutant arbors will be enlarged, whatever the host genotype. The two leading non-cell autonomous models, competition and homeostasis, make different predictions for the different chimera combinations. The competition model predicts that wildtype donor arbors in a *blu* mutant host will be larger, since they release more glutamate and excite postsynaptic tectal neurons more than the surrounding *blu* mutant arbors. Arbors from *blu* mutants in a wildtype host, on the other hand, are predicted to be smaller than wild-type arbors, since they excite postsynaptic tectal neurons less than surrounding wildtype arbors.

For these experiments donor embryos were obtained from a cross of *blu* heterozygotes, both of which were homozygous for the *Brn3c:mGFP* transgene described above. Host embryos came from a cross of *blu* heterozygotes. Thus, donor RGCs would express mGFP. In order to visualize other donor-derived cells, donor embryos were injected with biotin-dextran prior to transplantation. Biotin-dextran injected at the 1-cell stage remained concentrated enough over the course of development to be quite visible even at 7dpf when imaging was performed. To be included in the analysis, GFP-positive arbors had to project into the tectal neuropil and not overlap with any biotin-dextran positive processes, whether they be GFP-negative RGCs or neuritis belonging to tectal

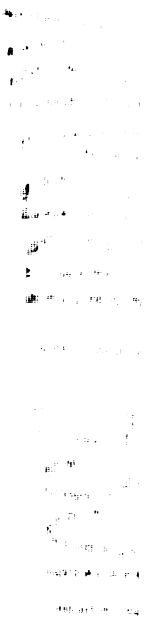

neurons. Morphometric measurements were made as above. The investigator doing the measuring was blind to donor genotype. Donors embryos were fixed after transplantation, and were genotyped by a mismatch RFLP-PCR strategy.

In both *blu* ➜ wildtype chimeras (n = 9) and wildtype ➜ *blu* (n = 10) chimeras, donor RGC axons had normal sizes and morphologies, similar to untransplanted wild-type axons or wild-type ➜ wild-type chimeras (n = 11) (Fig. 5). *blu* ➜ *blu* chimeras were not encountered in our transplantation experiments. The finding that *blu* mutant axons are of normal size in a wildtype host rules out a cell-autonomous mechanism for the enlarged axon arbors. Our transplant data also suggest that the differences in activity levels observed here between mutant and wildtype are too subtle to be able to skew the competition between neighboring axons for target territory. Instead, our data are consistent with a mechanism in which the postsynaptic cell stimulates presynaptic arbor growth until some set point of postsynaptic activity is reached. We account for the normal sized arbors in wildtype ➜ *blu* chimeras by proposing that a single wildtype arbor evokes sufficient activity to reach the set-point. Such a homeostatic mechanism, in which the presynaptic arbor grows in order to make room for more synapses, may explain the strong residual glutamatergic transmission despite the reduction in quantal amplitude.

Discussion

The synaptic deficits in the *blu* mutant compromise the precision of the retinotectal map. During embryonic development (in zebrafish beginning at 2 dpf), RGC axons project into the superficial layers of the contralateral tectum in retinotopic order, i. e., preserving the neighborhood relationships of their cell bodies in the retina (Johnson and Harris, 2000; McLaughlin et al., 2003a; Schmidt and Buzzard, 1990). In *blu* mutants,

previous DiI labeling studies had shown that, while coarse retinotopy was intact, the termination zones of small groups of RGC axons appeared more dispersed in the tectum (Baier et al., 1996; Trowe et al., 1996). By single-axon tracing, we were able to attribute this multi-axon phenotype to the expansion of individual arbors.

The fidelity of the retinotopy of the retinotectal projection depends on two factors: arbor size, how much of the map the projection of a single RGC covers, and arbor scatter, how well the ordering of the arbors of different cells preserves their arrangement in the retina. Because arbors cover greater area in *blu* mutants, we can say that the fidelity of the retinotectal map has been compromised. We investigate the functional consequences of blurred retinotopy in the next chapter. We did not measure arbor scatter in our experiments for technical reasons. Measuring arbor scatter would require measurements not only of the positions of arbors in the tectum, but also the positions of labeled cell bodies in the retina. Measuring cell body position in the retina is difficult, because of the larval eye's small size and pigmentation. In larger animals, it is commonplace to cut open and flatten the retina (Brown et al., 2000a), but because of the small size of the larval zebrafish eye, we were unable to successfully use this technique. It is possible to block the synthesis of pigment pharmacologically with PTU, but this treatment has severe effects on vision (Page-McCaw et al., 2004), and may thus perturb activity patterns and levels in the RGCs. Indeed, PTU treatment seems to have a significant effect on arbor size (T. Xiao, personal communication). So, even without measuring axon arbor scatter in the retinotectal map, because RGC axon arbors are nearly twice as large as normal, we can say that the fidelity of retinotopy is reduced in *blu*

mutants. If anything, an effect on arbor scatter is likely to make retinotopy even less precise than the effect on arbor size clearly already does.

We performed chimera analysis to investigate the mechanistic basis for the enlarged arbors in *blu* mutants. The larger arbors could result either from a lack of activity-dependent pruning, which is thought to depend on competitive interactions with neighboring axons (Hua and Smith, 2004; Ruthazer et al., 2003), or from homeostatic growth in response to lowered synaptic activity (Burrone and Murthy, 2003; Marek and Davis, 2003), or from a direct effect of the lack of glutamate on axon growth (Kreibich et al., 2004). By transplantation of single *blu* cells into a wildtype host, we showed that mutant RGC arbors were normal-sized when surrounded by wildtype axons. Conversely, wildtype axons transplanted into a mutant environment formed normal-sized arbors.

These results do not conform to the predictions of any the simplest models sketched above, and are perhaps most informative for the possible models they eliminate. We can rule out a cell-autonomous effect of reduced vesicular glutamate uptake on arbor growth. For instance, we can eliminate the possibility that *vglut2a* might have some role in intracellular glutamate trafficking unrelated to synaptic transmission, which might somehow result in enlarged arbors. We can also rule out the idea that an axon might sense the amount of glutamate released by its own terminals and adjust its arbor size accordingly.

Our data also invalidates to the prediction of a competitive model in which relative activity levels determine arbor size. Our findings complement those of Hua et al. (2005), who interfered with the activity of individual or small numbers of RGCs and found

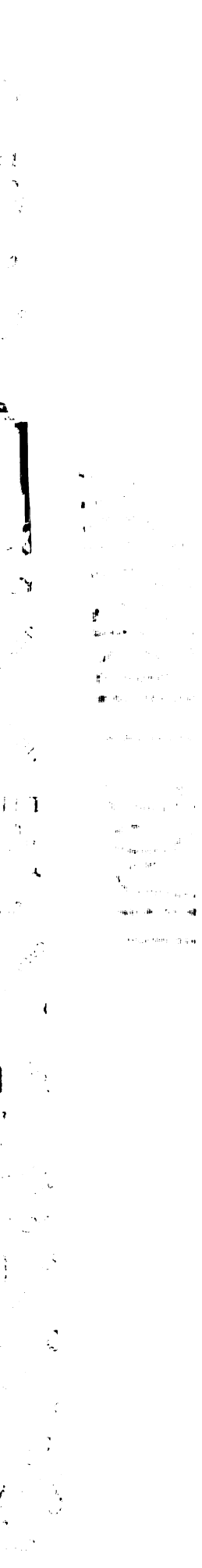

evidence for a role of activity in regulating axon arbor growth. In their study, activity was blocked by expressing either a potassium channel (Kir2.1), which hyperpolarizes cells and prevents them from reaching firing threshold, or a dominant negative VAMP (VAMPm), which impedes vesicle fusion. The result was that inactive axon arbors were smaller than those of active axons, suggesting they were at a competitive disadvantage when surrounded by normally active neighbors. The effect of activity on axon arbor size was not detectable when all axons were uniformly inactivated by the sodium channel blocker tetrodotoxin (Hua et al., 2005), similar to earlier findings in zebrafish larvae (Gnuegge et al., 2001; Stuermer et al., 1990). In contrast, we see that Vglut2a-deficient arbors are larger when surrounded by other mutant axons, and are normal-sized when surrounded by wildtype axons. One difference between the effects of the *blu* mutation and those of Kir2.1 (or VAMPm) overexpression is the degree of blockage. While Kir2.1 is likely to completely inhibit spiking, and VAMPm is likely to abolish synaptic exocytosis, the perturbation caused by absence of Vglut2a is much milder. Another notable difference between the two experiments is the cellular process that was inhibited: Hua et al. (2005) impeded synaptic transmission upstream of the *blu* mutant's defect in vesicular glutamate uptake, while excitability and exocytosis should be normal, or nearly so, in *blu* mutants.

Our results, taken together with those of Hua et al. (2005), suggest that neural activity may sculpt RGC axon arbors through both competition and homeostasis. Note that our findings eliminate the possibility that small differences in release can skew competition for synaptic space, but do not rule out a role for activity pattern-based competition. Indeed, Hebbian models of refinement are based on the correlation between

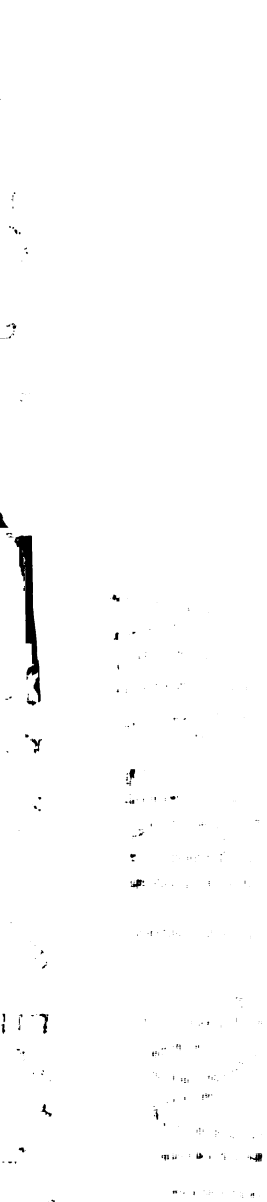

the firing of pre- and post- synaptic cells. Activity patterns in our chimeric animals should not differ from that in a wild-type animal. Rather, it is only the transfer of those activity patterns via glutamate release that should differ between donor cells and the host cells surrounding them. The perturbations used by Hua et al. (2005) not only introduced absolute differences in activity *levels* – by effectively silencing the synaptic output of transfected RGCs, they have changed the activity *patterns* of transfected RGCs, albeit in an extreme way. Interesting in this regard is recent work in mouse mutants deficient for the beta2-adrenergic acetylcholine receptor (McLaughlin et al., 2003b), which have normal levels of retinal ganglion cell activity but which lack the spontaneous waves of activity that normally propagate across the ganglion cell layer during development (Meister et al., 1995). These mutants show disrupted retinotectal topography, underscoring the importance of activity patterns in map formation. Perhaps the difference between our chimera results and the results of Hua et al. (2005) are not due to the degree of difference in activity levels but rather due to differences in activity patterns. It will therefore be interesting to test the effect on tectal mapping of perturbations that only change patterns and not levels of activity in zebrafish RGCs.

Having disproven the cell-autonomous and competitive models for our findings, we suggest that arbor overgrowth most likely reflects a homeostatic mechanism, in which the postsynaptic cell promotes growth of the presynaptic arbor to compensate for reduced synaptic drive (Burrone and Murthy, 2003; Marek and Davis, 2003). A similar homeostatic mechanism may underlie the enlargement of retinal arbors following treatment with MK-801, a blocker of glutamate receptors of the NMDA-subtype (Schmidt et al., 2000) and a similar effect in *mao* mutants, in which RGCs fail to generate

action potentials after 5 dpf (Gnuegge et al., 2001). According to this model, *blu* mutant axons in a wild-type host may grow to normal size because convergent wild-type RGC inputs evoke a wild-type level of postsynaptic activity. The normal size of wild-type axon arbors in a mutant host, on the other hand, implies that a single wild-type axon can evoke sufficient levels of activity in postsynaptic cells to produce normal growth. This model thus postulates that synaptic activity is monitored by a postsynaptic activity sensor. When activity levels fall below a set point, the activity sensor sends a retrograde signal promoting RGC axon arbor growth. To explain our findings, this sensor must be non-synapse-specific, summing the inputs of multiple RGCs. The putative retrograde signal would then promote arbor growth and synaptogenesis within a localized region.

Since it appears that arbors in *blu* mutants grow more in order to add more synapses, this compensating for the weakened release of individual synapses, it would have been informative to directly count synapses in the tectum to verify whether *blu* mutant arbors do indeed form more synapses. Technical limitations forbade the performance of such experiments. Immunofluorescent detection of presynaptic markers does not work, because the synaptic density in the optic tectal neuropil is so high that individual synapses cannot be resolved and thus cannot be counted (Kay, J.N., Nevin, L.M., H.B., unpublished observations). Presynaptic GFP-fusion proteins have been useful for this purpose in other organisms (Shen and Bargmann, 2003) but the only zebrafish fusion protein of which we are aware, VAMP-GFP (Hua et al., 2005), does not localize to presynaptic puncta, but rather partitions itself diffusely throughout the axon. Furthermore, fluorescent localization to puncta does not definitively prove the presence of a synapse. Any fluorescent method of synapse detection must first be validated by

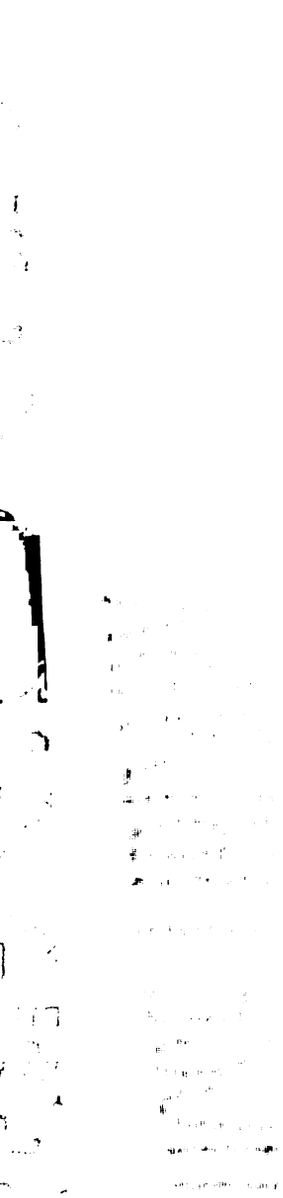

electron microscopy, and to our knowledge no light microscopic methods of presynaptic protein visualization have been thus validated in the zebrafish tectum. So, electron microscopy is the only acceptable method to definitively count synapses, but since our lab is unequipped for this technique, we will need a collaborator to count synapses in *blu* mutants.

Our results show that the fidelity of retinotopy is compromised in *blu* mutant tecta. Mutant RGC axon arbors cover a larger than normal area. Our chimera analysis suggests that this change compensates for weakened synaptic release. This homeostatic change thus represents a tradeoff between accurate mapping and aggregate synaptic strength. As a result, the visual computations performed by neurons in the tectum will be performed upon a less accurate visual input. In the next chapter, we will test whether the reduced accuracy of the *blu* mutant retinotectal projection has functional consequences. We hypothesized that the reduced accuracy of the retinotectal projection should alter the size and/or spatial structure of the receptive fields of tectal neurons. These neurons should consequently have reduced spatial resolution. To test this hypothesis, we performed behavioral tests which challenge the spatial acuity of zebrafish vision.

METHODS

Single axon arbor analysis

To drive GFP expression in RGCs, 6 kb of sequence upstream of the zebrafish *brn3c* gene, a transcription factor expressed in most RGCs, was cloned upstream of the

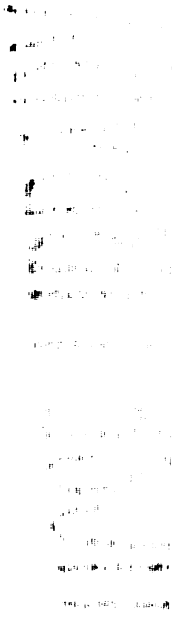

Gal4 transcription factor (Hua et al., 2005; Xiao et al., 2005). The same plasmid contained a membrane-targeted GFP (Kay et al., 2004) under control of the Gal4 upstream activating sequence (UAS). The *Brn3c:Gal4*; *UAS:mGFP* construct was incorporated into RGCs in either of two ways: microinjection into one-cell stage embryos (as above for PAC injection), which results in mosaic expression, and single cell electroporation (Haas et al., 2002; Hua et al., 2005), which consists of passing electrical pulses through a micropipette filled with a DNA solution (1-3 mg/ml in H_2O) inserted into the retina of 2-3 dpf larvae. At 7 dpf, larvae were embedded in 1% agarose and imaged on a Bio-Rad MRC 1024 confocal microscope. To qualify for our analysis, imaged axons had to arborize within the tectal neuropil and had to be traceable back into the optic nerve. Individually resolvable RGC arbors were analyzed using the public domain image-processing application Object-Image (http://rsb.info.nih.gov/). Morphometric measurements were performed by an investigator blind to the genotype of the specimen. Each arbor was traced from its first branch point out to all branch tips. From this tracing, we extracted a measurement of total branch length and the number of branches. The tracing was then projected and rotated to a plane parallel to the tectal neuropil. A polygon enclosing all branches of the arbor was then drawn to measure its coverage area. Comparison of the axons obtained by injection and electroporation revealed no significant difference between the two methods, so their results were pooled for comparison of *blu* and wild type.

Transplantations and chimera analysis

Chimeric embryos were generated as previously described (Ho and Kane, 1990; Woo and Fraser, 1995). Progeny from a cross between two *blu/+;*

Brn3c:mGFP/Brn3c:mGFP carriers were used as donors and non-transgenic *blu/+* progeny were used as hosts. Donors were injected with a solution containing 5% biotin-dextran, 5% rhodamine-dextran in 120 mM KCl at the one-cell stage. At the 1000-cell stage, small numbers of cells were transferred from the vertex of donor embryos (the site of the presumptive eye field) to the vertex of host embryos. Hosts were screened at ~24 hpf, and embryos with small clones of donor cells in the eye were kept for further analysis. At 7 dpf, GFP-expressing donor axon arbors were imaged and analyzed as above by an investigator blind to the genotypes of the chimera. The absence of donor cells in the host optic tectum was verified by absence of rhodamine fluorescence. Host embryos were scored by their VBA phenotype, while donor embryos were genotyped using a mismatch PCR-RFLP strategy, in which a restriction site was added to amplified genomic sequence using a primer containing additional bases adjacent to the site of the *blu* mutation. The primer sequence added an Mbo II site to the mutant allele, which was absent from the wild-type allele.

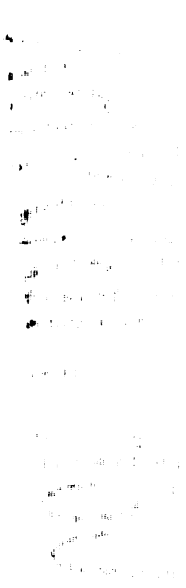

Figure 4, Smear et al.

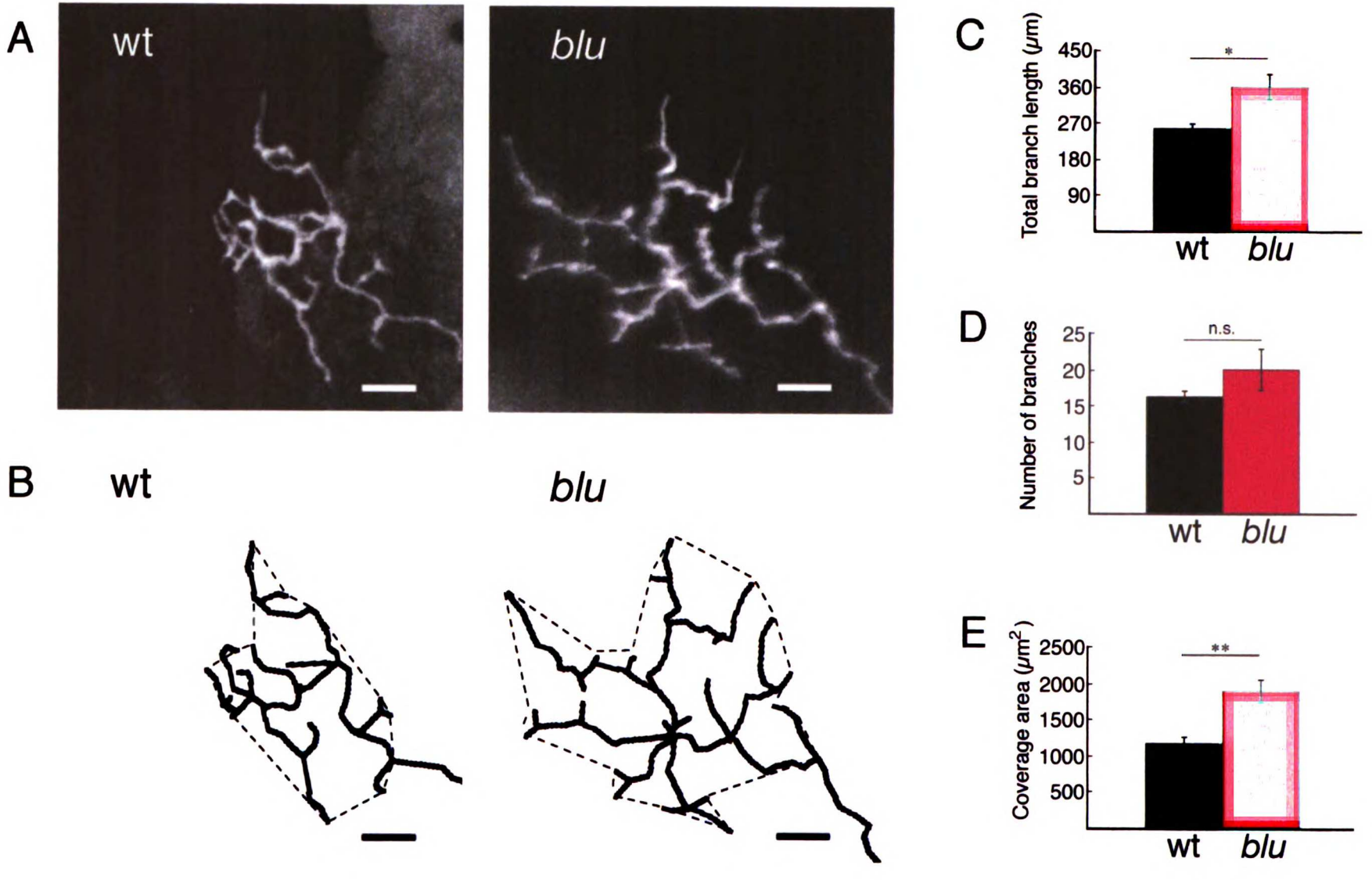

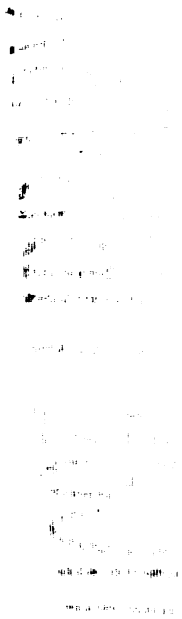

Figure 4. *blu* mutants have enlarged RGC axon arbors. **A,** Confocal projections of GFP-labeled RGC axon arbors imaged *in vivo* at 7 dpf. **B,** Arbors were traced in three dimensions from each branchtip to the first branchpoint of the arbor. Tracings were rotated into a plane parallel to the tectal neuropil and projected. Hatched lines around arbors demarcate the coverage area of the arbor. Scale bar, 10 μm. **C-E,** Quantitative morphometric analysis of RGC axon arbor size reveals that total branch length (C), and coverage area (E) are increased in the mutant, while the number of branches (D) is not statistically different. $*P < 0.05$, $**P < 0.01$. Wt, $n = 22$ cells; *blu*, $n = 11$ cells.

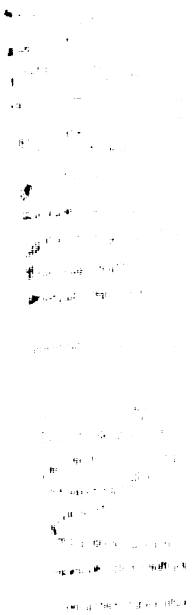

Figure 5, Smear et al.

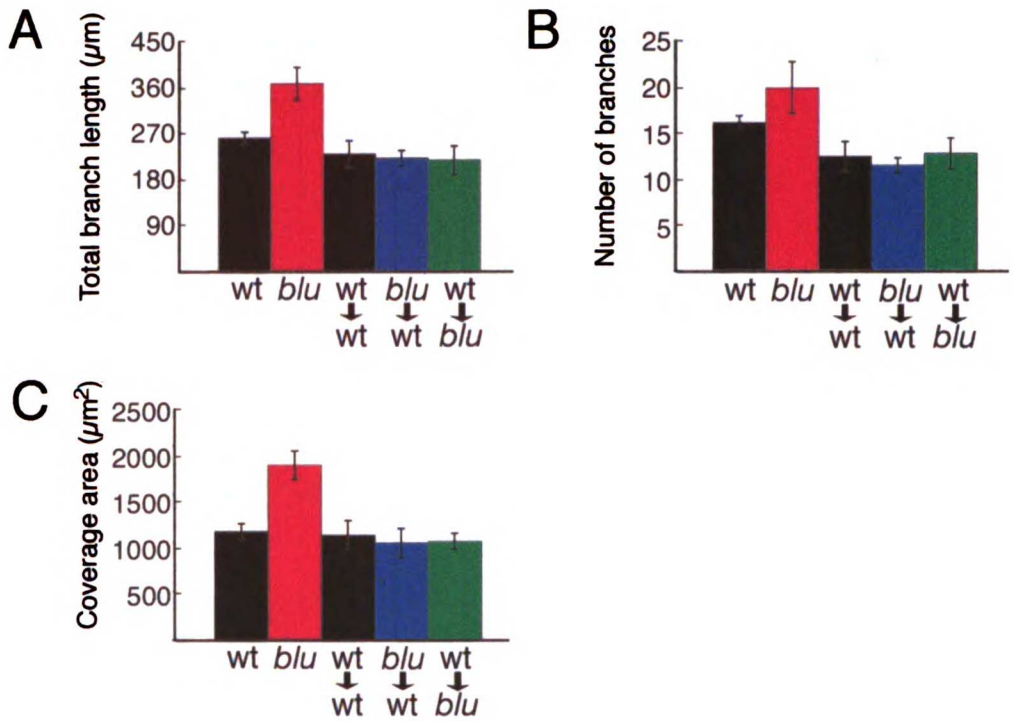

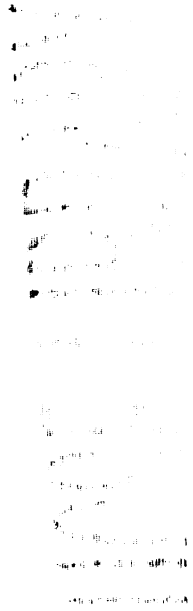

Figure 5. Chimera analysis of RGC arbor morphology. Transplantations were performed at the 1000-cell stage. *Brn3c:mGFP*-expressing donor axons were imaged at 7 dpf and analyzed as in Fig. 4. Wildtype and *blu* data are included for comparison. A, Total branch length. B, Number of branches. C, Coverage area. wt ➜ wt, $n = 11$; *blu* ➜ wt, $n = 9$; wt ➜ *blu* , $n = 10$.

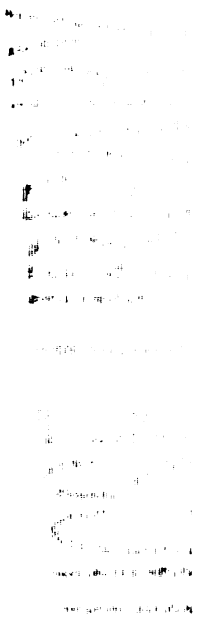

Chapter 4: *blu* mutants have reduced acuity in two visual behaviors

In the first chapter, I showed that *blumenkohl* encodes a vesicular glutamate transporter. In the second, I presented the evidence that *blu* mutants have phenotypes at the retinotectal synapse, most notably an increase in short-term depression, which makes these synapses less efficient at transmitting information when RGCs fire rapidly. In the third chapter, I demonstrated that *blu* mutants have enlarged RGC axon arbors, which reduces the retinotopic fidelity of the tectal map. The physiological and anatomical phenotypes of *blu* mutants should have functional consequences. Poor transmission at high firing rates should reduce the visibility of fast-changing stimuli. Degraded retinotopic mapping should compromise visual acuity. In this chapter, I confirm these predictions using behavioral assays I and others have developed in our lab. Because of the unique nature of these behavioral assays and the central role that the development of these assays has played my thesis work, I will discuss the assays themselves in some depth as well.

One might reasonably question why we have chosen the zebrafish as a model organism for visual psychophysics. The visual system of the zebrafish is not particularly impressive. Their vision is roughly three orders of magnitude less acute than the human's (Kelly, 1979; Rinner et al., 2005). They don't even have a cortex, the structure in which the majority of visual neurophysiologists make their living. So why zebrafish? One would start one's case by listing two of their immediately apparent virtues: small

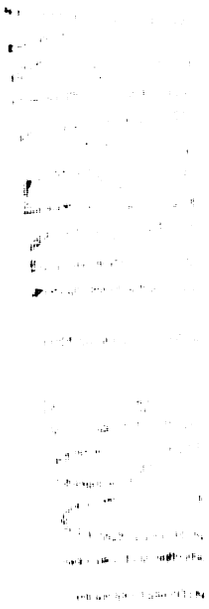

size and optical transparency, which has made them popular among developmental biologists. Another incontestable virtue of the zebrafish is its fecundity. The ease and rapidity with which large numbers of baby zebrafish can be obtained has made it possible to do forward genetic screens. Zebrafish are the only vertebrate species in which forward genetics is really tractable. Also, while it is true that the zebrafish have no cortex, other parts of their visual system, including the retina and optic tectum, bear a strong resemblance to their equivalents in higher vertebrates, certainly more so than the invertebrate species in which forward genetics has traditionally been practiced.

But the primary virtue of the zebrafish for those who are interested in the visual system is their repertoire of visual reflex behaviors. These behaviors have made it possible to show that the zebrafish attains a great deal of visual function remarkably early in development. Just three days after fertilization they are using their sight for numerous tasks. The fact that these behaviors are reflexive is quite a boon to studies of visual function. The animals needn't be trained to show any particular response to a visual stimulus – the outputs of their visual reflexes are hardwired. Thus, in a sense, they're born ready to "tell" us what they can see. The visual behaviors of the larval zebrafish include visual background adaptation, the dorsal light reflex, the optokinetic response, the optomotor response, and prey capture (Easter and Nicola, 1996; Gahtan and Baier, 2004; Neuhauss, 2003; Neuhauss et al., 1999; Orger et al., 2004). I have performed assays for the last two of these behaviors, so I will describe them in detail.

The optomotor response

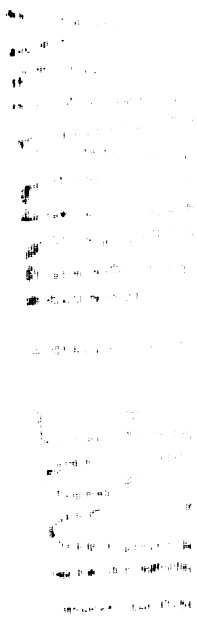

The optomotor response is one of several visual reflexes designed to counter retinal slip (Simpson, 1984). Movement of the animal's body relative to the surroundings makes those surroundings move relative to the eye, thus creating retinal slip, motion of the retinal image. This retinal slip blurs the retinal image, making image features more difficult to detect, and is therefore disadvantageous to the animal. To prevent retinal slip, animals reflexively move their eyes, their heads or, in the case of the optomotor response, their whole body to counter self-motion. Fish have to contend with a particularly important source of self-motion in their environment: water currents. Without the optomotor response, fish would be passively borne downstream, or worse, into the sucking mouth of a predator. In the lab, the optomotor response can be evoked by visual stimuli that occupy most of the visual field (Orger et al., 2000). Because the world appears to move opposite the direction of self-motion, and the optomotor response exists to cancel self-motion, these large motion stimuli evoke swimming in the direction that the stimulus is moving. Thus whether fish swim to follow a given moving stimulus gives a straightforward index of what the fish can see.

Traditional studies of the optomotor response have utilized drums with interior surfaces carrying a stimulus rotating around a circular tank containing the stimulated fish (Rock and Smith, 1986; Springer et al., 1977). Our lab instead uses a CRT monitor placed on its back (screen facing up) atop which sit long horizontal tanks in which fish swim (Neuhauss et al., 1999). Our setup, since it allows the use of computer-generated stimuli, carries the advantage of greater versatility in the stimuli that may be shown. We have developed a system to automate the imaging of the fish as they behave in the assay, and have also automated the subsequent image analysis used to score the performace of

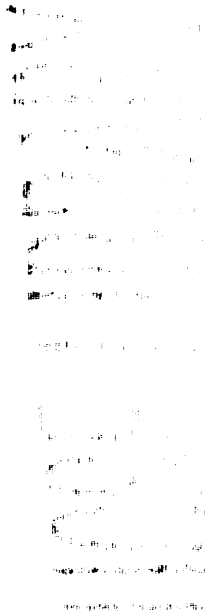

the fish in responding to different stimuli (Orger et al., 2000). The efficiency of this system has allowed us to use the OMR assay as part of the large-scale genetic screen our lab has conducted (Muto et al, in press), which I will discuss briefly below. In addition, it has made it possible for us to conduct sophisticated psychophysical tests, demonstrating that the fish can see second-order motion (Orger et al., 2000), delineating the contribution of different cone types to the optomotor response (Orger and Baier, 2005), and the thorough testing of the spatiotemporal sensitivity function in wildtype and *blu* mutants, which I will discuss in detail below.

We do not know what brain structures are necessary for the OMR. Lesion of the tectum in the adult goldfish had previously been reported to abolish the OMR (Springer et al., 1977). However, our lab has shown that laser ablation of the retinal input to the optic tectum in larval zebrafish spares the OMR (Roeser and Baier, 2003). We thus know that the structure in which we performed the electrophysiological and anatomical analyses described in the previous chapters is not necessary for the tectum. This is a major caveat to our arguments relating the neural phenotypes in *blu* to the OMR deficits described below. Nevertheless, because *vglut2a* is expressed by all RGCs, RGCs that project to central targets aside from the tectum will have similar synaptic and axon arbor phenotypes. Preliminary evidence suggests that laser ablation of one of the pretectal nuclei can block the OMR (Goold, C., HB, unpublished observations).

Prey capture

Animals must feed themselves to survive. For a predator, this entails identifying, tracking, and capturing prey species. The zebrafish larva matures into a predator very

rapidly. At the age of only one week after fertilization and with a body length of less than half a centimeter, readily prey upon live paramecia, by either chasing the prey or by remaining stationary and sucking the prey into their mouths (Borla et al., 2002). Our lab has developed a simple assay to test prey capture in larval zebrafish (Gahtan & Baier, in press). Paramecia are added to a small dish containing a few larvae. At time zero and at intervals thereafter over the course of 1-3 hours, a short movie is captured of the dish. For each movie, the paramecia are counted, and the rate of decline in the number of paramecia is quantified. This gives an index of how well the fish capture prey.

Our lab has previously used this assay to show that prey capture by larval zebrafish is largely mediated by vision. The rate of prey capture is greatly reduced for normal fish in the dark and for blind fish (Gahtan and Baier, in press). Furthermore, tectally-ablated fish perform indistinguishably from blind fish or normal fish in the dark. This indicates that the tectum mediates the visual component of prey capture. In addition, imaging of individual capture events demonstrates in what aspect of prey capture tectum-ablated fish are impaired. Tectum-ablated fish, when a paramecium is near, fail to initiate strikes far more often than normal fish, indicating that they are impaired at detecting prey, rather than being too uncoordinated to strike accurately at prey (Gahtan and Baier, in press). The prey capture assay thus nicely complements the OMR assay in that it directly tests tectal function.

We used these behavioral assays to test hypotheses about the functional consequences of the physiological and anatomical phenotypes described in the previous chapters. The physiological phenotype we thought might have an impact on vision was

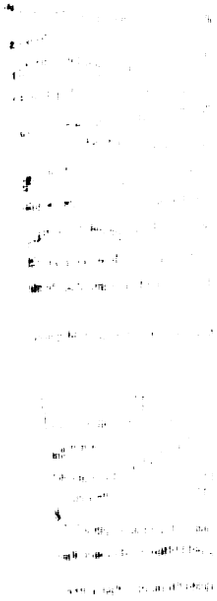

the depression we saw in paired-pulse and train stimulus experiments. We postulated that the inability of *blu* mutants' RGC synapses to fire at normal levels when RGCs are stimulated at high rates would constrain the temporal resolution of vision. What normally sets the temporal resolution of vision? It is thought that phototransduction kinetics set an upper bound to the ability to discriminate events in time (Baylor, 1996). Thus the rate at which the phototransduction cascade can be activated, quenched, and re-activated again sets a temporal sampling frequency for vision. We hypothesized that the *blu* mutant synaptic phenotype might create a bottleneck for the transfer of information at high firing rates. In numerous synaptic circuits, from cortex to the electrosensory system of electric fish, short-term plasticity has been postulated to play a computational role, by boosting certain signals when firing occurs at rates evoking facilitation, and dampening signals when firing rates engender short-term depression (Fortune and Rose, 2001; Tsodyks and Markram, 1997). Thus short-term depression and facilitation can be thought of as temporal filters on synaptic transmission. Short-term depression, in this way of thinking, can be described as a low-pass filter, limiting the transfer of information at high firing rates. The abnormal short-term depression we've observed in *blu* mutants should have this effect – limiting the transfer of information when RGCs fire at high rates.

What makes RGCs fire at high rates? It has long been known that RGCs which linearly sum the luminance within their receptive fields modulate their firing rates at the modulation frequency of sinusoidal stimuli (Hochstein and Shapley, 1976). This finding also holds true for goldfish, the species closest to zebrafish in which physiological recordings from RGCs have been made (Bilotta and Abramov, 1989). If firing rate is directly proportional to stimulus modulation rate, then we would expect RGC synapses in

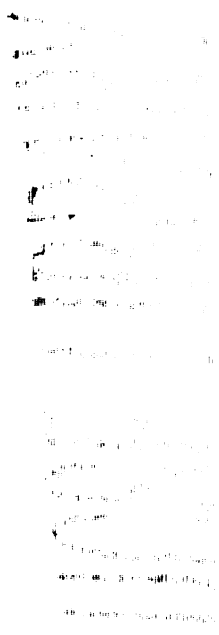

blu mutants to transmit poorly when the animal is stimulated with rapidly-modulated sinusoidal stimuli. Since all visual information must pass through retinofugal synapses to get to the brain and influence behavior we would expect this synaptic phenotype to cause a behavioral phenotype: impaired vision for rapidly-modulated sinusoidal stimuli. Our OMR assay has enabled us to test this hypothesis.

In addition, we hypothesized that *blu* mutants' enlarged RGC axon arbors would have an adverse effect on vision. Visual neurons have receptive fields of a certain size, shape, and spatial structure. The receptive fields of a given neuron can be traced back through the neurons from which it receives synapses, further back through successive synaptic connections, and eventually back to a certain subset of photoreceptors. The portion of the visual field sampled by these photoreceptors defines that neuron's receptive field. In other words, the structure of a visual neuron's receptive field is set by the arrangement of its synaptic inputs (Brown et al., 2000b; Reid and Alonso, 1995). The fidelity of retinotopy of the retinotectal map is reduced in *blu* mutants. As a result, retinorecipient neurons connect back to more of the photoreceptors, spread out over a larger region of the retina. The sensitivity of retinorecipient neurons thus becomes spread over a larger portion of visual space, reducing the responsiveness of these neurons to fine spatial detail. This would in turn reduce the animal's visual acuity. The spatial resolution of vision should depend on the accuracy of retinotopic mapping (Barlow, 1975; Marshall, 1942). We have tested this hypothesis using our assays for the OMR and for prey capture.

Results

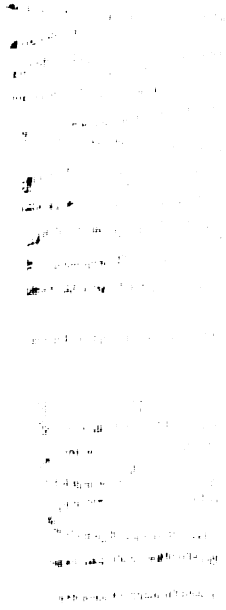

Automating the optomotor assay

When I began in the lab, the optomotor assay consisted of a system for displaying computer-generated stimuli to zebrafish larvae. The larvae swim in long horizontal tanks which spanned the horizontal axis of a CRT monitor. To score the behavior, the experimenter made a subjective judgment of whether the fish were responding (Neuhauss et al., 1999). In collaboration with Michael Orger, I made several improvements to this system. We felt that developing an automated system of scoring the behavior would have several advantages: speed, objectivity, and sensitivity. To do a behavioral screen with this assay, it needed to be fast and reliable. Furthermore, we wanted to use the assay to perform fairly sophisticated psychophysical experiments. The stimuli used in such experiments evoke small and inconsistent responses. An automated system of analysis would permit repeated, quantitative measurements, providing the statistical power needed to ask the questions we wanted to ask.

The optomotor response has several components including orientation to the stimulus and following the stimulus. While the kinematics of optomotor response initiation is an interesting problem in its own right, we chose to disregard this complexity, focusing instead on how much of a response a given stimulus elicited. Since the OMR consists of swimming to follow a visual stimulus, we define the size of a response as how far a fish swims in response to a given stimulus. Furthermore, to take advantage of the fecundity of the zebrafish, we designed our system to test groups of fish, up to 50 per tank. The response is then defined as how much the distribution of the fish in a given tank shifts along the axis of stimulus motion in response to a given stimulus. To make this measurement, we use a consumer-grade digital still camera (Nikon Coolpix), to take

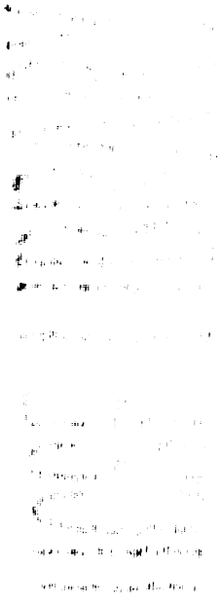

pictures of tanks of fish before an after the stimulus. We analyze these images using macros we wrote in NIH Image, which use the particle analysis feature to determine the position of all the fish in the tanks. This method has allowed us to perform a genetic screen (Orger et al., 2004) (Muto et al., in press), demonstrate that zebrafish can see non-Fourier motion (Orger et al., 2000), determine the contribution of different cone types to the OMR (Orger and Baier, 2005), and test our hypotheses about what visual deficits might be caused by *blu* mutants' neural defects.

A genetic screen for visual acuity mutants

We screened 5,934 crosses from 1,896 ENU-mutagenized F2 families (1 to 8 per F2 family) for mutants with defects in the OMR, in addition to other visually elicited behaviors and morphological defects. Each successful mating yielded a clutch of 10 to several hundred individual larvae, of which up to 50 were subjected to optomotor tests. Fish were generally scored on the seventh day after fertilization (at 7 dpf). Including retests, over 400,000 individual fish were screened in the course of three years. Statistical calculations, taking into account the number of F1 fish used to generate the F2 families, the number of F2 families, the number of crosses for each family, and the number of F3 larval fish, suggest that our screen encompassed 1,688 ENU-mutagenized haploid genomes.

Mutants detected by our assay were kept and tested in subsequent generations. (Table 1). To select against phenotypes with general defects, we discarded mutants with overt developmental problems, as well as those that were poor swimmers, with a few exceptions. Putative F2 carriers were mated at least twice more for confirmation of the phenotype in their progeny, before they were outcrossed. The OMR screen picked up 361

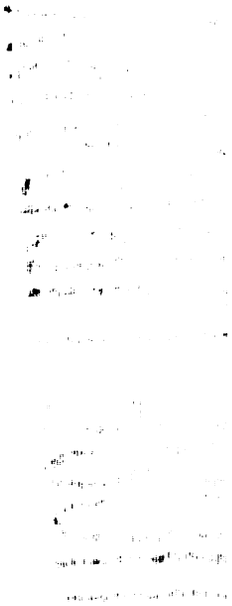

putants, 34 of which (9%) were confirmed and successfully propagated. The initial false-positive rate of this behavioral screen greatly exceeded that of a morphological screen for small-eye mutants carried out in parallel. However, almost all our mutants were recovered in the following generation. Our strategy of extensive re-testing as part of the primary screen therefore dramatically decreased the number of false positives and made this screen practical.

In parallel to the main OMR screen, which was designed to pull out OMR-minus mutants, we carried out screens for visual acuity and color vision. The purpose was to detect mutants with more subtle, stimulus-attribute-specific defects, as we thought these might be likely to result from interesting neural phenotypes similar to *blu*. The cone-isolating stimuli used for the color screen were found to evoke responses that were too small and inconsistent to be useful for screening, so this assay was abandoned. The visual acuity screen utilized a stimulus of relatively high spatial frequency, to sensitize the assay for mutants with spatial acuity deficits. This assay was found to give an acceptably low false positive rate (Table 1). The acuity OMR screen picked up 81 putants. To date, we have continued to maintain eight acuity mutants for at least two generations. However, no progress has been made in identifying the mutant genes or in characterizing additional neural phenotypes. The problem is that the higher spatial frequency stimuli used in this assay, while they can reliably detect mutant clutches, cannot be used reliably to sort mutant larvae from wildtype. Higher spatial frequency stimuli evoke weaker responses than lower spatial frequency stimuli, even in wildtype fish. Thus, when sorting the clutches, a considerable fraction of wildtype fish will fail to respond. No mutant discovered in this screen has a sufficiently strong impairment to

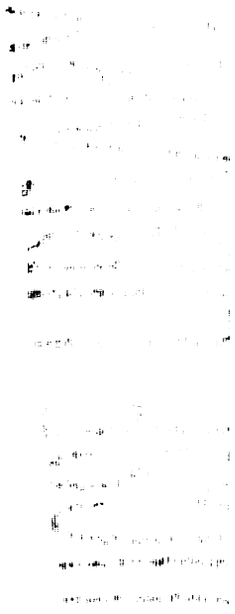

allow reliable sorting. This is also true for *blu* mutants – their OMR deficits are not strong enough to have been sortable using our present methods. Perhaps future work will develop an assay that can provide reliable for sorting on the basis of visual acuity. Until then, mutants will need to be sorted by means of other assays in order to be subjected to the rigorous characterization of the contrast sensitivity function which we describe below for *blu* mutants.

TABLE 1 OMR SCREEN STATISTICS

	OMR Screen	OMR Acuity Screen
F2 Families tested	1,896	1,896
Putants	361	81
Confirmed mutants	34	8
False positive rate	91%	90%

Optomotor responses reveal reduced temporal resolution by the *blu* mutant

In the previous chapters, we have shown that defective vesicular glutamate transport results in two phenotypes, (i) increased depression to fast stimulus trains and (ii) enlarged RGC axon arbors, while leaving visual responses overall intact. We asked if we could identify distinct perceptual correlates for these two defects using the zebrafish larval optomotor response (OMR) to motion of sinusoidal gratings as a quantitative behavioral assay (Orger et al., 2000). The synaptic depression observed at short ISIs (<400 ms) reduces the ability of RGC synapses to transmit information at high firing

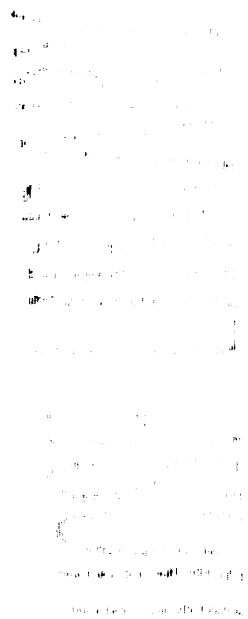

rates (>2.5 Hz; (Fortune and Rose, 2001; Tsodyks and Markram, 1997). RGCs fire at high rates *in vivo* in response to fast visual stimuli (Bilotta and Abramov, 1989; Hochstein and Shapley, 1976). We hypothesized that fast-moving stimuli will therefore be less visible to the mutant. The larger axon arbors are not expected to affect temporal resolution.

The OMR is driven by an innate tendency of zebrafish larvae to swim along with whole-field motion stimuli. In our assay, groups of fish are transferred to long, thin tanks, which sit atop a computer monitor facing up (Neuhauss et al., 1999; Orger et al., 2000). The response is quantified by measuring how far the fish swim in response to a given stimulus. We first measured the contrast sensitivity function of the OMR of mutant and wild-type fish. In preliminary experiments, we found that responses to strong motion stimuli (high contrast, low spatial frequency) are measurably reduced in the mutants (Neuhauss et al., 1999). This effect could be due to visual deficits; but because our assay requires the fish to swim a considerable distance, reduced responses in *blu* mutants may also be attributed to non-visual phenotypes owing to the absence of Vglut2a at other synapses outside the visual system. For instance, the fish may be subtly uncoordinated or perhaps more prone to fatigue.

In order to eliminate this possible confound and isolate the effects on the visual system, we used a motion-nulling technique (Chichilnisky et al., 1993; Orger and Baier, 2005), in which stimuli consist of two superimposed components, a reference stimulus moving in one direction and a test stimulus moving in the opposite direction (Fig. 6A). At low test-stimulus contrast, the fish swim in the direction of the reference stimulus (left

value in Fig. 6A), while at high test-stimulus contrast the fish follow the test stimulus (right value in Fig. 6A). At some intermediate contrast, the fish show no net movement (middle value in Fig. 6A). This "null contrast" gives an index of sensitivity to that stimulus. Because the fish make no net movement at the null contrast, any possible locomotor deficits do not contaminate this measurement. We determined the null contrasts for a range of test stimuli of varying temporal frequencies, while holding spatial frequency constant. Consistent with our hypothesis, mutants show normal sensitivity to low temporal frequency stimuli, but are impaired at temporal frequencies greater than 2.5 Hz (Fig. 6B). This cutoff frequency corresponds to stimulus period of 400 ms and is thus quantitatively concordant with the ISI below which abnormal synaptic depression was observed (see Fig. 2F). We conclude that *blu* mutants are less able to resolve fast motion.

Optomotor responses to fine gratings are impaired in *blu* mutants

We next tested spatial acuity, again using our motion-nulling method. The enlargement of RGC axon arbors generates a greater overlap of neighboring arbors, thus blurring the retinotectal map of visual space. Convergence of a greater number of RGCs onto individual retinorecipient neurons will enlarge their receptive fields and decrease the ability to detect fine spatial detail. We therefore hypothesized that enlarged RGC arbors would reduce the visibility of small stimuli. Consistent with this hypothesis, if temporal frequency is held constant, mutants respond normally to the low spatial frequency gratings but are deficient at high spatial frequencies (Fig. 6C). Finally, we confirmed that the deficits in temporal and spatial resolution are additive. For stimuli at a given constant velocity (where spatial and temporal frequency vary together), mutants show normal

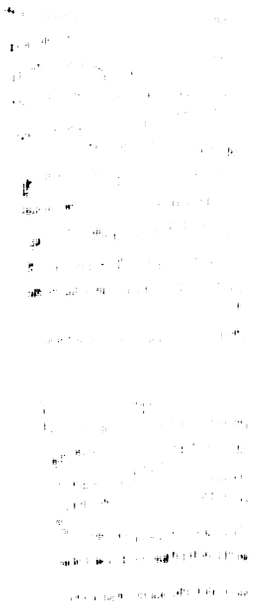

sensitivity to low spatial and low temporal frequency stimuli, but are substantially less sensitive to stimuli of high spatial and high temporal frequency (Fig. 6D).

blu mutants have a selective deficit in the capture of small prey, a tectum-dependent behavior

The behavioral data presented above indicate that vision in *blu* mutants is impaired in a manner that is consistent with the physiological and anatomical alterations in the retinotectal system. However, an important caveat of these behavioral measurements is that the OMR does not require an intact tectum (Roeser and Baier, 2003). Rather, another, currently unknown area receiving retinal input appears to extract the large-field motion stimuli that trigger the OMR. Because *vglut2a* is expressed in all RGCs, it is reasonable to assume that synaptic properties, particularly the kinetics of transmitter release, are similar across the entire RGC population. Nevertheless, the behavioral deficits as measured with the OMR assay cannot be matched up directly with the retinotectal phenotypes. We therefore decided to investigate another behavior, prey capture, which is largely visually mediated and dependent on the tectum (Gahtan and Baier, in press).

Larval zebrafish pursue, catch, and consume small protozoa, such as paramecia, at an early age. We asked whether *blu* mutants have a spatial acuity deficit for prey capture. To sensitize the assay for *blu's* postulated acuity deficit, we used two species of paramecia, which differ greatly in size. *P. multimicronucleatum* are about 200-350 μm in length, while *P. aurelia* are 120-180 μm (see Protist Information Server at http://taxa.soken.ac.jp/www/). In our assay, fish are placed in a small Petri dish, each

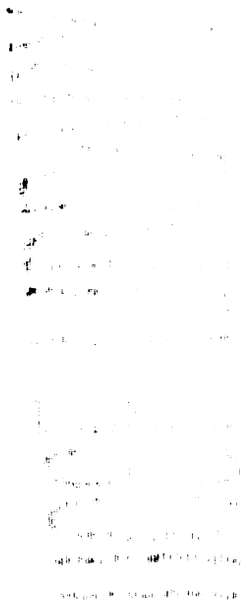

with 20-100 paramecia. At varying time intervals thereafter, the paramecia remaining in the dish are counted (Fig 7A; see Experimental Procedures). These data are fit with an exponential function, derived from the Lotka-Volterra differential equations, assuming steady rate of consumption of prey by a constant number of predators (see Experimental Procedures). The time constant of prey decline is inversely related to the efficiency of prey capture. We found that this time constant does not depend on the number of paramecia at the start of the experiment. In parallel to all experiments, we routinely ran dishes without any fish, in order to determine the spontaneous rate of change (death or proliferation) of paramecia.

We found that *blu* mutants consumed the large species, *P. multimicronucleatum*, at the same rate as wildtype siblings (wt, n = 14 dishes; *blu*, n = 15 dishes), demonstrating that the mutation does not disrupt appetite or locomotor capabilities (Fig. 7B; F-test, $P > 0.5$). In contrast, the mutants took much longer than wildtype to capture the smaller species, *P. aurelia* ($P < 0.001$; wt, n = 21 dishes; *blu*, n = 23 dishes). Thus, while wildtype fish consumed the two species with similar speeds, *blu* mutants were significantly less efficient in catching *P. aurelia* than *P. multimicronucleatum* ($P < 0.01$). The two species of paramecia do not differ in their swimming speeds (note the lengths of the swimming trajectories in Fig. 7A) and are unlikely to differ in their ability to evade capture. Therefore, the most likely explanation for the mutant's greater difficulty in catching *P. aurelia* is a deficiency in visual acuity, which makes the smaller species harder to detect. These results support our hypothesis that the enlargement of RGC axon arbors degrades the fine spatial structure of visual information as it is transmitted to the tectum.

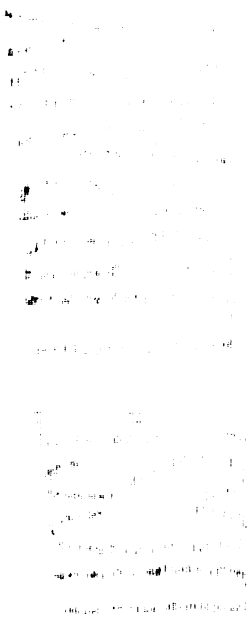

DISCUSSION

Even at a very young age, the larval zebrafish can use its visual system for many purposes. We have demonstrated the ease with which one can determine what a zebrafish sees, and we have designed sensitive behavioral assays to study zebrafish vision. These behavioral assays have allowed us to isolate novel mutations, and, most importantly for this thesis, perform a careful analysis of a previously discovered mutant, *blu*. Having shown that *blu* mutant RGCs are deficient at transmitting at high firing rates, and that RGCs form a retinotectal map with blurred retinotopy, we wanted to ask whether these neural phenotypes would affect vision. Specifically, we predicted that *blu* mutants' physiological phenotype would impair the visibility of rapidly-modulated stimuli, and that their anatomical phenotype would limit their vision's spatial resolution. Using assays for the OMR and prey capture, we confirmed these hypotheses.

Our OMR screen uncovered many previously undiscovered mutants, with novel phenotypes in phototransduction, neurogenesis, axon guidance, and more (Muto et al., in press). Further study of these mutants will thus provide insight into a host of biological problems. Unfortunately, our color and visual acuity screens were less successful. This is especially disappointing given that the kinds of behavioral phenotypes these screens would have revealed had they been sufficiently reliable would most likely have been the most interesting from a systems-level standpoint. Nevertheless, our experience will hopefully provide guidance to future zebrafish behavioral geneticists. If nothing else, the more sophisticated psychophysical techniques can be quite useful as secondary screening tools for mutants that can be sorted on the basis of other phenotypes. As increasing

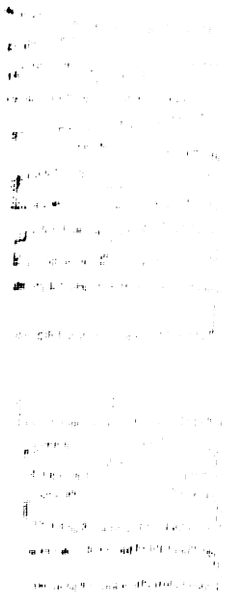

numbers of GFP lines with informative expression patterns make large-scale neuroanatomical screens more common in zebrafish (Xiao et al., 2005), the behavioral methods we have developed will prove useful for researchers looking to relate structure to function.

A particularly exciting possible behavioral screen will be one which utilizes prey capture as a primary assay. While the method we have used to measure the rate of prey capture, manually counting the number of paramecia remaining in a test dish as a function of time, is too slow and labor-intensive to be feasible for a large scale screen, there seem to be several possible ways to accelerate the assay. Writing an image-processing program that can reliably count paramecia will be a difficult, but probably feasible task. Another possibility would be to use a fluorescently-labeled prey species which could be detected in the digestive tract of zebrafish. Or perhaps one could engineer a prey-species to be toxic, thus selecting for fish that do not eat. However one gets it to work, a prey capture screen could give valuable insight into tectal development and function.

We have used the OMR and prey capture assays to test important principles of sensory coding. Just as temporal resolution of vision is limited by the kinetics of phototransduction (Baylor, 1996), temporal resolution should also be depend on the properties of synaptic transmission further downstream in the visual system. Rapid modulation of visual stimuli results in higher firing rates in RGCs (Bilotta and Abramov, 1989; Hochstein and Shapley, 1976). We therefore predicted that the synaptic depression to high frequency stimulation would make fast-changing stimuli less visible to the mutant

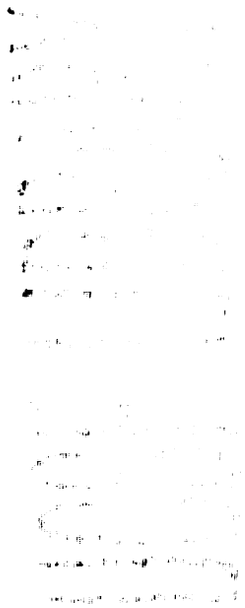

fish. We used the OMR to drifting gratings as a behavioral assay to test this prediction. Because we can vary temporal frequency, spatial frequency, and contrast of the grating stimulus independently, this assay provides a sensitive method for teasing apart spatial and temporal aspects of vision (Orger et al., 2000). Furthermore, the motion-nulling method we have devised (Orger and Baier, 2005) eliminates the contribution of any non-visual factors to our measurements. In agreement with our prediction, gratings that move at high temporal frequencies were less visible to the mutants, even when the grating was very coarse. The temporal frequency range in which the mutants showed an impairment (>2.5 Hz) is in striking agreement with the inter-stimulus-interval range (<400 ms) in which their retinotectal synapses showed increased depression to repetitive stimulation.

We further predicted that the enlarged arborizations of mutant RGCs should degrade the visual map, leading to reduced visual acuity. Roger Sperry (Sperry, 1943) showed that eye rotation in frogs leads to the formation of a rotated representation of visual space, as evidenced by their orientation and localization behavior. While this manipulation established the critical importance of map polarity for vision, the importance of map precision has, to our knowledge, not been directly tested. Because RGC axon arbors are larger and more overlapping in *blu* mutants, a given postsynaptic target neuron is likely to receive synaptic input from a larger number of RGCs spread over a greater area within the retina. While the spacing of photoreceptors puts physical limits on visual acuity (Geisler, 1984; Hirsch and Hylton, 1984), perceptual thresholds are more likely dependent on the size of receptive fields further downstream in the visual circuits (Barlow, 1975; Enroth-Cugell, 1966; Jacobs and Blakemore, 1988; Kiorpes, 2003). In young zebrafish larvae, the theoretical resolution limit set by intercone

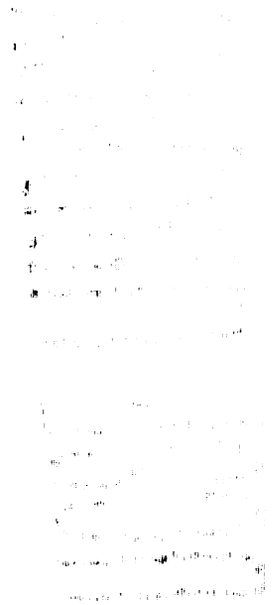

distances, the Nyquist frequency, is greater than 0.34 cycles/degree (less than 3° of the visual field) after 4 dpf (Easter and Nicola, 1996), while grating acuity does not exceed 0.16 cycles/degrees (about 6°) at 5-7 dpf (Rinner et al., 2005).

We demonstrated that *blu* mutants have reduced visual acuity in two visual tests. Using the OMR assay and our motion-nulling technique, we found that the mutants were indeed less able to detect fine gratings, even when the drift velocity was very slow. Our lab has shown previously that the OMR does not require an intact tectum (Roeser and Baier, 2003). This suggests that whatever retinorecipient area or areas are necessary for the OMR have perturbed retinotopy, as does the tectum. In the future, we hope to identify the brain circuit that mediates the OMR. When the retinorecipient area or areas in this circuit have been identified, it will be interesting to determine whether the RGC axons that project to this area or areas also have enlarged axon arbors.

In addition to the OMR, we tested visually guided prey capture. We find that *blu* mutants were substantially more impaired at catching a small prey species (*P. aurelia*) than they were at catching a species twice as large (*P. multimicronucleatum*). These experiments point to the retinotectal map as one of the stages in visual processing where the layout of neuronal circuitry can limit spatial acuity. These experiments complement our analyses of the optomotor response in several valuable ways. First we know that this behavior is tectum-dependent (Gahtan and Baier, in press), thus allowing us to directly test the behavioral outcome of the degraded retinotopy we have shown in the tectum of *blu* mutants. Furthermore, it allows us to test the function of the tectum using a naturalistic stimulus, a sharp contrast from the grating stimuli we use to test the OMR.

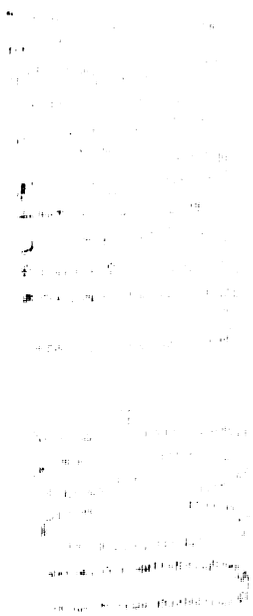

The drawback is that we have far less stimulus control – we were able to use two species of very different size to test the spatial acuity of *blu* mutants' prey capture. A broader survey of the species of paramecia and other protozoans that zebrafish will eat may allow us to ask more questions using the prey capture assay. For instance, we cannot presently test the temporal resolution of prey capture. Maybe this would become possible if we could find an especially fast-moving prey species.

Methods

Optomotor response assay

The OMR was tested as previously described (Orger et al., 2000). Heterozygous *blu* fish were mated, and their offspring were raised on a 14 hour light/10 hour dark cycle to 7 dpf. Mutant and sibling fish were separated and poured in groups of 30-40 into long rectangular tanks, which sat atop a cathode ray tube monitor facing up. The mean luminance and gamma function of the monitor was measured with a photometer. The gamma function was corrected by look-up table adjustment. Stimuli were generated in MATLAB using the Psychophysics Toolbox extensions (Brainard, 1997; Pelli, 1997). A Nikon Coolpix digital still camera was suspended above the fish and triggered by serial commands sent from MATLAB. Images were captured before and after each stimulus. These images were analyzed using custom-written Object-Image macros to determine the position of the fish in each image. The average distance traveled by the fish in a given tank was computed and used as the measure of response strength for a given stimulus. All measurements are an average of the response of at least twelve tanks. For motion-nulling experiments, stimuli consisted of a 10% contrast 0.012 cycles/degree, 0.93 Hz grating

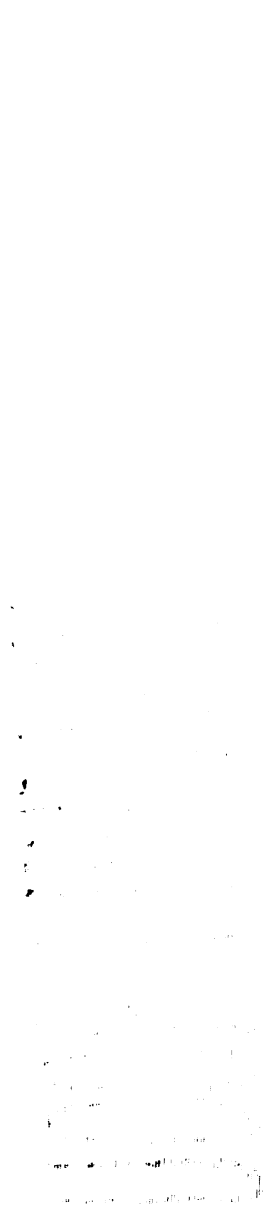

stimulus, moving in one direction (the reference stimulus), superimposed on a stimulus of variable spatial and temporal frequency (the test stimulus), moving in the opposite direction. For the test stimulus, the contrast varied from 0, which evokes a response from the fish in the direction of the reference stimulus, to a contrast at which the test stimulus nulls the reference stimulus. For each test stimulus, a contrast just below and just above that necessary to change the direction of the OMR were repeated and the zero-crossing point of the line connecting them were taken as the null point. The standard error of these measurements was calculated by converting the y-dimension (response size) standard error into the x-dimension (contrast) standard error according to the slope.

Prey capture assay

Prey capture was assayed as previously described (Gahtan and Baier, in press). *Paramecium multimicronucleatum* and *Paramecium aurelia* were obtained from Carolina Biological Supplies (Burlington, NC). Approximately 20-100 paramecia of one of the two species were transferred to a small Petri dish, along with either three *blu* mutant or wildtype fish. Immediately after the fish were added, the dish was placed on a glass platform, illuminated obliquely from below by a ring light, and imaged from above by a high-speed camera (Redlake Imaging, San Diego, California). At this time point and twice at varying time intervals thereafter, a 4 second long movie was captured for each dish. These movies were analyzed offline by taking the standard deviation of the z-projection of each movie, in which the paramecia's movement gives them the appearance of streaks. By counting these streaks, we obtained the number of paramecia in the dish at each time point. The original movies were consulted to resolve any ambiguities in the z-

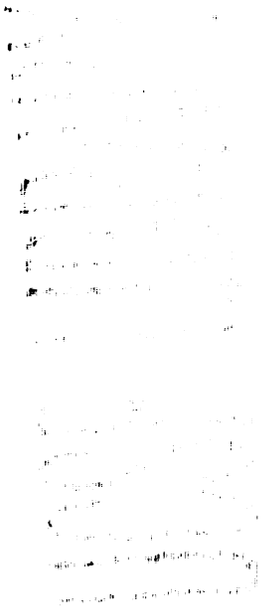

projection, such as overlapping trajectories of several paramecia. The time constant of paramecia decline was obtained by fitting the data to an exponential function derived from the Lotka-Volterra differential equations, in MATLAB. The movies were coded and subsequently scrambled so that the experimenter carrying out the analysis was blind to the time point being measured and the genotype of the fish. Dishes containing only paramecia and no fish were run simultaneously with the dishes containing fish in order to measure the spontaneous rate of change of the paramecia. The spontaneous rate of change (proliferation or death) was also estimated by exponential fits. These were used to correct estimated time constants for prey capture.

Figure 6, Smear et al.

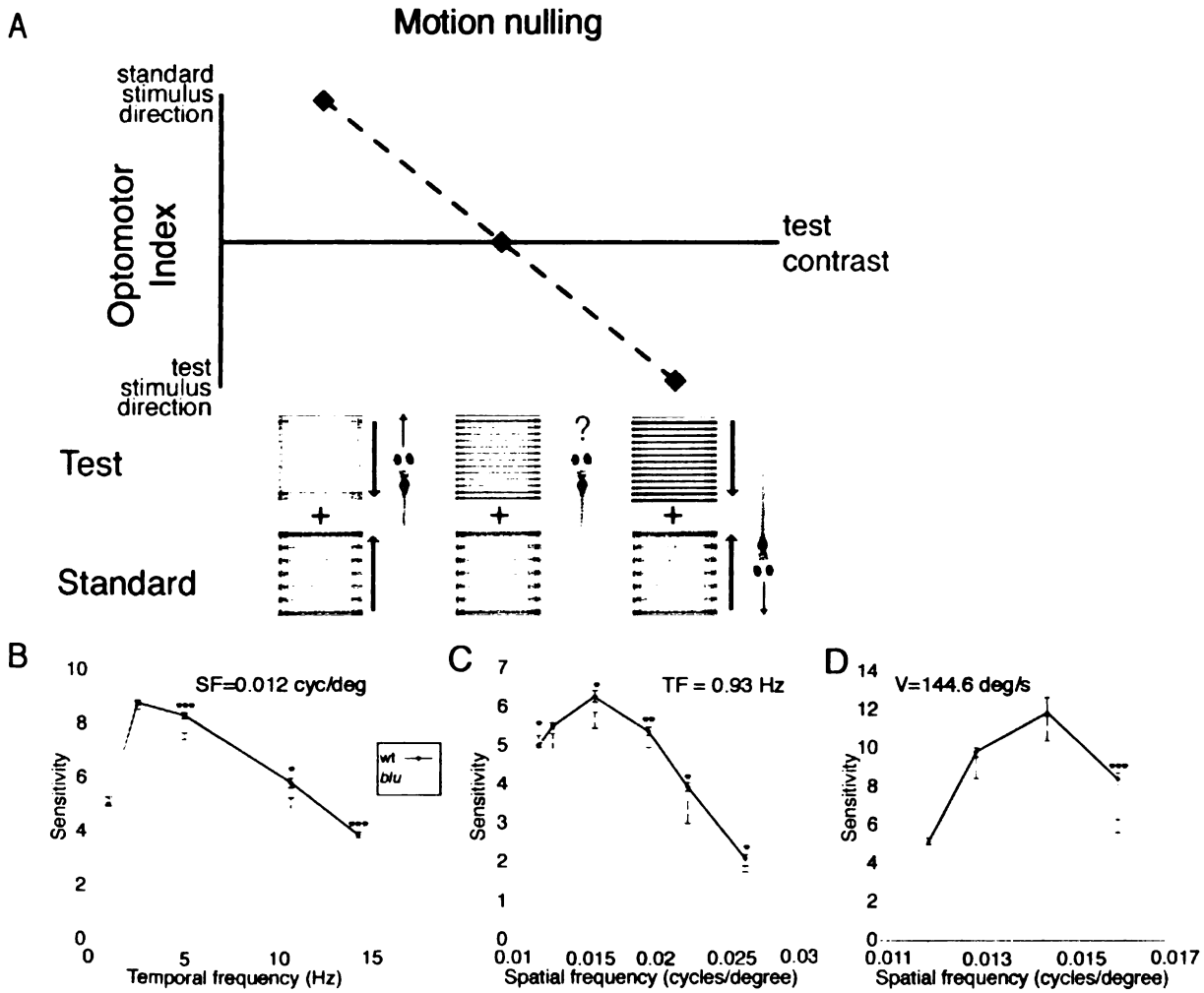

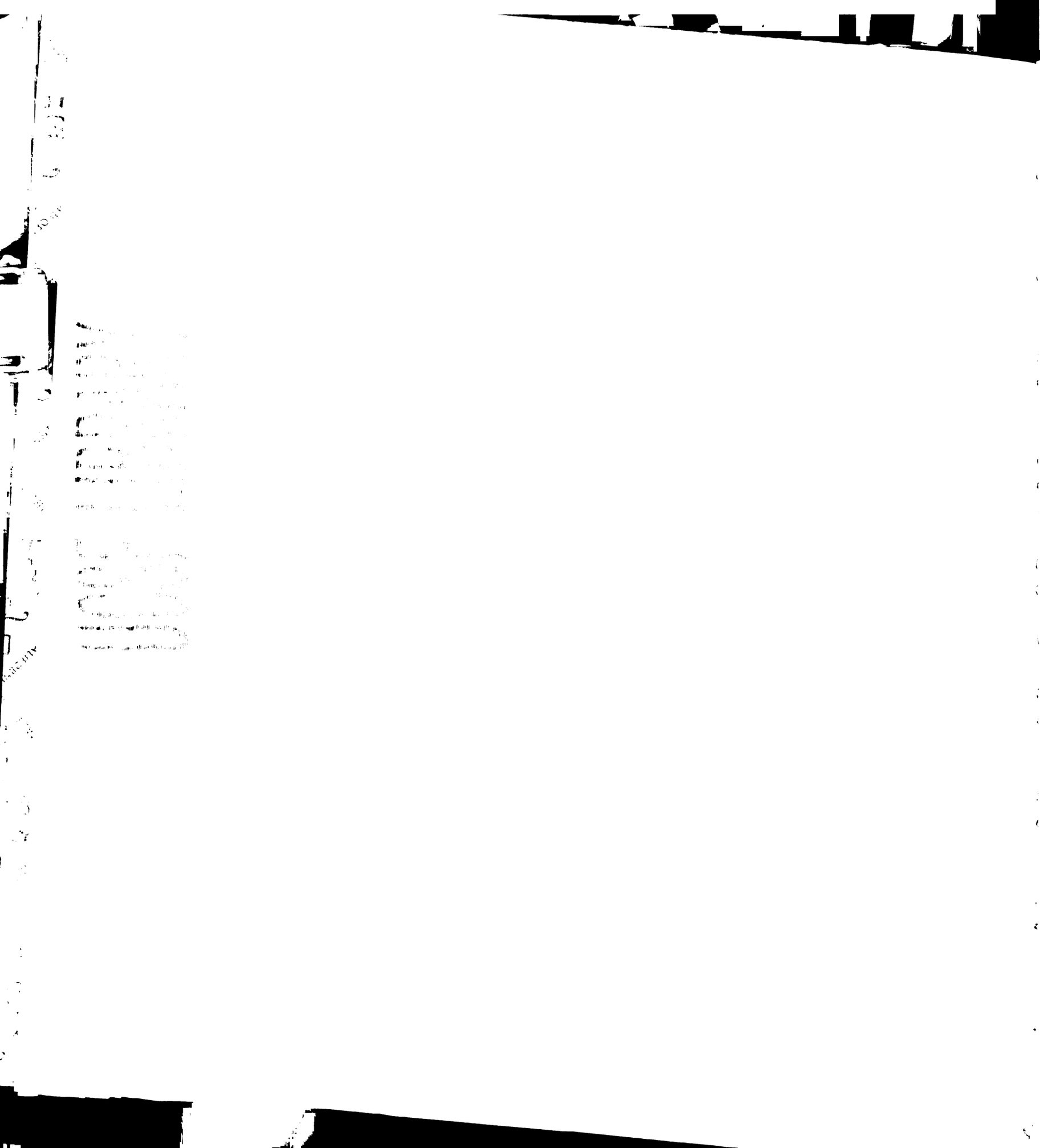

Figure 6. The OMR of *blu* mutants has reduced spatial and temporal resolution. **A**, Schematic diagram of the motion-nulling technique. Stimuli consist of two superimposed drifting sinusoids, a standard stimulus, held constant across all stimuli, and a test stimulus of a given spatial frequency (SF) and temporal frequency (TF). The test and standard stimuli move in opposite directions. For each test stimulus, the contrast is varied. At low test stimulus contrast, the standard stimulus is stronger, and the fish swim in the direction of the standard stimulus (left point). At high test stimulus contrast, the fish swim in the direction of the test stimulus (right point). At some intermediate contrast, the standard and test stimulus are of equal strength, and the fish show no net motion (middle point). This inverse of this "null contrast" is used as the index of sensitivity to that stimulus. Importantly, because the fish show no net motion at the null contrast, this index of sensitivity is not influenced by non-visual factors, such as locomotor ability. **B**, Sensitivity to stimuli of constant SF (0.012 cycles/degree) and varying TF, measured by motion-nulling. Mutants are significantly less sensitive to high TFs. **C**, Sensitivity to stimuli of constant TF (0.93 Hz) and varying SF, measured by motion nulling. Mutants are significantly less sensitive to high SFs. **D**, Sensitivity to stimuli of constant velocity (V = 144.6 degrees/second) and increasing SF, measured by motion nulling. TF co-varies with SF, according to V = TF / SF. Mutants are dramatically less sensitive to high SFs and TFs. Error bars were calculated by converting the x-dimension standard area into the y-dimension standard error by the slope. Statistical significance was determined with a two-tailed *t*-test. $*P < 0.05$, $**P < 0.01$, $***P < 0.001$.

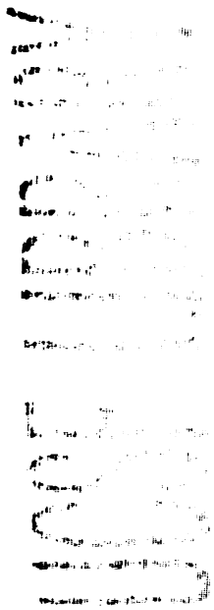

Figure 7, Smear et al.

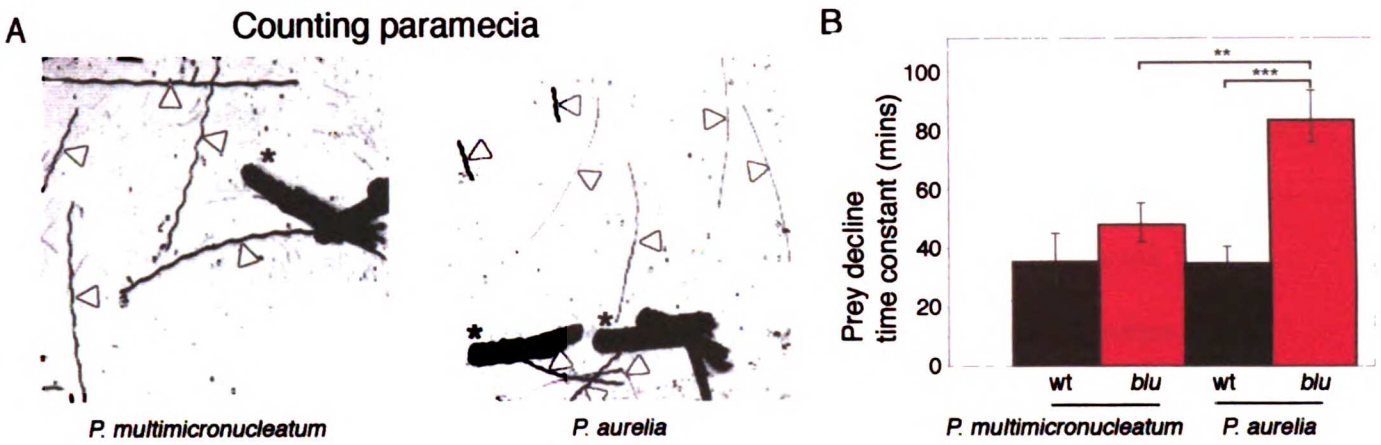

Figure 7. Prey capture by *blu* mutants has reduced spatial resolution. **A,** Example images used to quantify prey capture. Zebrafish larvae (thick black silhouettes, marked by asterisks) are placed in small Petri dishes with 20-100 paramecia. The number of paramecia remaining in the dish is monitored over time. At varying time points over the course of 90 minutes, four-second long movies are recorded and the frames are superimposed by standard deviation time projection. The swimming trajectories of paramecia appear as thin straight streaks (white arrowheads) and are counted. The small species (*P. aurelia*, right) leaves thinner, but equally long, streaks than the big species (*P. multimicronucleatum*, left). **B,** Mutants are impaired in capturing *P. aurelia*, but consume *P. multimicronucleatum* at almost normal rates. Prey capture performance is inversely proportional to the time constant of the decline of the prey population. Error bars are the 95% confidence interval for the estimate of the time constant *P. aurelia,* wt, n = 23; *blu,* n = 24. *P. multimicronucleatum,* wt, n = 14; *blu,* n = 15. Statistical significance was determined with an F-test. $^{**}P < 0.01$, $^{***}P < 0.001$.

Conclusion

The zebrafish *blu* mutant was initially discovered in a forward genetic screen for retinotectal mutants and later shown to have impairments in visual behavior (Baier et al., 1996; Neuhauss et al., 1999; Trowe et al., 1996). We show here by positional cloning that the *blu* gene encodes *vglut2a*, a member of the vesicular glutamate transporter gene family, which mediates the uptake of glutamate by presynaptic vesicles (Bellocchio et al., 2000; Takamori et al., 2001). The *vglut2a* gene is expressed in all RGCs, but was not detectable in glutamatergic neurons presynaptic to RGCs. Thus, the synapses formed by retinofugal axons in central areas are the first in the visual pathway to be affected by the absence of this transporter in *blu* mutants. All visual signals must pass through the RGCs on their way from the eye to the brain. Therefore the deficits in behavioral responses observed here are likely due to changes in synaptic transmission from RGCs to neurons in the tectum and other retinorecipient nuclei. Our own localization studies and those of others have shown that *vglut2a* is also expressed in the olfactory epithelium, the ventral diencephalon, and the spinal cord (Higashijima et al., 2004). It will be interesting to investigate in the future how this mutation affects other CNS functions beyond the visual system.

We asked how the absence of Vglut2a affected retinotectal transmission, with the aim of finding correspondences between the physiological phenotype and alterations in sensory perception and behavior. We chose to record from tectal neurons, which receive synaptic input from RGCs and are located near the dorsal surface of the brain, making them especially accessible to electrodes. We find that substantial glutamatergic

transmission remains at retinotectal synapses despite the mutation in *vglut2a*. One possibility is that the blu^{tz257} allele might be a hypomorph, leaving the mutant Vglut2a protein with some residual transport activity. However, the nature of the genetic lesion in blu^{tz257} argues against this interpretation. The mutation is in a nucleotide necessary for splicing and the resultant splicing error creates a premature stop codon. As a result of this base pair change, the mutant mRNA lacks an exon, and the mutant protein is expected to be truncated to less than a third of its normal length, lacking several transmembrane domains (Fremeau et al., 2001).

A more likely explanation for the mildness of the phenotype is that vesicular glutamate uptake in zebrafish RGCs is only partially dependent on Vglut2a. At least five other members of the *vglut* gene family are present in the zebrafish genome, and these constitute the prime candidates for this partially redundant function. The present incomplete state of the zebrafish genome sequencing project currently makes the cloning and characterization of these additional *vglut* genes prohibitively difficult. In the future it will be interesting to find out the expression pattern of these other *vgluts*, to determine whether one or more of them is indeed expressed by RGCs along with *vglut2a*. If so, loss of function studies for these *vgluts*, achieved either through mutation or morpholino knockdown, will be informative. Does loss of function of whatever additional *vglut* is expressed in RGCs reduce glutamatergic transmission by RGCs? Does this loss of function combined with the *blu* mutation completely abolish glutamatergic transmission by RGCs?

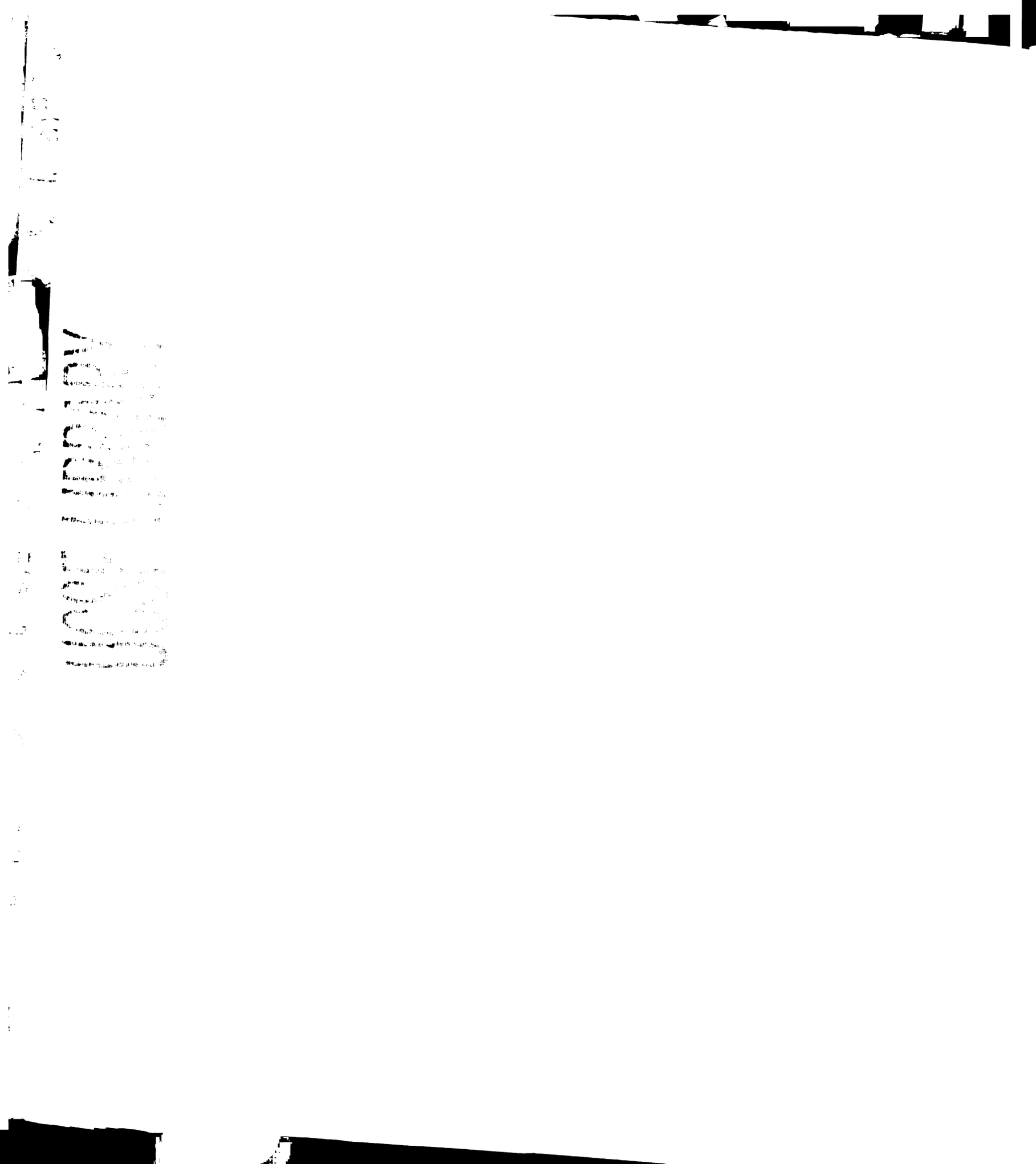

Although synaptic transmission is grossly normal in *blu* mutants, our mEPSC and paired-pulse ratio analyses revealed several deficits. First of all, mEPSC amplitudes are smaller, consistent with a reduction of vesicular glutamate uptake in the mutant. Previous studies of autaptic cultures of hippocampal neurons from *vglut1* mutant mice (Wojcik et al., 2004) and overexpression experiments at the *Drosophila* neuromuscular junction (Daniels et al., 2004) have shown that quantal amplitude is directly related to the number of transporter molecules. In apparent contrast to our zebrafish mutant, mEPSC amplitudes remained unaltered in hippocampal slice recordings from *vglut1* null mice (Fremeau et al., 2004). This finding has been explained by the co-expression of Vglut1 and Vglut2, which segregate to distinct populations of synapses in these neurons. Although we cannot exclude a similar segregation principle at retinotectal synapses, our data are most parsimonously explained by co-localization of Vglut isoforms in the same vesicle.

Second, we found that mEPSC frequency is increased in our mutant. This change may be due either to an increase in the probability of release and/or to an increase in the number of release sites. Either of these mechanisms would work to counteract the reduction in transmitter content per vesicle and thus may account for the relatively normal evoked EPSC amplitude in *blu* mutants. Our findings suggest that both mechanisms might be at work in *blu* mutants (discussed below).

Third, we found that evoked EPSCs are depressed to a significantly larger degree in the mutant when pulses are applied at high rates. The difference is not seen at pulse intervals greater than 400 ms. This kind of synaptic depression is commonly attributed to

depletion of the readily releasable pool of vesicles – synapses with higher release probability tend to show a reduced PPR (Zucker and Regehr, 2002). In *blu* mutants, a single pulse may deplete the readily releasable pool of vesicles enough to cause increased depression to the second pulse. Alternatively or in addition, recently-recycled vesicles might take longer to refill, in agreement with the presence of fewer transporters per vesicle (Gasnier, 2000). When these vesicles are recruited to respond to the second pulse, they would contain less glutamate and thus would lower the amplitude of the second response. Whatever the exact nature of this deficit, our results led us to predict that transmission of visual information should be impaired at high presynaptic firing rates.

Our mEPSC frequency data suggest that both probability of release and the number of release sites may be increased in *blu* mutants, thus working to counteract the reduction in vesicular glutamate concentration. There may well be other homeostatic compensations in *blu* mutants which also work to compensate for reduced vesicular glutamate uptake. One particularly strong possibility is that optic tectal neurons increase the surface concentration of glutamate receptors postsynaptically, thereby increasing postsynaptic glutamate sensitivity and thus boosting mEPSC amplitude. If anything, we expect that our mEPSC amplitude distribution data underestimates the difference in presynpatic glutamate release between wildtype and *blu* mutant synapses, because *blu* mutant synapses have activated mechanisms to enhance postsynaptic glutamate sensitivity. There is evidence that such postsynaptic compensations can be evoked by reductions of presynaptic activity levels *in vivo* in the *Drosophila* neuromuscular junction (Marek and Davis, 2003) and in the mammalian cortex (Turrigiano and Nelson, 2004), as well *in vitro* studies of cultured mammalian hippocampus neurons (Burrone and Murthy,

2003). The best way to test whether such changes are taking place at retinotectal synapses in *blu* mutants would be to exogenously apply glutamate to optic tectal neurons, thereby measuring postsynaptic sensitivity to glutamate directly. Several additional mechanisms might allow the *blu* mutant retinotectal synapse to compensate for deficiently filled vesicles. These include reducing reuptake by plasma membrane transporters, which would work to boost the amount of glutamate permeating the synaptic cleft following exocytosis. Another possibility would be to increase the excitability of postsynaptic neurons, for instance by increasing the surface expression or conductivity of voltage-gated channels in optic tectal neurons.

Our evidence shows that synaptic deficits in the *blu* mutant precipitate enlarged arborizarions by RGC axon arbors. During embryonic development (in zebrafish beginning at 2 dpf), RGC axons project into the superficial layers of the contralateral tectum in retinotopic order, i. e., preserving the neighborhood relationships of their cell bodies in the retina (Johnson and Harris, 2000; McLaughlin et al., 2003a; Schmidt and Buzzard, 1990). In *blu* mutants, previous DiI labeling studies had shown that, while coarse retinotopy was intact, the termination zones of small groups of RGC axons appeared more dispersed in the tectum (Baier et al., 1996) (Trowe et al., 1996) . By single-axon tracing, we were able to attribute this multi-axon phenotype to the expansion of individual arbors. Larger arbors may accommodate more presynaptic active zones, a hypothesis consistent with the observed increase in mEPSC frequency. An increased number of synaptic contacts, together with, or in lieu of, an increased probability of release, could thus explain the rather mild electrophysiological deficits observed in the mutant. The additional space for synapses comes at the expense of the retinotectal map.

Thus it would appear that the homeostatic mechanisms at work in *blu* mutant RGC axons represent a tradeoff between attaining a certain level of activity and maintaining the representation of fine-grained spatial patterns within that activity.

The larger arbors could result either from a lack of activity-dependent refinement, which is thought to work through competition between inputs (Hua and Smith, 2004; Ruthazer et al., 2003). Another possibility is that extra arbor growth is a homeostatic response to lowered synaptic activity (Burrone and Murthy, 2003; Marek and Davis, 2003). Or the mechanism might be cell-autonomous, reflecting a direct effect of the lack of glutamate on axon growth (Kreibich et al., 2004). By chimera analysis, we showed that mutant RGCs form normal-sized axon arbors in a wildtype host. This result excludes a cell-autonomous mechanism of reduced glutamate release on arbor growth, for instance one in which an axon might adjust its arbor size accordingly to the amount of glutamate released by its release sites. Conversely, wildtype RGCs formed normal-sized arbors when transplanted into a mutant environment. This result runs counter to a competitive model in which relative activity levels determine arbor size (Hua et al., 2005).

We therefore suggest that arbor overgrowth most likely reflects a homeostatic mechanism. We propose that the postsynaptic cell promotes growth of the presynaptic arbor to compensate for reduced synaptic drive (Burrone and Murthy, 2003; Davis and Bezprozvanny, 2001). This model can also explain the effects on RGC arbor growth caused by pharmacological blockade of NMDA channels (Schmidt et al., 2000) and by a mutation in voltage-gated sodium channels (Gnuegge et al., 2001). According to this model, *blu* mutant axons in a wild-type host grow normal-sized arbors because

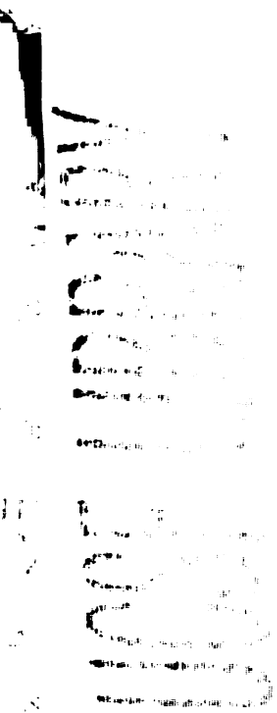

convergent wild-type RGC inputs evoke a sufficient level of postsynaptic activity. The normal size of wild-type axon arbors in a mutant host, on the other hand, implies that a single wild-type axon can evoke sufficient levels of activity in postsynaptic cells to produce normal growth. To test whether this compensatory mechanism indeed employs a retrograde signal, it would be useful to be able to block or reduce activity specifically in tectal neurons, without blocking that of RGCs. Blocking tectal activity should produce enlarged retinotectal axon arbors. Perhaps in the future it will be possible to engineer a transgenic fish to meet this specification.

We have shown that RGC axon arbor morphogenesis is altered in *blu* mutants. It will also be fruitful to study how the *blu* mutation affects dendritic morphogenesis in optic tectal neurons. Perhaps tectal dendrites arborize more profusely, in order to provide more surface for the insertion of additional postsynaptic densities. If this causes tectal neurons to spread their arbors over more of the retinotectal map, it might further degrade the retinotopy and exacerbate the loss of spatial acuity for tectally-mediated behaviors. A recent *in vivo* study using a PSD-95 GFP fusion protein to label tectal synapses has provided evidence consistent with the idea that nascent synapses stabilize dendritic filopodia (Niell et al., 2004). Since *blu* mutant RGCs are likely to form more synapses, such a mechanism would suggest that dendritic arbors will have increased numbers of branches, since more will be stabilized.

The physiological and anatomical phenotypes described above are predicted to have adverse effects on vision. The zebrafish larva has a rich repertoire of visually mediated behaviors (Easter and Nicola, 1996), and we have designed assays for these behaviors,

with the intent of studying mutants discovered in genetic screens for other phenotypes, like *blu* (Baier et al., 1996; Neuhauss et al., 1999; Trowe et al., 1996). As shown in the 4th chapter of this thesis and discussed below we have used these behaviors to ask questions about the functional effects of the neural phenotypes we have discovered. In addition, we attempted to use the OMR to discover novel mutants, with phenotypes ranging from total absence of OMR to subtler stimulus-specific OMR impairments, as we have found for *blu* mutants. Our screen has succeeded in revealing new OMR-negative mutants, with neural phenotypes ranging from photoreceptor dysfunction to aberrant RGC axon wiring (Muto et al., in press). These mutants will provide unique insights into visual system development and function.

Our attempts to isolate mutants on the basis of subtler deficits like reduced spatial acuity have succeeded. We have found several mutations with visual acuity deficits which have been detectable in the offspring of at least two generations. We have failed to make further progress with these mutants because their deficits, while detectable, are not severe enough to allow them to be reliably sorted from wildtype siblings. This unsortability impedes progress in genetic mapping and the search for anatomical phenotypes. Without criteria by which clutches may be sorted into pure wildtype and pure mutant groups, we obscure any "signal" in which mutants and wildtype might differ. If more sensitive methods for sorting these clutches can be developed, these mutants will become useful for what they may reveal about visual system function and development. For now further progress with them remains intractable. For mutants like *blu,* which can be sorted on the basis of an unambiguous difference in pigmentation, our behavioral assays can be quite powerful, as this thesis demonstrates. For now it seems the best

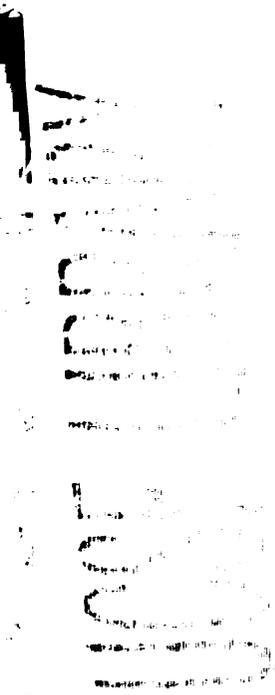

strategy for studying vision in zebrafish mutants is to first find a way to sort them by other criteria, and then use behaviors in secondary assays. As the development of more and more lines of transgenic fish with useful patterns of GFP expression become available (Xiao et al., 2005), anatomical screens will produce more and more mutants for which analysis of visual behaviors will be useful. Our analyses of *blu* mutant vision are testament to the power of zebrafish psychophysics.

The neural phenotypes we have demonstrated in *blu* mutants make clear predictions about visual impairments. One of these is that depression of retinofugal synapses produced by rapid stimulation would impair the temporal resolution of the mutant visual system. It is thought the temporal resolution of vision is set by the rate at which phototransduction can be activated and quenched (Baylor, 1996). Similarly, temporal resolution should also be constrained by the kinetics of synaptic transmission further downstream in the visual system. It is well-known that rapidly modulated visual stimuli evoke higher firing rates in RGCs (Bilotta and Abramov, 1989; Hochstein and Shapley, 1976). These stimuli should therefore evoke weaker responses in retinorecipient neurons.

We tested this prediction using a behavioral assay for the OMR to drifting gratings. Because we can control stimulus parameters like spatial frequency, temporal frequency and contrast, this assay provides a strong method for isolating spatial and temporal aspects of vision (Orger et al., 2000). Furthermore, the motion-nulling method we have devised (Orger and Baier, 2005) prevents non-visual factors like coordination and fatigue from influencing our measurements. As we predicted, mutants were less sensitive to high

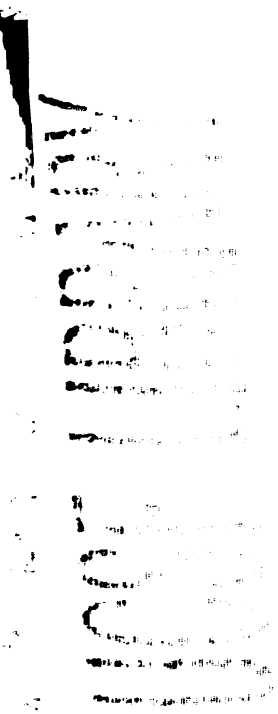

temporal frequency gratings, even for gratings with very low spatial frequency. Impressively, the range of temporal frequencies in which the mutants showed reduced sensitivity (>2.5 Hz) matches with the inter-stimulus-interval range (<400 ms) in which their retinotectal synapses showed increased depression to repetitive stimulation. In other words, the visual stimuli which we would predict to evoke the firing at the rates where retinotectal transmission is impaired (since RGCs modulate their firing rate to match the stimulus modulation rate (Bilotta and Abramov, 1989; Hochstein and Shapley, 1976)), are indeed harder for *blu* mutants to see.

The enlarged arborization of *blu* mutant RGCs reduces the precision of the retinotectal map. A given postsynaptic target neuron makes synaptic contact with more RGCs, whose somata are distributed over a larger area within the retina, and thus becomes sensitive to an enlarged chunk of visual space. The spacing of photoreceptors physically limits visual acuity (Geisler, 1984; Hirsch and Hylton, 1984), but perceptual thresholds also depend on the size of receptive fields further downstream in the visual circuits (Barlow, 1975; Enroth-Cugell, 1966; Jacobs and Blakemore, 1988; Kiorpes, 2003). We reasoned that the degraded retinotopy in *blu* mutants would enlarge receptive fields and thus compromise visual acuity. Using the OMR assay and our motion-nulling technique, we found that the mutants were less sensitive to fine gratings, even when the drift velocity was slow.

A caveat to relating OMR deficits to physiological and anatomical phenotypes in *blu* mutants is that we have demonstrated these phenotypes in the tectum, a structure we know to be unnecessary for the OMR (Roeser and Baier, 2003). Because *vglut2a* is

expressed in all RGCs, we feel that it is likely that the retinorecipient structure(s) necessary for the OMR will have similar wiring defects. However, we will be unable to demonstrate that this is true until we know the identity of this structure and can visualize the morphology of RGC axon arbors which connect to it. Therefore, we elected to perform an assay for another visual behavior: visually guided prey capture. Our lab has shown that this behavior is largely tectum-dependent (Gahtan and Baier, in press). We find that *blu* mutants were substantially more impaired at catching a small prey species (*P. aurelia*) than they were at catching a species twice as large (*P. multimicronucleatum*). These experiments point to the retinotectal map as one of the stages in visual processing where the layout of neuronal circuitry can limit spatial acuity.

We have shown that *blu* mutants have behavioral impairments that are predictable based on their physiological and anatomical phenotypes. In the future, we hope to make receptive field measurements from retinorecipient neurons in *blu* mutants, to determine whether these have the receptive field abnormalities our behavioral experiments indicate. Ideally, we would like to perform receptive field measurements on tectal neurons, which are required for prey capture, and from the yet-to-be-identified population of retinorecipient neurons required for the OMR. We would predict that these neurons should be less responsive to rapidly-modulated and fine-grained stimuli. In the spatial domain, we would predict that the receptive fields of tectal domains would be enlarged, thus reducing their responsiveness for small or high spatial frequency stimuli.

In addition to enlarging the size of receptive fields of retinorecipient neurons, the expansion of RGC arbors might also disrupt their fine spatial structure. A greater number

and spread of glutamatergic synapses in the tectum may produce local imbalances between transmitter systems or between inputs from different RGC subtypes. Receptive fields in the zebrafish tectum are shaped by both excitatory and inhibitory inputs (Sajovic and Levinthal, 1983). A recent calcium imaging study of the zebrafish tectum (Niell and Smith, 2005) has revealed a tectal cell type with large receptive fields selective for moving stimuli that subtend only a small sub-region of the receptive field. Such cells with "negative spatial summation" may be particularly important for prey capture, and their receptive field structure may be compromised in a mutant with larger axon arbors. It will be rewarding to study receptive field properties in the *blu* mutant tectum. Two methods of functional study should be possible. Calcium imaging allows the properties of many receptive fields to be characterized simulataneously from the same animal, with the drawback that the information is acquired with low temporal resolution. The alternative would be to adapt electrophysiological recording methods similar to that used recently in *Xenopus* tadpoles (Tao and Poo, 2005).

Another potentially interesting line of experiments would be to look at the effect of *vglut2a* over-expression. Over-expressing vglut proteins is predicted to increase the vesicular glutamate concentration at equilibrium (Gasnier, 2000). This has been shown in *in vitro* studies of cultured hippocampal neurons transfected to over-express VGLUT1 (Wilson et al., 2005; Wojcik et al., 2004). Even more interesting is an *in vivo* study of the effect of over-expressing DVGLUT, the *Drosophila* vesicular glutamate transporter, on neuromuscular transmission (Daniels et al., 2004). *Drosophila* motoneurons that over-express DVGLUT also show increased vesicular glutamate concentration. Further, the synapse makes a homeostatic adjustment, reducing the probability of release. This

change is thus symmetrical to the effect we see in *blu* mutants, which likely have reduced vesicular glutamate concentration. It would be interesting to over-express *vglut2a* to see whether the retinotectal synapse makes homeostatic changes opposite to those it makes in *blu* mutants. Would RGC axons grow smaller arbors and make fewer synapses in the tectal neuropil? What effect would this have on behavior?

Our physiological, anatomical, and behavioral investigations into the zebrafish *blu/vglut2a* mutant demonstrate a tight correspondence between specific perceptual abilities and the arrangement and function of the underlying synaptic circuitry. The most parsimonious interpretation of these results is that resolution of fast-changing visual scenes depends on rapid recovery of synaptic transmission, while high-acuity spatial vision requires precise retinotopic mapping. It is noteworthy that the primary physiological deficit of the mutant (reduced synaptic drive) seems to precipitate secondary physiological and anatomical changes (increased synapse number and, possibly, increased probability of release), which largely compensate for the initial perturbation. Homeostatic regulation may thus account for the relatively normal postsynaptic responses, but it comes at the expense of visual acuity. Our study has revealed a likely causal link between a circumscribed synaptic deficit and a change in the processing of sensory information by a behaving animal.

References

Aihara, Y., Mashima, H., Onda, H., Hisano, S., Kasuya, H., Hori, T., Yamada, S., Tomura, H., Yamada, Y., Inoue, I., *et al.* (2000). Molecular cloning of a novel brain-type Na(+)-dependent inorganic phosphate cotransporter. J Neurochem *74*, 2622-2625.

Attwell, D., Barbour, B., and Szatkowski, M. (1993). Nonvesicular release of neurotransmitter. Neuron *11*, 401-407.

Avery, L. (1993). The genetics of feeding in Caenorhabditis elegans. Genetics *133*, 897-917.

Baier, H., and Bonhoeffer, F. (1992). Axon guidance by gradients of a target-derived component. Science *255*, 472-475.

Baier, H., Klostermann, S., Trowe, T., Karlstrom, R. O., Nusslein-Volhard, C., and Bonhoeffer, F. (1996). Genetic dissection of the retinotectal projection. Development *123*, 415-425.

Barlow, H. B. (1975). Visual experience and cortical development. Nature *258*, 199-204.

Baylor, D. (1996). How photons start vision. Proc Natl Acad Sci U S A *93*, 560-565.

Bellocchio, E. E., Hu, H., Pohorille, A., Chan, J., Pickel, V. M., and Edwards, R. H. (1998). The localization of the brain-specific inorganic phosphate transporter suggests a specific presynaptic role in glutamatergic transmission. J Neurosci *18*, 8648-8659.

Bellocchio, E. E., Reimer, R. J., Fremeau, R. T., Jr., and Edwards, R. H. (2000). Uptake of glutamate into synaptic vesicles by an inorganic phosphate transporter. Science *289*, 957-960.

Bilotta, J., and Abramov, I. (1989). Spatial properties of goldfish ganglion cells. J Gen Physiol *93*, 1147-1169.

Borla, M. A., Palecek, B., Budick, S., and O'Malley, D. M. (2002). Prey capture by larval zebrafish: evidence for fine axial motor control. Brain Behav Evol *60*, 207-229.

Brainard, D. H. (1997). The Psychophysics Toolbox. Spatial Vision *10*, 433-436.

Brown, A., Yates, P. A., Burrola, P., Ortuno, D., Vaidya, A., Jessell, T. M., Pfaff, S. L., O'Leary, D. D., and Lemke, G. (2000a). Topographic mapping from the retina to the midbrain is controlled by relative but not absolute levels of EphA receptor signaling. Cell *102*, 77-88.

Brown, S. P., He, S., and Masland, R. H. (2000b). Receptive field microstructure and dendritic geometry of retinal ganglion cells. Neuron *27*, 371-383.

Burrill, J. D., and Easter, S. S., Jr. (1994). Development of the retinofugal projections in the embryonic and larval zebrafish (Brachydanio rerio). J Comp Neurol *346*, 583-600.

Burrone, J., and Murthy, V. N. (2003). Synaptic gain control and homeostasis. Curr Opin Neurobiol *13*, 560-567.

Cajal, S. R. (1995). Histology of the Nervous System, Vol. 1 (New York, Oxford University Press).

Cheng, H. J., Nakamoto, M., Bergemann, A. D., and Flanagan, J. G. (1995). Complementary gradients in expression and binding of ELF-1 and Mek4 in development of the topographic retinotectal projection map. Cell *82*, 371-381.

Chichilnisky, E. J., Heeger, D., and Wandell, B. A. (1993). Functional segregation of color and motion perception examined in motion nulling. Vision Res *33*, 2113-2125.

Chklovskii, D. B., Schikorski, T., and Stevens, C. F. (2002). Wiring optimization in cortical circuits. Neuron *34*, 341-347.

Cline, H. (2003). Sperry and Hebb: oil and vinegar? Trends Neurosci *26*, 655-661.

Cline, H. T., and Constantine-Paton, M. (1989). NMDA receptor antagonists disrupt the retinotectal topographic map. Neuron *3*, 413-426.

Constantine-Paton, M., and Law, M. I. (1978). Eye-specific termination bands in tecta of three-eyed frogs. Science *202*, 639-641.

Daniels, R. W., Collins, C. A., Gelfand, M. V., Dant, J., Brooks, E. S., Krantz, D. E., and DiAntonio, A. (2004). Increased expression of the Drosophila vesicular glutamate transporter leads to excess glutamate release and a compensatory decrease in quantal content. J Neurosci *24*, 10466-10474.

Davis, G. W., and Bezprozvanny, I. (2001). Maintaining the stability of neural function: a homeostatic hypothesis. Annu Rev Physiol *63*, 847-869.

Del Castillo, J., Katz, B. (1954). Statistical factors involved in neuromuscular facilitation and depression. J Physiol *124*, 574-585.

Dent, J. A., Davis, M. W., and Avery, L. (1997). avr-15 encodes a chloride channel subunit that mediates inhibitory glutamatergic neurotransmission and ivermectin sensitivity in Caenorhabditis elegans. Embo J *16*, 5867-5879.

DeVries, S. H. (2000). Bipolar cells use kainate and AMPA receptors to filter visual information into separate channels. Neuron *28*, 847-856.

Drescher, U., Kremoser, C., Handwerker, C., Loschinger, J., Noda, M., and Bonhoeffer, F. (1995). In vitro guidance of retinal ganglion cell axons by RAGS, a 25 kDa tectal protein related to ligands for Eph receptor tyrosine kinases. Cell *82*, 359-370.

Easter, S. S., Jr., and Nicola, G. N. (1996). The development of vision in the zebrafish (Danio rerio). Dev Biol *180*, 646-663.

Engert, F., Tao, H. W., Zhang, L. I., and Poo, M. M. (2002). Moving visual stimuli rapidly induce direction sensitivity of developing tectal neurons. Nature *419*, 470-475.

Enroth-Cugell, C., Robson, J.G. (1966). The contrast sensitivity of retinal ganglion cells of the cat. J Physiol *187*, 517-552.

Featherstone, D. E., Rushton, E., and Broadie, K. (2002). Developmental regulation of glutamate receptor field size by nonvesicular glutamate release. Nat Neurosci *5*, 141-146.

Feldheim, D. A., Kim, Y. I., Bergemann, A. D., Frisen, J., Barbacid, M., and Flanagan, J. G. (2000). Genetic analysis of ephrin-A2 and ephrin-A5 shows their requirement in multiple aspects of retinocollicular mapping. Neuron *25*, 563-574.

Fortune, E. S., and Rose, G. J. (2001). Short-term synaptic plasticity as a temporal filter. Trends Neurosci *24*, 381-385.

Fremeau, R. T., Jr., Burman, J., Qureshi, T., Tran, C. H., Proctor, J., Johnson, J., Zhang, H., Sulzer, D., Copenhagen, D. R., Storm-Mathisen, J., *et al.* (2002). The identification of vesicular glutamate transporter 3 suggests novel modes of signaling by glutamate. Proc Natl Acad Sci U S A *99*, 14488-14493.

Fremeau, R. T., Jr., Kam, K., Qureshi, T., Johnson, J., Copenhagen, D. R., Storm-Mathisen, J., Chaudhry, F. A., Nicoll, R. A., and Edwards, R. H. (2004). Vesicular glutamate transporters 1 and 2 target to functionally distinct synaptic release sites. Science *304*, 1815-1819.

Fremeau, R. T., Jr., Troyer, M. D., Pahner, I., Nygaard, G. O., Tran, C. H., Reimer, R. J., Bellocchio, E. E., Fortin, D., Storm-Mathisen, J., and Edwards, R. H. (2001). The expression of vesicular glutamate transporters defines two classes of excitatory synapse. Neuron *31*, 247-260.

Frisen, J., Yates, P. A., McLaughlin, T., Friedman, G. C., O'Leary, D. D., and Barbacid, M. (1998). Ephrin-A5 (AL-1/RAGS) is essential for proper retinal axon guidance and topographic mapping in the mammalian visual system. Neuron *20*, 235-243.

Gahtan, E., and Baier, H. (2004). Of lasers, mutants, and see-through brains: functional neuroanatomy in zebrafish. J Neurobiol *59*, 147-161.

Gasnier, B. (2000). The loading of neurotransmitters into synaptic vesicles. Biochimie *82*, 327-337.

Geisler, W. S. (1984). Physical limits of acuity and hyperacuity. J Opt Soc Am A *1*, 775-782.

Gesteland, R. F., Cech, T., and Atkins, J. F. (1999). The RNA world : the nature of modern RNA suggests a prebiotic RNA, 2nd edn (Cold Spring Harbor, N.Y., Cold Spring Harbor Laboratory Press).

Gnuegge, L., Schmid, S., and Neuhauss, S. C. (2001). Analysis of the activity-deprived zebrafish mutant macho reveals an essential requirement of neuronal activity for the development of a fine-grained visuotopic map. J Neurosci *21*, 3542-3548.

Goodman, C. S., and Shatz, C. J. (1993). Developmental mechanisms that generate precise patterns of neuronal connectivity. Cell *72 Suppl*, 77-98.

Haas, K., Jensen, K., Sin, W. C., Foa, L., and Cline, H. T. (2002). Targeted electroporation in Xenopus tadpoles in vivo--from single cells to the entire brain. Differentiation *70*, 148-154.

Hartline, H. K. (1940). The receptive fields of optic nerve fibers. 1940, 690-699.

Hebb, D. O. (1949). The Organization of Behavior (New York, John Wiley and Sons).

Higashijima, S., Mandel, G., and Fetcho, J. R. (2004). Distribution of prospective glutamatergic, glycinergic, and GABAergic neurons in embryonic and larval zebrafish. J Comp Neurol *480*, 1-18.

Hindges, R., McLaughlin, T., Genoud, N., Henkemeyer, M., and O'Leary, D. D. (2002). EphB forward signaling controls directional branch extension and arborization required for dorsal-ventral retinotopic mapping. Neuron *35*, 475-487.

Hirsch, J., and Hylton, R. (1984). Quality of the primate photoreceptor lattice and limits of spatial vision. Vis Res *24*, 347-356.

Ho, R. K., and Kane, D. A. (1990). Cell-autonomous action of zebrafish spt-1 mutation in specific mesodermal precursors. Nature *348*, 728-730.

Hochstein, S., and Shapley, R. M. (1976). Quantitative analysis of retinal ganglion cell classifications. J Physiol *262*, 237-264.

Hua, J. Y., Smear, M. C., Baier, H., and Smith, S. J. (2005). Regulation of axon growth in vivo by activity-based competition. Nature *434*, 1022-1026.

Hua, J. Y., and Smith, S. J. (2004). Neural activity and the dynamics of central nervous system development. Nat Neurosci *7*, 327-332.

Jacobs, D. S., and Blakemore, C. (1988). Factors limiting the postnatal development of visual acuity in the monkey. Vision Res *28*, 947-958.

Johnson, K. G., and Harris, W. A. (2000). Connecting the eye with the brain: the formation of the retinotectal pathway. Results Probl Cell Differ *31*, 157-177.

Kaas, J. H. (1997). Topographic maps are fundamental to sensory processing. Brain Res Bull *44*, 107-112.

Kaethner, R. J., and Stuermer, C. A. (1992). Dynamics of terminal arbor formation and target approach of retinotectal axons in living zebrafish embryos: a time-lapse study of single axons. J Neurosci *12*, 3257-3271.

Katz, B., and Miledi, R. (1968). The role of calcium in neuromuscular facilitation. J Physiol *195*, 481-492.

Katz, L. C., and Shatz, C. J. (1996). Synaptic activity and the construction of cortical circuits. Science *274*, 1133-1138.

Kay, J. N., Roeser, T., Mumm, J. S., Godinho, L., Mrejeru, A., Wong, R. O., and Baier, H. (2004). Transient requirement for ganglion cells during assembly of retinal synaptic layers. Development.

Keegan, B. R., Feldman, J. L., Lee, D. H., Koos, D. S., Ho, R. K., Stainier, D. Y., and Yelon, D. (2002). The elongation factors Pandora/Spt6 and Foggy/Spt5 promote transcription in the zebrafish embryo. Development *129*, 1623-1632.

Kelly, D. H. (1979). Motion and vision. II. Stabilized spatio-temporal threshold surface. J Opt Soc Am *69*, 1340-1349.

Kiorpes, L., Movshon, J.A. (2003). Neural limitations on visual development in primates. In The visual neurosciences, L. M. Chalupa, Werner, J.S., ed. (Cambridge, MA, MIT Press), pp. 234-259.

Knudsen, E. I., du Lac, S., and Esterly, S. D. (1987). Computational maps in the brain. Annu Rev Neurosci *10*, 41-65.

Kreibich, T. A., Chalasani, S. H., and Raper, J. A. (2004). The Neurotransmitter glutamate reduces axonal responsiveness to multiple repellents through the activation of metabotropic glutamate receptor 1. J Neurosci *24*, 7085-7095.

Kuffler, S. W. (1953). Discharge patterns and functional organization. Neurophysiology *16*, 37-68.

Lee, R. Y., Sawin, E. R., Chalfie, M., Horvitz, H. R., and Avery, L. (1999). EAT-4, a homolog of a mammalian sodium-dependent inorganic phosphate cotransporter, is necessary for glutamatergic neurotransmission in caenorhabditis elegans. J Neurosci *19*, 159-167.

Liu, Y., and Edwards, R. H. (1997). The role of vesicular transport proteins in synaptic transmission and neural degeneration. Annu Rev Neurosci *20*, 125-156.

Marek, K. W., and Davis, G. W. (2003). Controlling the active properties of excitable cells. Curr Opin Neurobiol *13*, 607-611.

Marshall, W. H., Talbott, S.A. (1942). Recent evidence for neural mechanisms in vision leading to a general theory of sensory acuity. Biol Symp *7*, 117-164.

Maycox, P. R., Hell, J. W., and Jahn, R. (1990). Amino acid neurotransmission: spotlight on synaptic vesicles. Trends Neurosci *13*, 83-87.

McLaughlin, T., Hindges, R., and O'Leary, D. D. (2003a). Regulation of axial patterning of the retina and its topographic mapping in the brain. Curr Opin Neurobiol *13*, 57-69.

McLaughlin, T., and O'Leary, D. D. (2005). Molecular gradients and development of retinotopic maps. Annu Rev Neurosci *28*, 327-355.

McLaughlin, T., Torborg, C. L., Feller, M. B., and O'Leary, D. D. (2003b). Retinotopic map refinement requires spontaneous retinal waves during a brief critical period of development. Neuron *40*, 1147-1160.

Meister, M., Lagnado, L., and Baylor, D. A. (1995). Concerted signaling by retinal ganglion cells. Science *270*, 1207-1210.

Nakamoto, M., Cheng, H. J., Friedman, G. C., McLaughlin, T., Hansen, M. J., Yoon, C. H., O'Leary, D. D., and Flanagan, J. G. (1996). Topographically specific effects of ELF-1 on retinal axon guidance in vitro and retinal axon mapping in vivo. Cell *86*, 755-766.

Nakamura, H., and O'Leary, D. D. (1989). Inaccuracies in initial growth and arborization of chick retinotectal axons followed by course corrections and axon remodeling to develop topographic order. J Neurosci *9*, 3776-3795.

Neuhauss, S. C. (2003). Behavioral genetic approaches to visual system development and function in zebrafish. J Neurobiol *54*, 148-160.

Neuhauss, S. C., Biehlmaier, O., Seeliger, M. W., Das, T., Kohler, K., Harris, W. A., and Baier, H. (1999). Genetic disorders of vision revealed by a behavioral screen of 400 essential loci in zebrafish. J Neurosci *19*, 8603-8615.

Ni, B., Rosteck, P. R., Jr., Nadi, N. S., and Paul, S. M. (1994). Cloning and expression of a cDNA encoding a brain-specific Na(+)-dependent inorganic phosphate cotransporter. Proc Natl Acad Sci U S A *91*, 5607-5611.

Niell, C. M., Meyer, M. P., and Smith, S. J. (2004). In vivo imaging of synapse formation on a growing dendritic arbor. Nat Neurosci *7*, 254-260.

Niell, C. M., and Smith, S. J. (2005). Functional imaging reveals rapid development of visual response properties in the zebrafish tectum. Neuron *45*, 941-951.

O'Rourke, N. A., and Fraser, S. E. (1990). Dynamic changes in optic fiber terminal arbors lead to retinotopic map formation: an in vivo confocal microscopic study. Neuron *5*, 159-171.

Orger, M. B., and Baier, H. (2005). Channeling of red and green cone inputs to the zebrafish optomotor response. Vis Neurosci *22*, 275-281.

Orger, M. B., Gahtan, E., Muto, A., Page-McCaw, P., Smear, M. C., and Baier, H. (2004). Behavioral screening assays in zebrafish. Methods Cell Biol *77*, 53-68.

Orger, M. B., Smear, M. C., Anstis, S. M., and Baier, H. (2000). Perception of Fourier and non-Fourier motion by larval zebrafish. Nat Neurosci *3*, 1128-1133.

Page-McCaw, P. S., Chung, S. C., Muto, A., Roeser, T., Staub, W., Finger-Baier, K. C., Korenbrot, J. I., and Baier, H. (2004). Retinal network adaptation to bright light requires tyrosinase. Nat Neurosci *7*, 1329-1336.

Pelli, D. G. (1997). The VideoToolbox software for visual psychophysics: transforming numbers into movies. Spatial Vision *10*, 437-442.

Reh, T. A., and Constantine-Paton, M. (1985). Growth cone-target interactions in the frog retinotectal pathway. J Neurosci Res *13*, 89-100.

Reid, R. C., and Alonso, J. M. (1995). Specificity of monosynaptic connections from thalamus to visual cortex. Nature *378*, 281-284.

Rinner, O., Rick, J. M., and Neuhauss, S. C. (2005). Contrast sensitivity, spatial and temporal tuning of the larval zebrafish optokinetic response. Invest Ophthalmol Vis Sci *46*, 137-142.

Rock, I., and Smith, D. (1986). The optomotor response and induced motion of the self. Perception *15*, 497-502.

Roeser, T., and Baier, H. (2003). Visuomotor behaviors in larval zebrafish after GFP-guided laser ablation of the optic tectum. J Neurosci *23*, 3726-3734.

Rubin, B. D., and Katz, L. C. (1999). Optical imaging of odorant representations in the mammalian olfactory bulb. Neuron *23*, 499-511.

Ruthazer, E. S., Akerman, C. J., and Cline, H. T. (2003). Control of axon branch dynamics by correlated activity in vivo. Science *301*, 66-70.

Ruthazer, E. S., and Cline, H. T. (2004). Insights into activity-dependent map formation from the retinotectal system: a middle-of-the-brain perspective. J Neurobiol *59*, 134-146.

Sajovic, P., and Levinthal, C. (1983). Inhibitory mechanism in zebrafish optic tectum: visual response properties of tectal cells altered by picrotoxin and bicuculline. Brain Res *271*, 227-240.

Schmidt, J. T. (1985). Apparent movement of optic terminals out of a local postsynaptically blocked region in goldfish optic tectum. J Neurophysiol *53*, 237-251.

Schmidt, J. T., and Buzzard, M. (1990). Activity-driven sharpening of the regenerating retinotectal projection: effects of blocking or synchronizing activity on the morphology of individual regenerating arbors. J Neurobiol *21*, 900-917.

Schmidt, J. T., Buzzard, M., Borress, R., and Dhillon, S. (2000). MK801 increases retinotectal arbor size in developing zebrafish without affecting kinetics of branch elimination and addition. J Neurobiol *42*, 303-314.

Schmidt, J. T., and Easter, S. S. (1978). Independent biaxial reorganization of the retinotectal projection: a reassessment. Exp Brain Res *31*, 155-162.

Schuske, K., and Jorgensen, E. M. (2004). Neuroscience. Vesicular glutamate transporter--shooting blanks. Science *304*, 1750-1752.

Schwartz, E. A. (1987). Depolarization without calcium can release gamma-aminobutyric acid from a retinal neuron. Science *238*, 350-355.

Shen, K., and Bargmann, C. I. (2003). The immunoglobulin superfamily protein SYG-1 determines the location of specific synapses in C. elegans. Cell *112*, 619-630.

Shimoda, N., Knapik, E. W., Ziniti, J., Sim, C., Yamada, E., Kaplan, S., Jackson, D., de Sauvage, F., Jacob, H., and Fishman, M. C. (1999). Zebrafish genetic map with 2000 microsatellite markers. Genomics *58*, 219-232.

Simpson, J. I. (1984). The accessory optic system. Annu Rev Neurosci *7*, 13-41.

Sperry, R. W. (1943). Effect of 180 degree rotation of the retinal field on visuomotor coordination. J Exp Zool *92*, 263-279.

Sperry, R. W. (1963). Chemoaffinity in the Orderly Growth of Nerve Fiber Patterns and Connections. Proc Natl Acad Sci U S A *50*, 703-710.

Springer, A. D., Easter, S. S., Jr., and Agranoff, B. W. (1977). The role of the optic tectum in various visually mediated behaviors of goldfish. Brain Res *128*, 393-404.

Stent, G. S. (1973). A physiological mechanism for Hebb's postulate of learning. Proc Natl Acad Sci U S A *70*, 997-1001.

Sterling, P. (2003). How retinal circuits optimze the transfer of visual information. In The visual neurosciences, L. M. Chalupa, Werner, J.S, ed. (Cambridge, MA, MIT Press).

Stevens, C. F., and Wesseling, J. F. (1998). Activity-dependent modulation of the rate at which synaptic vesicles become available to undergo exocytosis. Neuron *21*, 415-424.

Stuermer, C. A. (1988). Retinotopic organization of the developing retinotectal projection in the zebrafish embryo. Journal of Neuroscience *8*, 4513-4530.

Stuermer, C. A., Rohrer, B., and Munz, H. (1990). Development of the retinotectal projection in zebrafish embryos under TTX-induced neural-impulse blockade. J Neurosci *10*, 3615-3626.

Takamori, S., Rhee, J. S., Rosenmund, C., and Jahn, R. (2000). Identification of a vesicular glutamate transporter that defines a glutamatergic phenotype in neurons. Nature *407*, 189-194.

Takamori, S., Rhee, J. S., Rosenmund, C., and Jahn, R. (2001). Identification of differentiation-associated brain-specific phosphate transporter as a second vesicular glutamate transporter (VGLUT2). J Neurosci *21*, RC182.

Talbot, W. S., and Hopkins, N. (2000). Zebrafish mutations and functional analysis of the vertebrate genome. Genes Dev *14*, 755-762.

Tao, H. W., and Poo, M. M. (2005). Activity-dependent matching of excitatory and inhibitory inputs during refinement of visual receptive fields. Neuron *45*, 829-836.

Tokuoka, H., Yoshida, T., Matsuda, N., and Mishina, M. (2002). Regulation by glycogen synthase kinase-3beta of the arborization field and maturation of retinotectal projection in zebrafish. J Neurosci *22*, 10324-10332.

Trowe, T., Klostermann, S., Baier, H., Granato, M., Crawford, A. D., Grunewald, B., Hoffmann, H., Karlstrom, R. O., Meyer, S. U., Muller, B., *et al.* (1996). Mutations disrupting the ordering and topographic mapping of axons in the retinotectal projection of the zebrafish, Danio rerio. Development *123*, 439-450.

Tsodyks, M. V., and Markram, H. (1997). The neural code between neocortical pyramidal neurons depends on neurotransmitter release probability. Proc Natl Acad Sci U S A *94*, 719-723.

Turrigiano, G. G., and Nelson, S. B. (2004). Homeostatic plasticity in the developing nervous system. Nat Rev Neurosci *5*, 97-107.

Udin, S. B., and Gaze, R. M. (1983). Expansion and retinotopic order in the goldfish retinotectal map after large retinal lesions. Exp Brain Res *50*, 347-352.

Usrey, W. M., Reppas, J. B., and Reid, R. C. (1999). Specificity and strength of retinogeniculate connections. J Neurophysiol *82*, 3527-3540.

Walter, J., Henke-Fahle, S., and Bonhoeffer, F. (1987). Avoidance of posterior tectal membranes by temporal retinal axons. Development *101*, 909-913.

Wassle, H., and Boycott, B. B. (1991). Functional architecture of the mammalian retina. Physiol Rev *71*, 447-480.

Wilson, N. R., Kang, J., Hueske, E. V., Leung, T., Varoqui, H., Murnick, J. G., Erickson, J. D., and Liu, G. (2005). Presynaptic regulation of quantal size by the vesicular glutamate transporter VGLUT1. J Neurosci *25*, 6221-6234.

Wojcik, S. M., Rhee, J. S., Herzog, E., Sigler, A., Jahn, R., Takamori, S., Brose, N., and Rosenmund, C. (2004). An essential role for vesicular glutamate transporter 1 (VGLUT1) in postnatal development and control of quantal size. Proc Natl Acad Sci U S A *101*, 7158-7163.

Woo, K., and Fraser, S. E. (1995). Order and coherence in the fate map of the zebrafish nervous system. Development *121*, 2595-2609.

Xiao, T., Roeser, T., Staub, W., and Baier, H. (2005). A GFP-based genetic screen reveals mutations that disrupt the architecture of the zebrafish retinotectal projection. Development *132*, 2955-2967.

Zhang, L. I., Tao, H. W., Holt, C. E., Harris, W. A., and Poo, M. (1998). A critical window for cooperation and competition among developing retinotectal synapses. Nature *395*, 37-44.

Zucker, R. S., and Regehr, W. G. (2002). Short-term synaptic plasticity. Annu Rev Physiol *64*, 355-405.

For reference